

Single-cell spatial transcriptomics of fixed, paraffin-embedded biopsies reveals colitis-associated cell networks

Short Title: Spatial transcriptomics analysis of colitis

Elvira Mennillo^{1*}, Madison L. Lotstein^{2,3*}, Gyehyun Lee^{1§}, Vrinda Johri^{3§}, Christina Ekstrand^{2,3}, Jessica Tsui³, Julian Hou¹, Donna E. Leet¹, Jun Yan He^{5,7}, Uma Mahadevan¹, Walter Eckalbar^{3,4}, David Y. Oh^{5,7}, Gabriela K. Fragiadakis^{2,3,6,7#}, Michael G. Kattah^{1,2,7#}, Alexis J. Combes^{1,2,3,7,8#}

1. Division of Gastroenterology, Department of Medicine, University of California, San Francisco, San Francisco, CA 94143, USA
2. Biomedical Sciences graduate program, University of California, San Francisco, San Francisco, CA 94143, USA
3. UCSF CoLabs Initiative, University of California, San Francisco, San Francisco, CA 94143, USA
4. Division of pulmonary and intensive care, Department of Medicine, University of California, San Francisco, San Francisco, CA 94143, USA
5. Division of Hematology/Oncology, University of California, San Francisco, San Francisco, CA 94143, USA
6. Division of Rheumatology, University of California, San Francisco, San Francisco, CA 94143, USA
7. UCSF Bakar ImmunoX Initiative, University of California, San Francisco, San Francisco, CA 94143, USA
8. Department of Pathology, University of California, San Francisco, San Francisco, CA 94143, USA

*: These authors contributed equally to this work

§: These authors contributed equally to this work

#: Lead authors

Correspondence

Address correspondence to:

Alexis J. Combes PhD, 513 Parnassus Ave, S-859, San Francisco CA, 94143. e-mail:

alexis.combes@ucsf.edu

Michael G Kattah MD PhD, 513 Parnassus Ave, S-357G, San Francisco CA, 94143. e-mail:

<mailto:michael.kattah@ucsf.edu>,

Gabriela K Fragiadakis PhD, 513 Parnassus Ave, S-847C, San Francisco CA, 94143. e-mail:

<mailto:gabriela.fragiadakis@ucsf.edu>.

ABSTRACT

Background & Aims: Imaging-based, single-cell spatial transcriptomics (iSCST) using formalin-fixed, paraffin-embedded (FFPE) tissue could transform translational research by retaining all tissue cell subsets and spatial locations while enabling the analysis of archived specimens. We aimed to develop a robust framework for applying iSCST to archived clinical FFPE mucosal biopsies from patients with inflammatory bowel disease (IBD).

Methods: We performed a comprehensive benchmarking comparison of three iSCST platforms capable of analyzing FFPE specimens. We analyzed FFPE mucosal biopsies (n=57) up to 5 years old from non-IBD controls (HC; n=9) and patients with ulcerative colitis (UC;n=11). After platform-specific cell segmentation, we applied a uniform data processing pipeline to all datasets, including transcript detection, cell annotation, differential gene expression, and neighborhood enrichment. Transcriptomic signatures identified with iSCST were validated using external, publicly available bulk transcriptomic datasets.

Results: A custom 290-plex Xenium gene panel exhibited the highest sensitivity and specificity for transcript detection, enabling precise identification and quantification of diverse cell subsets and differentially expressed genes across cell types and disease states. We mapped transcriptionally distinct fibroblast subsets to discrete spatial locations and identified inflammation-associated fibroblasts (IAFs) and monocytes as a colitis-associated cellular neighborhood. We also identified signatures associated with Vedolizumab (VDZ) responsiveness. VDZ non-responders were characterized by an IAF-monocyte transcriptional signature, while responders exhibited enrichment of epithelial gene sets.

Conclusions: Our optimized iSCST framework for archived FFPE biopsies provides unique advantages for assessing the role of colitis-associated cellular networks in routinely collected clinical samples. FFPE-based biomarkers could integrate with existing clinical workflows and potentially aid in risk-stratifying patients.

Keywords: Spatial transcriptomics, ulcerative colitis, vedolizumab

INTRODUCTION

Single-cell multi-omics studies in inflammatory bowel disease (IBD) have rapidly accelerated our understanding of intestinal inflammation, highlighting critical roles for multiple cell subsets across stromal, epithelial, and immune compartments¹⁻⁸. While powerful, traditional single-cell multi-omics analyses of prospectively collected and digested colon biopsies suffer from several important limitations. These include cellular dropout or under-representation of epithelial and granulocyte subsets, loss of spatial information, and prolonged patient recruitment^{9,10}. As an example, neutrophils contribute to acute colitis and treatment non-response, but they are particularly difficult to capture with many single-cell multi-omics approaches, and their proximity and interactions with inflammatory fibroblasts are lost in disaggregated tissue^{8,10,11}. Analyzing cellular networks such as these before and after treatment in responders and non-responders across multiple therapies from prospectively collected samples requires prolonged recruitment. Spatial transcriptomics of formalin-fixed, paraffin-embedded (FFPE) tissue with subcellular resolution directly addresses these shortcomings by comprehensively capturing cell subsets and transcriptional states in mucosal biopsies, retaining spatial relationships, and accelerating recruitment for retrospective, longitudinal, case-control analyses of archived clinical specimens collected as part of standard of care.

Spatial transcriptomics technologies hold great promise for identifying tissue biomarkers and augmenting our understanding of disease and treatment response. These technologies are still emerging, and a growing body of literature leverages these approaches to study mouse models¹² or patient samples^{10,13}, but few studies have benchmarked different platforms for the optimal analysis of archived FFPE clinical specimens, and those that have were primarily focused on tumor tissues¹⁴⁻¹⁷. Hence, it is unclear whether prior iSCST comparisons extrapolate to archived clinical specimens from inflammatory disorders such as IBD. We performed a comparison of three commercially available imaging-based single-cell spatial transcriptomics (iSCST) platforms capable of analyzing FFPE specimens with subcellular resolution from tissue sections. These platforms were used to analyze FFPE colon mucosal biopsies archived for up to 5 years from non-IBD controls and patients with UC. Our primary comparison examined specific and non-specific transcript detection, cell-subset identification, and differential gene expression between healthy and inflamed tissue. We also examined cell segmentation and the impact of sample age on assay performance. Using our custom IBD panel, we identified transcriptionally and spatially distinct fibroblast subsets in health and disease, and we defined an inflammation-associated fibroblast (IAF)-monocyte cellular network that increased in abundance and spatial proximity in patients with active UC. We present an optimized iSCST pipeline for analyzing archived mucosal biopsies from patients with inflammatory intestinal disorders, offering unique advantages for evaluating colitis-associated cellular networks in routinely collected clinical samples.

RESULTS

Xenium Outperforms Competing iSCST Platforms in Sensitivity and Detection of Colon-Associated Cell Types.

To develop an iSCST pipeline for studying archived FFPE specimens, here focused on mucosal biopsies from IBD patients, we evaluated three commercially available imaging-based spatial transcriptomics platforms: Xenium (10X Genomics), CosMx (NanoString), and MERSCOPE (Vizgen). The CosMx dataset was previously generated using a 1,000 gene pre-designed CosMx Human Universal Cell Characterization RNA Panel on an FFPE tissue microarray (TMA) containing colon biopsies from UC patients and patients without IBD, referred to as healthy controls (HC), and was re-analyzed for this study (**Figure 1A, Supplementary Table 1**)⁹. The Xenium and MERSCOPE spatial platforms were used to test the same TMA that was used to generate the CosMx data. The custom Xenium panel contained 290 genes, and the custom MERSCOPE panel contained 280 genes (**Supplementary Table 2**). Both panels were designed to detect colon-associated mucosal and submucosal cell subsets and differentially expressed genes (DEGs) identified by single-cell RNA sequencing (scRNA-seq) of colon biopsies from UC and HC patients⁹. Due to difficulties with tissue clearing, MERSCOPE could not detect most of the genes in the panel (**Supplementary Figure 1A-B**). Even though some genes were detected as shown in the TMA scanned area (**Supplementary Figure 1C**), they were low quality and only 0.17% of cells passed quality control (QC) (**Supplementary Figure 1D**). Thus, MERSCOPE was excluded from the remainder of the analysis. The Xenium and CosMx panels shared 159 overlapping genes and were compared for transcript and gene detection, cell annotation, and differential gene expression (**Supplementary Table 2**).

We began by using the default cell segmentation settings for each platform to identify single cells. For the Xenium platform, we employed the integrated default nuclear expansion method, extending nuclear boundaries by 5 μm or until another cell boundary is encountered. In contrast, the CosMx platform combines nuclear and cell membrane staining for cell identification. Although this led to slight differences in the distribution of nuclear versus cytoplasmic transcripts between platforms (**Supplementary Figure 2A**), the median cell area was similar (**Supplementary Figure 2B**). To further investigate outlier cells with larger areas observed in the Xenium platform, we examined cell boundaries using the Xenium Explorer visualization tool from 10X Genomics. Some cells displayed expanded boundaries, but the distortion affected primarily cells adjacent to luminal space (**Supplementary Figure 2C**). Overall, the nuclear expansion cell segmentation inflated the cell area of a relatively small percentage of cells.

We then evaluated sensitivity metrics across the full gene panel for both the Xenium and CosMx platforms. The larger CosMx panel yielded a higher number of transcripts and unique features per cell (**Figure 1B-C**). However, when the analysis was restricted to the 159 overlapping genes between the two panels, Xenium detected significantly more transcripts and unique features per cell compared to CosMx (**Figure 1B-C**). Importantly, Xenium also exhibited ten times lower detection of negative probes per cell (0.03 vs 0.37, $p < 0.001$) (**Figure 1D**). Xenium demonstrated significantly higher transcript counts for the overlapping genes (**Figure 1E**). The higher signal per gene with reduced non-specific detection of negative probes yielded a markedly higher signal over

background for Xenium compared to CosMx (**Supplementary Table 3**). Upon examining dataset-specific genes unique to either the Xenium or CosMx panels, we found that most genes exhibited similar expression levels, typically ranging from 1 to 5 transcripts per cell. However, immunoglobulin genes expressed by B and plasma cells (*IGHG2*, *IGKC*, *IGHG1*, *IGHA1*) displayed higher expression levels (**Supplementary Figure 2D**). These highly expressed immunoglobulin genes could not be included in the Xenium panel due to their abundance and issues with optical crowding, pointing to one limitation of the signal amplification with Xenium. Notably, the age of the sample block had minimal impact on performance metrics for both methods, showing no meaningful differences in the median number of transcripts or genes detected per cell per core or FOV across 2-, 3-, 4-, and 5-year-old sample blocks (**Supplementary Figure 2E-F**). The HC samples were prospectively collected and processed in the laboratory, while the UC samples were retrospectively retrieved years after processing and storage through the usual standard of care. Despite this, the retrospectively retrieved UC samples exhibited equivalent or better transcript and feature detection compared to prospectively collected HC samples (**Figure 1F-G**).

A key advantage of iSCST is its ability to spatially locate transcriptomic cell states that were previously identified by unsupervised clustering of single-cell RNA sequencing (scRNA-seq) from dissociated tissue. We assessed how each platform's specificity and sensitivity affected unsupervised cell type identification in FFPE colon biopsies. Using the same data processing pipeline, we generated uniform manifold approximation and projection (UMAP), clustering, and annotation, and generated heatmaps of landmark genes and correlation matrices for Xenium (**Fig 2A-D**) and CosMx (**Fig 2E-H**). At both the coarse (**Figure 2A, 2E**) and fine level (**Figure 2B, 2F**), comparing this CosMx re-analysis and prior analysis⁹, Xenium enabled the identification of a broader range of colon-associated cell types, including various fine subsets of epithelial cells, fibroblasts, endothelial cells, and fragile innate immune cells like neutrophils and mast cells. Some subsets were difficult to confidently assign, such as intraepithelial lymphocytes (IELs), which is likely due in part to cell segmentation challenges. Overall, unsupervised clustering of single-cell gene expression profiles from Xenium produced more distinct gene expression signatures per cluster, yielding clearer cell cluster separation, as shown in heatmaps (**Figure 2C, 2G**) and correlation plots (**Figure 2D, 2H**). In contrast, the same data processing pipeline of the CosMx data from the same TMA resulted in >20% of cells being labeled as "Unassigned" due to indistinct transcriptomic profiles (**Figure 2I**). There was also a small percentage of cells labeled "ncount_hi" characterized by the high expression of B and plasma cell-related genes. Although finer cell annotation is possible with both the Xenium and CosMx datasets, here we applied comparable pipelines to provide a more direct comparison of subset identification. We then assessed the mutually exclusive co-expression rate (MECR) values for each platform, which provides a metric for lineage-specific genes that are unique to prominent cell types (**Supplementary Figure 3**). As a gold standard, we compared MECR values to previously published scRNA-seq data from HC and UC patient biopsies⁹. MECR values were generally similar for the two iSCST platforms, and neither was as specific as scRNA-seq, but the higher transcript counts for unique landmark genes enabled finer cell annotation with Xenium (**Supplementary Figure 3, Figure 2B**). Overall, the improved performance of Xenium for cell

identification in these colon FFPE samples is due to multiple factors, including higher cell number, a custom panel optimized for colon biopsies, and higher sensitivity and specificity for landmark gene expression. Then, to address reproducibility with the Xenium platform, we performed a replicate run of separate sections from the same TMA. We observed high reproducibility for gene expression levels (**Supplementary Figure 4A**) and the samples demonstrated a balanced representation of cell types across replicates (**Supplementary Figure 4B**). Doubling the number of cells in our dataset enhanced the accuracy of our detailed fine annotations (**Supplementary Figure 4C, Supplementary Figure 5A-B**). Taken together, our comprehensive comparison of three iSCST platforms for FFPE specimens indicates that the Xenium platform exhibits superior transcript and gene sensitivity, enables the detection of a greater range of colon-associated cell types and transcriptional states, exhibits high reproducibility across replicates, and is robust to tissue age.

A custom 290-plex iSCST Xenium panel differentiates cases and controls in UC FFPE colon biopsies, revealing spatial transcriptomic profiles of B Cells, epithelial cells, and mononuclear phagocytes.

Next, we aimed to extend our comparison of the CosMx and Xenium iSCST platforms beyond QC and cell identification metrics to evaluate their ability to identify transcriptomic signatures associated with UC pathology. Publicly available bulk transcriptomic data served as the comparator for this analysis, rather than scRNA-seq, because bulk RNA isolation methods do not involve digestion and, therefore, do not suffer from cellular or transcriptional dropout like scRNA-seq studies. We generated pseudobulk iSCST transcriptomic profiles by aggregating the transcript counts for all cells for each individual patient. We then performed a DEG analysis comparing UC biopsies before treatment with VDZ (UC PRE) to HC using the full gene panels for both platforms. Using a cutoff of >0.4 Log₂FC and q-value <0.1 , the transcriptomic profile obtained from the Xenium platform identified a broad range of upregulated genes in both UC and HC groups, with 32 genes significantly upregulated in UC PRE and 60 in HC (**Figure 3A**). The UC-associated DEGs included genes well-known for their association with inflammatory infiltrates, specifically neutrophils and monocytes (S100A8/S100A9) as well as lymphocytes (CD19, LTB, SELL, MS4A1), with cell identities confirmed in our Xenium iSCST dataset (**Supplementary Figure 5C**). Conversely, HC-associated genes included mostly genes associated with intact intestinal epithelial cells (IECs), such as *c15orf48*, *EPCAM*, *AQP8*, *FABP1*, *FABP2*, *PHGR1* (**Supplementary Figure 5C**). In contrast, data from the CosMx platform on the same TMA identified 57 genes upregulated in UC PRE and only one gene significantly upregulated in HC (**Figure 3B**). Unsupervised hierarchical clustering of a subset of the DEGs showed unique expression patterns that readily distinguished UC PRE patients and HC in the Xenium dataset (**Figure 3C**) but not CosMx (**Figure 3D**). CosMx identified a slightly higher number of DEGs in the UC PRE samples compared to Xenium, but only identified a single gene associated with HC (**Figure 3E**). It is important to acknowledge that testing more genes (1000 vs 290) leads to a statistical penalty for CosMx due to FDR correction. We then focused our comparison on the overlapping genes across platforms. This revealed a poor correlation between the differentially expressed genes identified by the two platforms ($R = 0.12$), with only *COL1A1*, *MZB1*, and *TIMP1* being significant in both datasets (**Figure 3F**). Overall, genes identified by Xenium exhibited a higher fold change compared to those from CosMx (**Figure 3F**). To further validate our Xenium gene

signatures identified for HC and UC PRE, we performed gene set enrichment analysis (GSEA) on an external bulk transcriptomic dataset¹⁸, confirming significant Normalized Enrichment Scores (NES) in HC and UC PRE, and nearly flawless validation of the UC PRE-associated signature (**Figure 3G**). CosMx showed a slightly lower NES compared to Xenium for the UC PRE signature (-2.49 vs -2.66; **Figure 3G** and **Supplementary Figure 6A**). To further adjudicate the conflicting DEGs between the Xenium and CosMx datasets (**Figure 3F**), we then determined whether the individual DEGs from the two iSCST methods exhibited concordance or discordance with up-regulation in the UC PRE external bulk transcriptomic dataset. Although both methods revealed significant concordance, CosMx demonstrated more discordance with bulk transcriptomic data, as 13 DEGs in the CosMx UC PRE signature were instead associated with HC in bulk transcriptomic data (**Supplementary Figure 6B**). These discordant CosMx genes included *KRT20* and *LGALS3*, which were enriched in HC in the external dataset and are expressed by intact IECs (**Supplementary Table 5**).

Finally, we leveraged the spatial information associated with each transcript to create spatial transcript scatter plots for the mucosal biopsies for subsets of DEGs identified by Xenium for HC and UC PRE patients. Transcript-level spatial scatter plots for IEC-specific genes (*AQP8*, *EPCAM*, and *PIGR*) were more abundant in HC tissue, while B cell-specific genes (*BANK1*, *IGHD*, *MS4A1*, and *SELL*) and MNP and neutrophil-specific genes (*S100A8*, *S100A9*, and *TIMP1*) were linked to disease (**Figure 3H**). Overall, the custom Xenium 290-plex gene panel identified more DEGs between HC and UC patients, with higher log fold changes and greater concordance with external validation bulk transcriptomic data. This strong differentiation between cases and controls in UC FFPE colon biopsies is marked by a shift in transcriptomic profiles, from epithelial cells predominating in HC to B cells, neutrophils and MNPs in UC.

Optimized iSCST pipeline identifies spatially and transcriptionally distinct fibroblast populations in FFPE colon biopsies.

Previous work by our group⁹ and others^{1,19} has highlighted the importance of distinct fibroblast subsets, characterized by unique transcriptional states, in colon tissue under steady-state conditions, as well as in UC pathology and treatment response. While the spatial location of those transcriptomic subsets has been recently described in IBD mouse models¹², equivalent detailed spatial characterization in clinical biopsies has been challenging and is still lacking. By leveraging the high sensitivity of the Xenium iSCST platform, unsupervised clustering from our custom 290-plex gene panel identified five transcriptionally distinct fibroblast subsets (S1, S2, S3, S4 and IAF; **Figure 2B** and **Supplementary Figure 5A**) that were previously characterized in scRNA-seq of human colonic stromal cells^{1,9,19}. In agreement with prior scRNA-seq studies, Xenium iSCST identified transcriptionally distinct S1 (*CCL8*, *ADAMDEC1*, *APOE*, *FABP5*), S2 (*F3*, *SOX6*, *PDGFRA*, *WNT5A*, *POSTN*, *CXCL14*), S3 (*GSN*, *OGN*, *CCDC80*, *C7*), S4 (*C3*, *TNFSF13B*, *IRF8*, *PTGDS*), and IAF (*IL1R1*, *TIMP1*, *CD44*, *IL13RA2*, *MMP1*, *MMP3*, *OSMR*, *NFKBIA*, *TNFAIP3*) subsets (**Figure 4A**). These subsets display a broad range of functions and identities, and some have previously been linked to specific locations in the colon²⁰. S1 fibroblasts have been linked to *PDGFRA*^{lo} colonic crypt fibroblasts (cCF) at the bottom of the colon crypts, S2

fibroblasts have been described to line the colonic crypt, and share features with *PDGFRA*^{hi} crypt top fibroblasts (CTFs) that are also high in *SOX6* and *WNT5A*^{1,9,19,20}. While IAF are disease-associated, S1-4 subsets were present at steady state. We spatially mapped the transcriptomic states present in colon tissue at steady state (**Figure 4B**). Spatial scatter plots showed that the S1-cCF fibroblasts were somewhat dispersed but were biased more toward the crypt base, while S2-CTF fibroblasts lined the colonic crypt as previously described (**Figure 4B**). S3 fibroblasts localize to the submucosal (**Figure 4B**), while S4 fibroblasts express fibroblastic reticular cell (FRC)-associated genes, including *TNFSF13B* or B-cell activating factor (BAFF) and colocalize with B cells in gut-associated lymphoid tissue (GALT) aggregates (**Figure 4B**). Together, this study provides a comprehensive spatial map of transcriptomic subsets of colonic fibroblasts at steady state in archived clinical FFPE mucosal biopsies using iSCST.

Inflammation-associated fibroblast–monocyte network and B cell abundance in GALT are associated with UC

Our spatially resolved Xenium iSCST dataset accurately identified 34 distinct transcriptomic cell states, including fragile populations such as neutrophils which are typically lysed during cryopreservation and thawing or are excluded by encapsulation in single-cell sequencing workflows⁹. This provided us with a unique opportunity to study cell composition, gene expression changes, and spatial location in undissociated colon tissue between HC and UC cases without cellular dropout. First, by comparing cell abundances between HC and UC PRE, we revealed 19 cell subsets that differed significantly after FDR correction (**Figure 5A and Supplementary Figure 7**). We observed significant variations associated with disease, specifically in monocyte, neutrophil, IAF, and S4 fibroblast abundance (**Figure 5A**). Furthermore, there was a significant increase across all endothelial subsets, pericytes, B and plasma cells, and both CD4 and CD8 T lymphocytes in UC PRE, with a reduction in IEC subsets (**Supplementary Figure 7**). iSCST with Xenium identified transcriptionally and spatially distinct colonic mucosal cell subsets in homeostasis and disease, providing a more comprehensive framework for interrogating stromal and immune subsets.

We then leveraged the spatial aspect of the dataset to explore the proximity and interactions between our annotated cell types, comparing HC and UC PRE. Spatial neighborhood graphs were constructed for the HC and UC PRE data subsets using the fine annotation cell type categories aggregating all patients. Using these spatial neighbor graphs, we calculated neighborhood enrichment z-scores for each cell type pair (**Supplementary Figure 8**). Comparing cellular neighborhoods between HC and UC PRE, we identified several notable changes for the monocytes, including neighborhood enrichment with IAFs, neutrophils, and B cells (**Supplementary Figure 8B**). Next, we focused on the neighborhood enrichment z-scores between IAFs and all other cell types in HC (**Figure 5B**) and UC PRE (**Figure 5C**). Monocytes exhibited the highest interaction scores in both HC and UC PRE, with a collectively higher value in UC PRE. The IAF-monocyte enrichment was followed by IAF-neutrophil enrichment, which has been described in recent single-cell analyses of UC biopsy specimens^{8,10}. Neutrophils and monocytes exhibit similarities in gene expression, so there could be overlap in

the annotation of neutrophils and monocytes. Here, the monocyte population exhibited higher *HLA-DRA*, *HLA-DRB1*, and *VCAN*, while the neutrophils expressed higher *CSF3R*, *FCGR3B*, *S100A8*, *S100A9*, and *TREM1* (**Supplementary Figure 8C**). To investigate this interaction further, we calculated the neighborhood enrichment z-scores between IAF and monocytes for each individual core and averaged the scores per patient. This revealed low enrichment scores in HC, with multiple instances where z-scores could not be calculated due to low or no abundance (**Figure 5D**). UC PRE biopsies showed a trend (p value 0.07) toward increased z-scores for IAFs and monocytes, consistent with the increased abundance and proximity of IAFs and monocytes in colitis. Spatial scatter plots of these subsets within representative HC and UC PRE samples confirmed these findings (**Figure 5E**). Taken together, we define an IAF-monocyte cellular network that increases in abundance and spatial proximity in patients with active UC.

Finally, we examined the biopsies from UC patient's pre-treatment with vedolizumab, stratified by subsequent treatment response, to assess the association of spatial cellular network with treatment outcomes. We performed a pseudobulk DEG analysis, stratifying the UC PRE group into responders (UC PRE R) and non-responders (UC PRE NR) to VDZ (**Supplementary Figure 9, Supplementary Table 6**). Consistent with previous findings⁹, our Xenium dataset identified response-associated genes linked to IEC crypts, including *AGR2*, *PIGR*, and *SPINK4*. Additionally, we observed an increase in IAF and MNP-associated genes, such as *MMP1*, *MMP3* for IAF and *FCER2*, *CD1C* for the MNP, in non-response (**Supplementary Figure 9A-C**). Moreover, the Xenium dataset enabled the detection of differences in genes associated with B cells (*CD19*, *MS4A1*, *BANK1* and *SELL*) in UC PRE NR versus UC PRE R (**Supplementary Figure 9A-B**). These B cell genes were located spatially in GALT aggregates (**Supplementary Figure 9C**). This raised the possibility that VDZ non-responders have higher levels of GALT pre-treatment compared to responders, supporting recent work showing that VDZ reduces GALT in responders after treatment²¹. We then performed GSEA of external bulk transcriptomic data using our Xenium-defined gene sets from VDZ responders and non-responders. GSEA validated our Xenium VDZ response signature, comprised largely of epithelial genes (**Supplementary Figure 9D**). Interestingly, the overall Xenium VDZ non-response signature was not validated by GSEA in this external dataset. We then divided the Xenium VDZ non-response signatures into two separate signatures, one comprised of genes from IAF, monocytes, and neutrophils, and the other comprised of genes enriched in GALT aggregates, including B cell, DC, and S4 fibroblast landmark genes. The IAF-monocyte-neutrophil signature was enriched in VDZ non-responders by GSEA in the external dataset, but the GALT-B-DC-S4 fibroblast signature was not, suggesting that there may be some heterogeneity in VDZ non-responders. These data demonstrate the potential for Xenium to identify pre-treatment response and non-response signatures using archived clinical FFPE specimens.

DISCUSSION

To identify the optimal spatial transcriptomics platform for analyzing archived, clinical FFPE mucosal biopsies of non-IBD patients and patients with UC, we compared three commercially available platforms on the same FFPE TMA. The Vizgen MERSCOPE was not able to analyze these samples due to difficulties with tissue clearing.

Comparing 10X Genomics Xenium and Nanostring CosMx, the Xenium detected more transcripts and genes per cell for overlapping genes with significantly lower non-specific probe detection. The smaller custom Xenium panel, optimized for mucosal biopsies of patients with IBD, enabled the identification, annotation, and quantitation of more cell subsets and identified more differentially expressed genes across cell subsets and disease states. The default nuclear expansion cell segmentation with Xenium inflated the cell sizes of a small percentage of cells but identified comparable median cell area to other algorithms with minor impact on the overall results. Using this improved spatial pipeline, we mapped transcriptionally distinct fibroblast subsets to discrete spatial locations, and we identified increased abundance and trends toward increased spatial proximity of IAFs and monocytes in patients with UC. We also identified signatures associated with response or non-response to VDZ, highlighting IAF-monocyte networks and B cell-GALT abundance in non-responders as well as IEC gene sets in responders. Spatial transcriptomics preserves cell subset frequency and transcriptional states with high fidelity, and these methods can facilitate robust tissue profiling using archived FFPE.

Several recent studies have examined imaging-based spatial platforms on tumor tissue, and the results are largely consistent with this study^{14–16}. One study found higher sensitivity and broader dynamic range with Xenium for FFPE prostate cancer samples¹⁵. Another study of FFPE tumor blocks originating from breast, colorectal, lung, ovary, bladder, and lymphoma similarly observed better gene clustering, fewer false positives, and better correlation with whole transcriptome approaches for Xenium as compared to CosMx¹⁶. A third study of 7 tumor types and 16 normal tissues found higher transcript counts, higher specificity, and lower false discovery rates for Xenium compared to CosMx, and showed that MERSCOPE was the most dependent on RNA integrity¹⁶. The default Xenium cell segmentation consistently inflated cell sizes across all these studies, but the overall impact on performance was minor, consistent with our findings. It is important to note that the preferred spatial transcriptomics approach may depend on the upstream processing and tissue type. For example, one recent benchmarking study using fresh-frozen mouse brain samples demonstrated superior performance with Vizgen's MERSCOPE over the Xenium platform²². Therefore, considering the tissue type and sample processing protocol will be critical for choosing a spatial transcriptomics platform.

It is also important to acknowledge that some of the improvements in cell annotation we observed with Xenium were due to the customized panel for IBD, which included key landmark genes for our cell subsets of interest. This focused panel allowed us to map transcriptionally distinct fibroblast subsets to discrete spatial locations, for example, confirming S2 as sub-epithelial crypt-associated fibroblasts, S3 as submucosal fibroblasts, and S4 as follicular stromal cells co-localizing with lymphoid aggregates in GALT. Although it would be appealing to employ an unbiased universal panel across tissues, our results suggest that an optimized panel for a specific tissue type and disease state will capture more cells and genes of interest with improved performance. In IBD, there are ample reference tissue scRNA-seq datasets to guide panel design^{1–4,6,7,9}, but other tissues and disease processes may benefit from initial studies using larger, unbiased panels or whole transcriptome approaches. While we observed excellent cell subset identification using a smaller, custom IBD panel, this focused panel may not capture the breadth of differentially expressed genes offered by larger panels or whole transcriptome

methods. Due to optical crowding with imaging-based spatial transcriptomics platforms, there will likely continue to be a trade-off between the signal for each gene and the size of the panel. Therefore, multiple complementary spatial transcriptomics approaches might be necessary to adequately capture the transcriptional diversity of cell subsets and disease states in FFPE tissue. Whether focused or whole transcriptome methods are used, the transcript counts for these spatial methods are generally orders of magnitude lower than scRNA-seq, which could limit downstream differential gene expression analyses. Therefore, bulk RNA-seq and scRNA-seq will continue to be critical for dissecting tissue inflammation and informing spatial transcriptomics datasets.

The identification of both B cell abundance in GALT and IAF-monocyte networks in UC biopsies, including some VDZ non-responders, complements recent studies regarding UC and the effects of VDZ. Comprehensive flow cytometry analysis of mucosal biopsies identified a significant reduction of CD1c⁺ (BDCA1⁺) type 2 conventional dendritic cells (cDC2s) in UC patients on VDZ²³. We subsequently reported a shift of $\alpha4\beta7^+$ conventional dendritic cells (cDCs) from the tissue to the circulation in UC patients on VDZ⁹. Interestingly, another group reported that VDZ reduced naïve B and T cells and gut-homing plasmablasts, culminating in GALT attrition in VDZ responders²¹. Given the central role of cDCs in priming naïve T and B cells in lymphoid tissue, VDZ may reduce GALT by markedly inhibiting migratory cDCs from trafficking to the colon. Here, we identified higher B cell abundance and *CD1C* expression in some VDZ non-responders pre-treatment by Xenium. Given that both B cells and CD1c⁺ cDCs localize to GALT, these data imply that higher pre-treatment GALT area may be associated with VDZ non-response, although the GALT signature in VDZ non-responders was not validated in an external transcriptomic dataset. Recruitment of neutrophils and monocytes to inflamed colon tissue by IAFs has also been associated with UC and non-response to VDZ^{8,9}. In this study, we also observed an increased abundance and trend toward proximity of IAFs and monocytes in UC compared to HC, confirming prior associations of this cellular network with colitis. Neutrophils were also increased in abundance in patients with UC in this study, and given similarities in gene expression, there is likely some overlap in the annotation of neutrophils and monocytes using spatial transcriptomics. Finally, we identified pre-treatment spatial transcriptomics signatures in the epithelial compartment associated with a response to VDZ, suggesting a potential mechanism for mucosal healing. Namely, VDZ responders may have IECs that are poised to regenerate the epithelium once inflammation is suppressed.

There are important limitations of this study to consider, and several caveats regarding spatial transcriptomics in general. First and foremost, we compared healthy and inflamed colon biopsies and VDZ responders versus non-responders using a small number of patients. Future longitudinal spatial transcriptomics studies will need to include more patients on various therapies to identify signatures predictive of response or non-response. We also focused exclusively on archived human FFPE colon tissue, which is a unique tissue type. These endoscopic mucosal biopsies are placed directly in formalin within seconds of collection, they permeabilize easily due to their small size, and embedding is typically completed within a day or a few days. Thus, our findings may not extrapolate seamlessly to other specimens that vary in size and fixation times. As noted above, several studies have examined imaging-based spatial platforms on tumor and normal tissue, and the results largely align with

our study^{14–16}, but certain tissues or disease processes may be captured differently by various platforms. Moreover, additional gene sets would be required to adequately profile ileal samples. Another fundamental limitation of spatial transcriptomics is that annotating cells exclusively using transcriptional signatures has inherent drawbacks. For example, confidently differentiating naïve, effector, regulatory, and memory T cell subsets would be markedly improved with simultaneous spatial proteomic surface marker analysis. Similarly, the identification of polymorphonuclear cells (PMNs) and IELs would be greatly enhanced with expert concurrent annotation of H&E images by a pathologist, rather than relying solely on landmark gene expression. Spatial transcriptomics studies are also limited by sampling variability. For example, here we analyzed 4 μ m-thick sections of cores from 2-3mm biopsies meant to reflect the inflammatory status of an organ approximately one meter long. Adequate tissue sampling will be critical to consider in all future spatial transcriptomics studies.

In summary, we compared three commercially available platforms and optimized a custom spatial transcriptomics panel for analyzing archived FFPE colon mucosal biopsies from patients with or without colitis. Our custom IBD-specific Xenium panel detected more transcripts and genes per cell for overlapping genes, identified more unique cell subsets, quantitated more significant changes in cell frequency, and detected more differentially expressed genes across disease states. This approach yielded improved annotation and spatial analysis of fibroblast subsets and uncovered IAF-monocyte neighborhood enrichment in inflamed colon biopsies. This study adds to the growing body of literature identifying critical interactions among MNP, neutrophil, and fibroblast subsets in inflamed tissues across multiple diseases. We also identified increased B cell frequency in UC biopsies compared to HC, particularly in VDZ non-responders pre-treatment, demonstrating the ability of spatial transcriptomics to profile alterations in GALT across disease states. The capability of generating spatial transcriptomics data from routinely collected, archived clinical specimens with subcellular resolution could enable transformative translational research. Spatial transcriptomics could accelerate the identification and validation of candidate biomarkers and nominate novel therapeutic targets in affected tissue for a variety of inflammatory disorders.

METHODS

Study approval

The study was conducted according to the Declaration of Helsinki principles and was approved by the Institutional Review Board of the University of California, San Francisco (19-27302). Written informed consent was received from participants prior to inclusion in the study.

Study participants and biospecimen collection

For this study, both prospectively collected and retrospectively retrieved archived formalin-fixed paraffin-embedded (FFPE) samples were used. Healthy control (HC) patients refer to those without known or suspected inflammatory bowel disease (IBD) who were undergoing routine colonoscopy or sigmoidoscopy for various indications, such as colorectal cancer screening. HC biopsies were prospectively collected, placed in 10% formalin in 5 mL tubes for approximately 24h, then washed with PBS three times, and then transferred to 30%,

50%, and finally 70% ethanol, and they are stored in 70% ethanol for up to a month prior to paraffin embedding. All UC specimens were retrospectively retrieved. For retrospective retrieval, study subjects were identified by querying the electronic medical records of patients previously seen by UCSF Gastroenterology with existing archived specimens. This was followed by obtaining written informed consent and approval. Baseline demographic and clinical information about the study participants are provided in **Supplementary Table 1**. The CosMx dataset from this cohort was previously published and re-analyzed for this study⁹. Xenium and MERSCOPE analyses were acquired for this study as detailed below. We have consent to publish de-identified patient demographics including age at the time of sample collection, sex, diagnosis, and medical center. Demographic options were defined by the investigators, and participants chose their classifications. Biopsy samples were categorized based on the level of inflammation observed endoscopically: non-inflamed (score=0), mildly inflamed (score=1), moderately inflamed (score=2), or severely inflamed (score=3). Samples were assigned unique identifiers before biobanking.

Histology FFPE tissue microarray (TMA) construction

Tissue microarrays were constructed from FFPE blocks by Pantomics, with 1.1–1.5 mm cores. The IBD TMA contained multiple cores from 9 prospectively-collected HC and 11 retrospectively-retrieved UC patients. For UC patients, cores were obtained both before and after treatment with Vedolizumab. Core areas were selected based on individual H&E staining of each block, with representative areas chosen per core. Core samples from the same patients had at least duplicate cores from different locations, although some cores were not within the fiducials and final scanned area. The recipient TMA block was sectioned with a clearance angle of 10° and a thickness of 4 µm along the width of the block and was used for H&E staining. The TMA block was stored at 4 °C. Freshly cut TMA sections were prepared before each experiment, according to the recommended protocol for each spatial transcriptomic assay performed.

CosMx spatial transcriptomics tissue processing, staining, and imaging

FFPE TMA processing, staining, imaging, and cell segmentation were performed as previously described and published^{24,9}. The time from sectioning to CosMx SMI analysis was 9 days. For this analysis, the raw data files were re-loaded into our preprocessing and technical performance comparison Jupyter notebooks to ensure consistent analysis across spatial transcriptomics platforms.

Xenium spatial transcriptomics tissue processing, staining, and imaging

Xenium sections were prepared following the Xenium “In Situ- Tissue Preparation Guide protocol” (10X Genomics, Demonstrated Protocol, CG000578-Rev C). Briefly, 4 µm sections of the FFPE TMA block were sectioned, and shortly kept afloat in an RNase-free water bath at 42°C. They were then carefully transferred from the water bath to the marked sample area of the Xenium slide (PN-1000460). To remove excess of water, the slides were placed upright in a drying rack at room temperature for 30 minutes and then baked for 3 hours at 42°C. Thereafter, the slides were stored in a vacuum-sealed bag at room temperature until they were ready

for processing. The time from sectioning to Xenium analysis was 2 days for replicate 1 and 9 days for replicate 2. The Xenium slides were processed at UCSF according to the Xenium “In Situ for FFPE-Deparaffinization and Decrosslinking protocol” (10X Genomics, CG000580-Rev C). The slides were incubated at 60°C for 2 hours and then cooled down at room temperature for 7 minutes. After cooling, the slides were immersed first in xylene, then ethanol, and lastly, nuclease-free water to deparaffinize and rehydrate the tissue. Post rehydration, slides were assembled into the Xenium cassette (10X Genomics, PN-1000566) and the tissue sections were decrosslinked using the Xenium Slides and Sample Prep Reagents Kit (10X Genomics, PN-1000460). Decrosslinking involved a thermocycler incubation at 80°C for 30 minutes and then 22°C for 10 minutes with the decrosslinking buffer. The slides were washed multiple times with PBS-T and, subsequently, were hybridized following the Xenium “In Situ Gene Expression User Guide” (10X Genomics, CG000582 Rev D). Tissue slides were incubated at 50°C overnight with a customized gene panel, which included 290 genes (**Supplementary Table 2**). The next day, unbound probes were removed by washes with PBS-T and a thermocycler incubation at 37°C for 30 minutes with the post-hybridization wash buffer. After the removal of unbound probes, the junction between the RNA with its hybridized probes was ligated using the ligation mix in the thermocycler at 37°C for 2 hours. The probe-RNA product was then amplified at 30°C for 2 hours with the Amplification Master Mix to generate multiple gene-specific barcodes. Post amplification, the slides were washed and quenched with autofluorescence quencher to reduce signal noise. Lastly, before loading the Xenium cassette in the machine, nuclei were stained with DAPI. Xenium slides were imaged using the Xenium Analyzer following the guidelines provided in the Xenium Analyzer User Guide (10X Genomics, CG000584-RevB). The decoding modules A and B were transferred from 20°C to 4°C a night prior to the instrument run. On the day of the instrument run, first, the buffers (Wash Buffer A, Wash Buffer B, Xenium Instrument Wash Buffer, and Xenium Probe Removal Buffer) were prepared and loaded into the machine. Then, the decoding reagent plates, pipette tip rack, extraction tip, and the wetting consumable were loaded. Lastly, the Xenium cassettes containing the slides were loaded into the Xenium Controller machine. After successful loading, the machine took about an hour for a sample scan. From the output of the scan on the machine screen, we selected FOVs containing the tissue cores and started the run. Nucleus boundaries were identified using a nucleus segmentation algorithm applied to the nuclei-stained (DAPI) morphology image, and cell boundaries were determined by expanding the nucleus boundaries by 5 μm or until they intersected with another cell. The cell-specific and transcript-specific metadata, found in the cell summary and transcript output files, respectively, included several cell segmentation-related metrics: cell area (μm^2) and nucleus area (μm^2) for cells, and overlap with the nucleus (yes/no options) and nucleus distance (μm) for transcripts. After the Xenium run was completed, all data were stored in an organized output directory on the Xenium instrument. Data were downloaded and we used the cell summary file (cells.csv.gz) and the cell-feature matrix file (cell_feature_matrix.h5), which included the x and y coordinates for each individual cell. The transcript file (transcripts.csv) was used for the QC transcript-level comparisons.

MERSCOPE spatial transcriptomics tissue processing, and staining

MERSCOPE slides were prepared according to “MERSCOPE User Guide-Formalin-Fixed Paraffin-Embedded Tissue Sample Preparation” (91600112 Rev C). Briefly, 4 μm sections of the FFPE TMA block were sectioned, and placed onto the center of the MERSCOPE FFPE slide (PN 20400100). Then, slides were transferred to a drying rack to remove excess water. Slides were dried at 55°C for 15 minutes and then at room temperature until no visible water droplets were present. Dry slides were stored in a 60-mm petri dish and sealed with parafilm at -20°C until further processing. The slides were processed within 6 weeks of sectioning. Before running the samples with the full gene panel, one of the MERSCOPE slides was used to run sample verification kit (91600004 Rev D), targeting a housekeeping gene *EEF2* in *Homo sapiens* to verify RNA quality, assess background noise, and optimize protocol conditions. The assay using the full customized gene panel was then conducted. The MERSCOPE slide was equilibrated to room temperature for 30 minutes and underwent deparaffinization and decrosslinking steps. Subsequently, a pre-anchoring treatment (PN 20300116; PN 202300113) was performed at 37°C for 2 hours, followed by a cell boundary staining (PN20300100) with a primary staining solution at room temperature for 1 hour. Then, the MERSCOPE slide was washed three times with 1X PBS and incubated with a secondary staining solution at room temperature for 1 hour. After this step, samples were incubated with formamide wash buffer (PN 20300002) at 37°C for 30 minutes and subsequently incubated with RNA anchoring buffer (PN 20300117) at 37°C overnight. Following overnight incubation, another formamide wash was conducted at 47°C for 15 minutes and the slide was washed before proceeding to the gel embedding step (PN 30200004). For resistant FFPE tissues, a digestion step (PN 20300005) was performed at 37°C for 5 hours before incubation in clearing solution (PN 20300114) for 13 days at 37°C to ensure tissue transparency, instead of the recommended 7 days in clearing solution, based on guidance from the manufacturer. Tissue transparency was never fully achieved. Consequently, MERSCOPE slides underwent autofluorescence quenching using MERSCOPE photobleacher (PN 10100003). Next, clearing solution was removed and slides were washed and incubated with formamide wash buffer at 37°C for 30 minutes before incubating with the customized 280-plex gene panel (**Supplementary Table 2**) in a humidified 37°C cell culture incubator for at least 36 hours. Finally, a post-encoding probe hybridization wash was completed through two incubations with formamide wash buffer at 47°C for 30 minutes each. Then, the slide was washed twice with sample wash buffer and incubated with DAPI and PolyT staining reagents at room temperature for 15 minutes. The slide was then assembled into MERSCOPE flow chamber and loaded on the MERSCOPE instrument for imaging following the User guide (91600001 Rev G) for proper configuration and data acquisition. Segmentation parameters were selected and image processing was run using the Cellpose segmentation algorithm to produce single-cell outputs²⁵. The cell-feature matrix file (`cell_by_gene.csv`), cell metadata file (`cell_metadata.csv`), and cell and transcript location information file (`micron_to_mosaic_pixel_transform.csv`) were used for our data processing analysis.

Technical performance comparisons among spatial transcriptomics platforms

Our technical QC comparison between Xenium and CosMx platforms utilized transcript data, filtered to only include high-quality transcripts that passed platform-specific filters (Xenium platform phred-scaled quality value

(Q-Score) > 20; All CosMx QC flags = 'Pass') and our cell-level filtering schema, which included filtering out cells with <50 counts and <10 genes and filtering out genes with <1 count and detected in <10 cells.

The sources of the data values used for various QC comparisons are detailed below. To quantify cellular location classification for transcripts, we used the Xenium transcript metadata 'Overlaps Nucleus' metric (yes/no options) and the CosMx transcript metadata 'Cellular Compartment' metric (0, cytoplasm, membrane, and nuclear options). Post-filtering, we had 0 transcripts with 0 values. For the cellular location classification plot, we grouped cells as nuclear and non-nuclear for both platforms. Cell area was compared across platforms using μm^2 values. For Xenium, the cell area values were already provided in μm^2 . However, for CosMx, the cell area values were initially in pixels and were converted to μm^2 by multiplying each pixel value by 0.0144, as 1 pixel equals 0.12 μm . Negative probes per cell were quantified using the 'Control Probe Counts' cell metadata column in Xenium and 'nCount NegProbes' cell metadata column in CosMx. Signal over background metrics were calculated by dividing the mean expression of each gene within cells by the mean negative probe counts per cell. Block age was measured from the time of tissue collection until the assay was conducted. As a specificity measure, we calculated mutually exclusive co-expression rate (MECR) values for each dataset²². We used lineage-specific genes that are highly expressed in our cell types of interest within the Xenium, CosMx, and our previous scRNA-seq dataset performed on colon biopsies collected from HC and UC patients (GSE250487). Ideally, these lineage-specific genes should only be expressed within their corresponding cell types. The MECR metric quantifies the detected co-expression rate of two lineage-specific genes in individual cells, normalized for the abundance of each gene. MECR values were calculated for each gene pair by dividing the fraction of cells that express both markers by the fraction of cells that express at least one of the markers.

Data preprocessing and annotation

We developed and optimized a standard preprocessing pipeline using the Python packages scanpy, squidpy, and anndata, tailored for use with CosMx, Xenium, and MERSCOPE data^{26,27}. We created spatial data objects in Python for each data type using cell-level gene expression, metadata, and spatial location information. Low quality transcripts (as qualified by a Q-score < 20) were automatically removed from the Xenium cell-level data before processing steps. For the CosMx and Xenium data, we filtered out cells with <50 counts and <10 genes and genes with <1 count and detected in <10 cells. As the MERSCOPE dataset had very few cells passing QC, we tweaked our filtering schema to remove cells with <10 counts instead of <50 counts. The other filtering criteria remained the same. After filtering, we proceeded to normalize and log-transform the data and regress out unwanted sources of variation, specifically the number of transcripts per cell and the number of unique (gene) transcripts per cell. Next, we scaled the data and ran a Principal Component Analysis (PCA). We computed a neighborhood graph using $n_neighbors=10$ and $n_pcs=30$ (CosMx, Xenium) or $n_pcs=14$ (MERSCOPE). We embedded the neighborhood graph using UMAP, specifying $min_dist=0.2$ and $spread=1.5$ (CosMx, MERSCOPE) or $spread=1.75$ (Xenium), and clustered using Leiden community detection. We annotated cell clusters by known markers and spatial location, using the Chan-Zuckerberg CELLxGENE tool for refinement^{28,29}. The CosMx and Xenium datasets were processed with the same pipeline and settings, as noted above. For the

Xenium dataset, some Leiden clusters were further divided based on readily apparent, distinct landmark gene expression within subclusters. Cluster 07 was subdivided into neutrophils and monocytes, and the remaining cells expressed high levels of *BANK1*, *IGHD*, *MS4A1*, and *CD19* and were combined with the B cell clusters 11 and 16. Cluster 02 and 22 were combined into a coarse endothelial cluster, and then divided into arterial, venous, lymphatic, pericytes and Not Otherwise Specified (NOS) subsets. Cluster 15 was subdivided into S3 and S4 fibroblasts. A LYVE1⁺ macrophage subcluster was annotated macrophage cluster 10. Cluster 24 was subdivided into IAF and plasma cells, and those plasma cells were combined with plasma cell clusters 0, 24, and 30.

Integrating Xenium replicates

We created spatial data objects in Python for each Xenium replicate data using cell-level gene expression, metadata, and spatial location information. We added prefixes to the cell ID values to distinguish between replicates 1 and 2 and added a 'batch' metadata column. We proceeded to filter the datasets separately based on our standard filtering schema (filtered out cells with <50 counts and <10 genes and genes with <1 count and detected in <10 cells). Next, we concatenated the two replicate anndata objects along the observations axis (x-axis; rows) using the `anndata.concat` function. This process preserves all sub-elements of each object while stacking the observations in an ordered manner. By concatenating along the observations axis, we effectively combined data from different cells (observations) into a single dataset. We then added 15,000 to the x-coordinate value of each cell in replicate 2 to offset its value from those in replicate 1. This adjustment allowed us to visualize the spatial coordinates of the concatenated dataset with replicates 1 and 2 displayed side by side rather than overlapping. After concatenating, we proceeded with the preprocessing pipeline as usual: normalization and log-transformation of the data, regressing out unwanted sources of variation, and scaling the data. We ran a Principal Component Analysis (PCA), integrated the data with Harmony³⁰ to account for potential batch effects, and constructed a neighborhood graph using `n_neighbors=10` and `n_pcs=30`. We embedded the neighborhood graph using UMAP, specifying `min_dist=0.2` and `spread=1.5`, and clustered using Leiden community detection. We annotated cell clusters by known markers and spatial location, using the Chan-Zuckerberg CELLxGENE tool for refinement.

Neighborhood enrichment

We performed neighborhood enrichment analyses for fine annotation cell clusters within the Xenium HC and UC PRE data subsets using functions from the `squidpy` package. To do this, we constructed a spatial nearest-neighbor graph using Delaunay triangulation, which links cells based on their spatial proximity to each other within a connectivity matrix. We then calculated an enrichment z-score for each pair of fine annotation cell clusters based on cell proximity within the connectivity graph. These analyses were conducted for the Xenium HC and UC PRE data subsets in two ways: (1) by calculating neighborhood enrichment z-scores for each pair of fine annotation cell clusters across the entire dataset (all cores, all patients), (**Supplemental Figure 7A-B**), and (2) by calculating neighborhood enrichment z-scores specifically for our cell types of interest, `Fibroblast_IAF`

and MNP_monocyte cell clusters, within each individual core and then grouping these z-score values for each unique patient (**Figure 5D**).

Pseudobulk DE genes analysis and Gene Set Enrichment Analysis (GSEA)

Spatial transcriptomic data were used to perform pseudobulk differential expression (DE) analysis using DESeq2³¹. Three distinct Pseudobulk DE gene analyses were conducted: CosMx data comparing UC PRE to HC, Xenium data comparing UC PRE to HC and, Xenium data comparing UC PRE Non-Responders to UC PRE Responders. Samples were stratified by patients. The bulk transcriptomic dataset (GSE73661)¹⁸, consisting of colonic biopsies from HC and UC patients before and after various biologic treatments, was obtained from the GEO database and utilized for GSEA³². For this analysis, the bulk transcriptomic samples were categorized into HC (n=12) and UC PRE (n=43), or UC PRE VDZ R (n=11) and UC PRE VDZ NR (n=9). Data were normalized and z-scored before being processed in the GSEA program (version 4.3.3). HC and UC PRE signatures were defined based on the Pseudobulk DE analysis from Xenium spatial transcriptomic data. For CosMx, only the UC PRE gene signature was identified. Gene signatures obtained from Xenium for UC PRE R, UC PRE NR, IAF-monocyte-neutrophil and GALT-B-DC-S4 fibroblast were explored in the external cohort of patients pre-VDZ stratified by UC PRE R and UC PRE NR. GSEA was then conducted for each gene signature (**Supplementary Table 7**). The number of permutations was set to 1000, with no dataset collapse, using the Affymetrix Human Gene 1.0 ST Array and t-test. For each analysis, a Normalized Enrichment Score (NES) was calculated, and only NES values with a p-value < 0.05 and an adjusted q-value (FDR) < 0.1 were considered significant.

Statistics

For the comparative analysis among different spatial transcriptomic platforms, the non-parametric method using Mann-Whitney test, two-tailed was utilized. However, for the number of transcripts and unique features per cell per core or FOV, the Kruskal-Wallis test was used to assess differences in population medians across 2-, 3-, 4-, and 5-year old samples. Cell frequencies for Xenium comparing two groups were also assessed using the Mann-Whitney test, followed by a two-stage linear step-up procedure of Benjamini, Krieger and Yekutieli, which adjusts for multiple comparisons by controlling the false discovery rate (FDR). The q-value, representing the FDR-adjusted p-value, was set for discovery at $q < 0.1$. For DeSeq2 analysis, significance thresholds were defined as $\log_2fc > 0.4$ or < -0.4 and $q < 0.1$ and counts threshold of baseMean >500 for Xenium and >400 for CosMx (**Supplementary Table 4-6**). Additional statistical analyses were performed using GraphPad PRISM 10. The ComplexHeatmap R package was used to generate expression z-score heatmaps for DE genes.

Acknowledgements

MGK is supported by NIH K08 DK123202. MGK holds a Career Award for Medical Scientists from the Burroughs Wellcome Fund. GKF is supported by NIH U01DE028891-01A1, R01AI093615-11, R01DK103735, P30AR070155-05, U01AI168390, R01AI170239, P30 AI027763-31, R01DE032033, and support from the Chan Zuckerberg Initiative, the Bill and Melinda Gates Foundation, Eli Lilly, and the UCSF Bakar ImmunoX Initiative.

AJC is supported by NIH U01DE028891-01A1, R35CA242447-03, R01HL170038-01 and support from the Melanoma Research Alliance, the California Institute for Regenerative Medicine, Genentech, Eli Lilly, and the UCSF Bakar ImmunoX Initiative. This work was also supported by funding from UCSF ImmunoX and the Kenneth Rainin Foundation. Schematics created with BioRender.com. We also acknowledge the Research Core of the UCSF Division of Hospital Medicine. We thank Dr Peng He for his critical feedback on the manuscript. We would also like to acknowledge the valuable contributions from members of the UCSF CoLabs Spatial Transcriptomics Working Group. We thank the study participants for contributing to this research.

Author contribution statement

Conceptualization: GKF, MGK, AJC; patient recruitment and sample collection: GL, JH, UM, DYO, MGK; sample processing and data acquisition: EM, VJ, CE, GL, JT, JH, WE; cell subset annotation: EM, GL, DEL, JYH; spatial transcriptomics analysis: EM, ML; supervision: GKF, MGK, AJC; funding acquisition: GKF, MGK, AJC; all authors contributed to manuscript preparation.

Competing interests statement

The Kattah, Combes and Fragiadakis lab receive research support from Eli Lilly for work unrelated to this manuscript. The Combes lab receive research support from Genentech for work unrelated to this manuscript. MGK is a member of the scientific advisory boards of Santa Ana Bio and Switchback Therapeutics and has received consulting fees from Cellarity, Spyre Therapeutics, Morphic Therapeutic, Sonoma Biotherapeutics, and Surrozen. AJC is a member of the scientific advisory board of Foundry innovations and has received consulting fees from Survey Genomics. UM is a consultant for Abbvie, Janssen, Takeda, Pfizer, BMS, Gilead, Enveda, Lilly, Merck, Rani Therapeutics, Celltrion, Abivax and received grant support from Leona and Harry Helmsley Charitable Trust. DYO has received research support from Merck, PACT Pharma, the Parker Institute for Cancer Immunotherapy, Poseida Therapeutics, TCR2 Therapeutics, Roche/Genentech, and Nutcracker Therapeutics; travel and accommodations from Roche/Genentech and Poseida Therapeutics; and has consulted for Revelation Partners.

FIGURE LEGENDS

Fig. 1| Schematic of study design and technical performance comparison between Xenium and CosMx platforms. (A) Schematic of study design. Created with BioRender.com (B,C) Number of (B) transcripts and (C) unique features detected per cell within the Xenium and CosMx datasets, calculated using the complete gene panel for each platform (Xenium, 290 genes; CosMx, 1,000 genes; left) and limited to the 159 overlapping genes across both panels (right). (D) Number of negative probes detected per cell within the Xenium and CosMx (Xenium mean=0.03 and CosMx mean=0.37). (E) Correlation between average transcript counts in Xenium and CosMx for the 159 overlapping genes. (F,G) Number of (F) transcripts and (G) unique features detected per cell per core or FOV within the Xenium and CosMx datasets split by prospectively collected HC and retrospectively collected UC. For panels B, C, D, F and G box and whisker plots, the band indicates the median, the box indicates

the first and third quartiles, and the whiskers indicate minimum and maximum value within the upper/lower fence (upper fence= $Q3+1.5 \times IQR$ and lower fence= $Q1-1.5 \times IQR$), only outlier points are shown. Mann-Whitney, two-tailed tests, p-values are indicated.

Fig. 2| Cell type recovery across spatial transcriptomics platforms. (A,B) UMAP visualization of Xenium dataset (313,940 cells), colored by coarse (A) and fine (B) annotations. (C) Heatmap displaying gene expression of the top 5 landmark genes for each coarse annotation cell type within the Xenium dataset. (D) Correlation matrix displaying the correlation between coarse annotation cell types identified for Xenium. (E,F) UMAP visualization of CosMx dataset (126,368 cells), colored by coarse (E) and fine (F) annotations. (G) Heatmap displaying gene expression of the top 5 landmark genes for each coarse annotation cell type within the CosMx dataset. (H) Correlation matrix displaying the correlation between coarse annotation cell types identified for CosMx. (I) Stacked bar plots for coarse annotation displaying cell frequency (percent of total) for Xenium and CosMx.

Fig. 3| Pseudobulk DE gene analysis comparing UC PRE versus HC in both platforms and gene set enrichment analysis (GSEA) of an external, publicly available, bulk transcriptomic dataset using Xenium transcriptomic signatures. (A) Volcano plot of pseudobulk DE genes identified by DESeq2 with $\log_2fc > 0.4$ or < -0.4 and $q < 0.1$ in UC PRE vs HC for Xenium dataset. (B) Volcano plot of pseudobulk DE genes identified by DESeq2 with $\log_2fc > 0.4$ or < -0.4 and $q < 0.1$ in UC PRE vs HC for CosMx dataset. (C) Heatmap of expression z-scores for the indicated genes in UC PRE (Up/Down) relative to HC for Xenium dataset. (D) Heatmap of expression z-scores for the indicated genes in UC PRE (Up/Down) relative to HC for CosMx dataset. (E) Number of pseudobulk DE genes in the indicated platform with $\log_2fc > 0.4$ or < -0.4 in UC PRE relative to HC identified by DESeq2 analysis. (F) Volcano plot of significant overlapping genes identified by DESeq2 with $\log_2fc > 0.4$ or < -0.4 for Xenium and CosMx; genes are color coded (green, significant in both panels; blue, significant in Xenium panel only; orange, significant in CosMx panel only). (G) GSEA of Xenium HC and UC PRE spatial gene signatures in an external cohort of patients and relative Normalized Enrichment Scores (NES). (H) Representative spatial transcript scatter plots highlighting a subset of genes relatively increased in HC and UC PRE in Xenium dataset. For panels B and D, some genes are off-scale for visualization purposes, z-score set from -1 to 1.

Fig. 4| Xenium enabled identification and spatial localization of distinct fibroblast subsets in colon mucosal biopsies and identified increased myeloid and stromal cell subsets in UC. (A) Dot plot representation of landmark genes for the indicated subsets. (B) Transcriptionally distinct fibroblast subsets identified by relative spatial localization in colon tissue from representative cores for the indicated cell subsets.

Fig. 5| Neighborhood enrichment analysis of Xenium dataset reveals higher proximity of IAFs and monocytes in UC PRE biopsies. (A,B) Heatmaps displaying neighborhood enrichment z-scores for fine

annotation cell pairs within (A) HC and (B) UC PRE biopsies. Spatial enrichment of IAFs cells to all other cell types in (C) HC and (D) UC PRE biopsies. (E) Violin plots comparing the spatial enrichment of IAFs and monocytes by patient, each dot represents a core; nd, not defined. (F) Spatial scatter plot of representative cores highlighting IAF, crypt top (CT) colonocytes, and monocytes in HC and UC PRE biopsies. For panel E, Mann-Whitney test, p-value is indicated. For panels A and B, several values exceed the scale for visualization purposes and are denoted by a white asterisk.

Supplemental Fig. 1| MERSCOPE dataset analysis. (A,B) UMAP visualization of MERSCOPE dataset (212 cells), highlighting (A) transcript count per cell, (B) number of genes per cell, and (C) area of TMA scanned showing DAPI and detected transcripts (D) spatial scatter plot depicting the spatial location of cells in the MERSCOPE dataset in relation to the TMA slide, colored based on leiden clustering.

Supplemental Fig. 2| Xenium and CosMx dataset quality control and cell segmentation-related metrics.

(A) Bar plot comparing the percentage of nuclear versus non-nuclear transcripts within the Xenium and CosMx datasets. (B) Cell area plotted in μm^2 for each cell within the Xenium and CosMx dataset. (C) Representative Xenium cell segmentation visualization, displaying DAPI nuclei (white), nuclei outlines (red), cell borders (black), cells are pseudocolored by Xenium fine annotation labels. (D) Scatter plot of average transcript count per cell for genes specific to either the Xenium or CosMx (blue for Xenium, and orange for CosMx). (E,F) Number of (E) transcripts and (F) unique features detected per cell per Core or FOV within the Xenium and CosMx datasets, calculated using the complete gene panel for each platform (Xenium, 290 genes; CosMx, 1,000 genes; left) and limited to the 159 overlapping genes across both panels (right). Plotted points are categorized based on the age of FFPE blocks from which they originated. For panels B, E, and F, box and whisker plots, the band indicates the median, the box indicates the first and third quartiles, and the whiskers indicate minimum and maximum value within the upper/lower fence (upper fence= $Q3+1.5 \times IQR$ and lower fence= $Q1-1.5 \times IQR$), only outlier points are shown; Mann-Whitney, two-tailed tests. Panels E and F compared the difference in population medians between 2-, 3-, 4-, and 5-year-old samples, averaged by core or FOV, with Kruskal-Wallis rank sum statistic (h-statistic) indicated.

Supplemental Fig. 3| Using mutually exclusive genes to evaluate platform specificity. (A-C) Scatter plots of gene expression level (transcript counts per cell) for two representative mutually exclusive lineage-specific genes within (A) Xenium, (B) CosMx, and (C) scRNA-seq datasets generated from colon biopsies collected from HC and UC patients (GSE250487). Genes were selected based on cell types of interest and the overlapping genes between Xenium and CosMx panels. The mutually exclusive co-expression rate (MECR) value is listed for each scatter plot, with lower rates corresponding to greater technology specificity.

Supplemental Fig. 4| Reproducibility of Xenium replicates. (A) Scatter plot showing the gene expression level (transcript counts per cell) for all genes between Xenium replicates. (B) Cell frequency as a percent of

dataset total for fine annotations within Xenium replicates. **(C)** UMAP visualization of two integrated Xenium replicate runs, colored by fine annotations (582,188 total cells: 313,940 from replicate 1 and 268,248 from replicate 2). Xenium replicate data were obtained from different runs of different sections from same TMA block. **Supplemental Fig. 5| Xenium dataset landmark gene heatmap and correlation matrix for fine annotations, and DEGs between UC and HC.** **(A,B)** Fine cell annotation **(A)** heatmap displaying gene expression of the top 3 landmark genes and **(B)** correlation matrix in Xenium replicate 1. **(C)** Dot plot representation of a subset of genes from pseudobulk DEG analysis by coarse annotations.

Supplemental Fig. 6| GSEA of an external, publicly-available, bulk transcriptomic dataset using a CosMx transcriptomic signature associated with UC PRE biopsies. **(A)** GSEA of CosMx UC PRE spatial gene signature in an external cohort of patients and relative NES. **(B)** Number of DE genes in the UC PRE signature for Xenium and CosMx that are concordantly or discordantly expressed to the UC PRE patients from the publicly available dataset.

Supplemental Fig. 7| Quantitation of differential cell abundance in the Xenium integrated dataset. Cell frequencies of the indicated subsets comparing HC and UC PRE, each dot represents one patient; Mann–Whitney, two-tailed test with FDR correction; $q < 0.1$ threshold for discovery. Only statistically significant cell subsets are shown with exact p-value and q-value displayed.

Supplemental Fig. 8| Unsupervised Neighborhood enrichment analysis in Xenium FFPE colon biopsies and dot plot of neutrophil versus monocyte landmark genes. **(A,B)** Heatmaps displaying neighborhood enrichment z-scores for fine annotation cell pairs within **(A)** HC and **(B)** UC PRE biopsies. **(C)** Dot plot representation of landmark genes for the indicated subsets. For panels **A** and **B**, several values exceed the scale for visualization purposes (values greater than 200)..

Supplemental Fig. 9| Pseudobulk DE gene analysis comparing UC PRE Non-Responders (UC PRE NR) versus UC PRE Responders (UC PRE R) in the Xenium dataset. **(A)** Volcano plot of pseudobulk DE genes identified by DESeq2 with $\log_2fc > 0.4$ or < -0.4 and $q < 0.1$ in UC PRE NR vs UC PRE R. **(B)** Heatmap of expression z-scores for the indicated genes in UC PRE NR (Up/Down) relative to UC PRE R. **(C)** Representative spatial transcript scatter plots highlighting a subset of genes relatively increased in UC PRE R (left) and UC PRE NR (right). **(D)** GSEA of Xenium signatures in external cohort of patients pre-VDZ stratified by UC PRE NR and UC PRE R with relative Normalized Enrichment Scores (NES) and FDR q-value. For panel **B**, some genes are off-scale for visualization purposes, z-score set from -1 to 1.

Supplementary Table 1. Baseline demographic and clinical data for study participants. Categorical variables were analyzed by Chi-square test and continuous variables were compared using one-way ANOVA with FDR

correction or Mann-Whitney test where appropriate. ns, not significant; n/a, not applicable; pre, pre-VDZ treatment; post, post-VDZ treatment. VDZ-vedolizumab.

Supplementary Table 2. Gene panels for the different spatial transcriptomic platforms.

Supplementary Table 3. Summarized QC results.

Supplementary Table 4. Pseudobulk DE gene analysis of Xenium data comparing colon biopsies in UC PRE versus HC. Significance was set as $\log_2fc > 0.4$ or < -0.4 , $p\text{-adj} < 0.1$ and $\text{baseMean} > 500$.

Supplementary Table 5. Pseudobulk DE gene analysis of CosMx data comparing colon biopsies in UC PRE versus HC. Significance was set as $\log_2fc > 0.4$ or < -0.4 , $p\text{-adj} < 0.1$ and $\text{baseMean} > 400$.

Supplementary Table 6. Pseudobulk DE gene analysis of Xenium data comparing colon biopsies in UC PRE Non-Responders versus UC PRE Responders. Significance was set as $\log_2fc > 0.4$ or < -0.4 , $p\text{-adj} < 0.1$ and $\text{baseMean} > 500$.

Supplementary Table 7. iSCST gene signatures used for Gene Set Enrichment Analysis (GSEA). Numeric ID, Affymetrix numeric probe identifier corresponding to each gene.

REFERENCES

1. Kinchen, J. *et al.* Structural Remodeling of the Human Colonic Mesenchyme in Inflammatory Bowel Disease. *Cell* **175**, 372-386.e17 (2018).
2. Parikh, K. *et al.* Colonic epithelial cell diversity in health and inflammatory bowel disease. *Nature* **567**, 49–55 (2019).
3. Boland, B. S. *et al.* Heterogeneity and clonal relationships of adaptive immune cells in ulcerative colitis revealed by single-cell analyses. *Sci. Immunol.* **5**, eabb4432 (2020).
4. Smillie, C. S. *et al.* Intra- and Inter-cellular Rewiring of the Human Colon during Ulcerative Colitis. *Cell* **178**, 714-730.e22 (2019).
5. Konnikova, L. *et al.* High-dimensional immune phenotyping and transcriptional analyses reveal robust recovery of viable human immune and epithelial cells from frozen gastrointestinal tissue. *Mucosal Immunol.* **11**, 1684–1693 (2018).
6. Martin, J. C. *et al.* Single-Cell Analysis of Crohn's Disease Lesions Identifies a Pathogenic Cellular Module Associated with Resistance to Anti-TNF Therapy. *Cell* **178**, 1493-1508.e20 (2019).
7. Mitsialis, V. *et al.* Single-Cell Analyses of Colon and Blood Reveal Distinct Immune Cell Signatures of Ulcerative Colitis and Crohn's Disease. *Gastroenterology* (2020) doi:10.1053/j.gastro.2020.04.074.
8. Friedrich, M. *et al.* IL-1-driven stromal-neutrophil interactions define a subset of patients with inflammatory bowel disease that does not respond to therapies. *Nat. Med.* **27**, 1970–1981 (2021).
9. Mennillo, E. *et al.* Single-cell and spatial multi-omics highlight effects of anti-integrin therapy across cellular compartments in ulcerative colitis. *Nat. Commun.* **15**, 1493 (2024).

10. Garrido-Trigo, A. *et al.* Macrophage and neutrophil heterogeneity at single-cell spatial resolution in human inflammatory bowel disease. *Nat. Commun.* **14**, 4506 (2023).
11. Eshghi, S. T. *et al.* Molecular characterization of response to etrolizumab and anti-TNF reveals treatment resistance in ulcerative colitis is associated with an abundance of residual neutrophil subsets and inflammatory fibroblast populations. Preprint at <https://doi.org/10.1101/2024.07.02.601267> (2024).
12. Cadinu, P. *et al.* Charting the cellular biogeography in colitis reveals fibroblast trajectories and coordinated spatial remodeling. *Cell* **187**, 2010–2028.e30 (2024).
13. Kumar, T. *et al.* A spatially resolved single-cell genomic atlas of the adult human breast. *Nature* **620**, 181–191 (2023).
14. Cervilla, S. *et al.* Comparison of spatial transcriptomics technologies across six cancer types. Preprint at <https://doi.org/10.1101/2024.05.21.593407> (2024).
15. Cook, D. P. *et al.* A Comparative Analysis of Imaging-Based Spatial Transcriptomics Platforms. Preprint at <https://doi.org/10.1101/2023.12.13.571385> (2023).
16. Wang, H. *et al.* Systematic benchmarking of imaging spatial transcriptomics platforms in FFPE tissues. Preprint at <https://doi.org/10.1101/2023.12.07.570603> (2023).
17. Janesick, A. *et al.* High resolution mapping of the tumor microenvironment using integrated single-cell, spatial and in situ analysis. *Nat. Commun.* **14**, 8353 (2023).
18. Arijis, I. *et al.* Effect of vedolizumab (anti- α 4 β 7-integrin) therapy on histological healing and mucosal gene expression in patients with UC. *Gut* **67**, 43–52 (2018).
19. Fawkner-Corbett, D. *et al.* Spatiotemporal analysis of human intestinal development at single-cell resolution. *Cell* (2021) doi:10.1016/j.cell.2020.12.016.
20. Brügger, M. D. & Basler, K. The diverse nature of intestinal fibroblasts in development, homeostasis, and disease. *Trends Cell Biol.* **33**, 834–849 (2023).
21. Canales, P. *et al.* Gut-associated lymphoid tissue attrition associates with response to anti- α 4 β 7 therapy in ulcerative colitis. *C E N C E M M U N O O G* (2024).
22. Hartman, A. & Satija, R. Comparative analysis of multiplexed in situ gene expression profiling technologies. Preprint at <https://doi.org/10.7554/eLife.96949.1> (2024).
23. Boden, E. K. *et al.* Vedolizumab Efficacy Is Associated With Decreased Intracolonic Dendritic Cells, Not Memory T Cells. *Inflamm. Bowel Dis.* **30**, 704–717 (2024).
24. He, S. *et al.* High-plex imaging of RNA and proteins at subcellular resolution in fixed tissue by spatial molecular imaging. *Nat. Biotechnol.* (2022) doi:10.1038/s41587-022-01483-z.
25. Stringer, C., Wang, T., Michaelos, M. & Pachitariu, M. Cellpose: a generalist algorithm for cellular segmentation. *Nat. Methods* **18**, 100–106 (2021).
26. Wolf, F. A., Angerer, P. & Theis, F. J. SCANPY: large-scale single-cell gene expression data analysis. *Genome Biol.* **19**, 15 (2018).
27. Palla, G. *et al.* Squidpy: a scalable framework for spatial omics analysis. *Nat. Methods* **19**, 171–178 (2022).
28. Megill, C. *et al.* cellxgene: a performant, scalable exploration platform for high dimensional sparse matrices. Preprint at <https://doi.org/10.1101/2021.04.05.438318> (2021).
29. Kim, Y.-J. *et al.* Tutorial: Guidelines for Manual Cell Type Annotation of Single-Cell Multi-Omics Datasets Using Interactive Software. <http://biorxiv.org/lookup/doi/10.1101/2023.07.11.548639> (2023) doi:10.1101/2023.07.11.548639.
30. Korsunsky, I. *et al.* Fast, sensitive and accurate integration of single-cell data with Harmony. *Nat. Methods* **16**, 1289–1296 (2019).
31. Love, M. I., Huber, W. & Anders, S. Moderated estimation of fold change and dispersion for RNA-seq data with DESeq2. *Genome Biol.* **15**, 550 (2014).
32. Subramanian, A. *et al.* Gene set enrichment analysis: A knowledge-based approach for interpreting genome-wide expression profiles. *Proc. Natl. Acad. Sci.* **102**, 15545–15550 (2005).

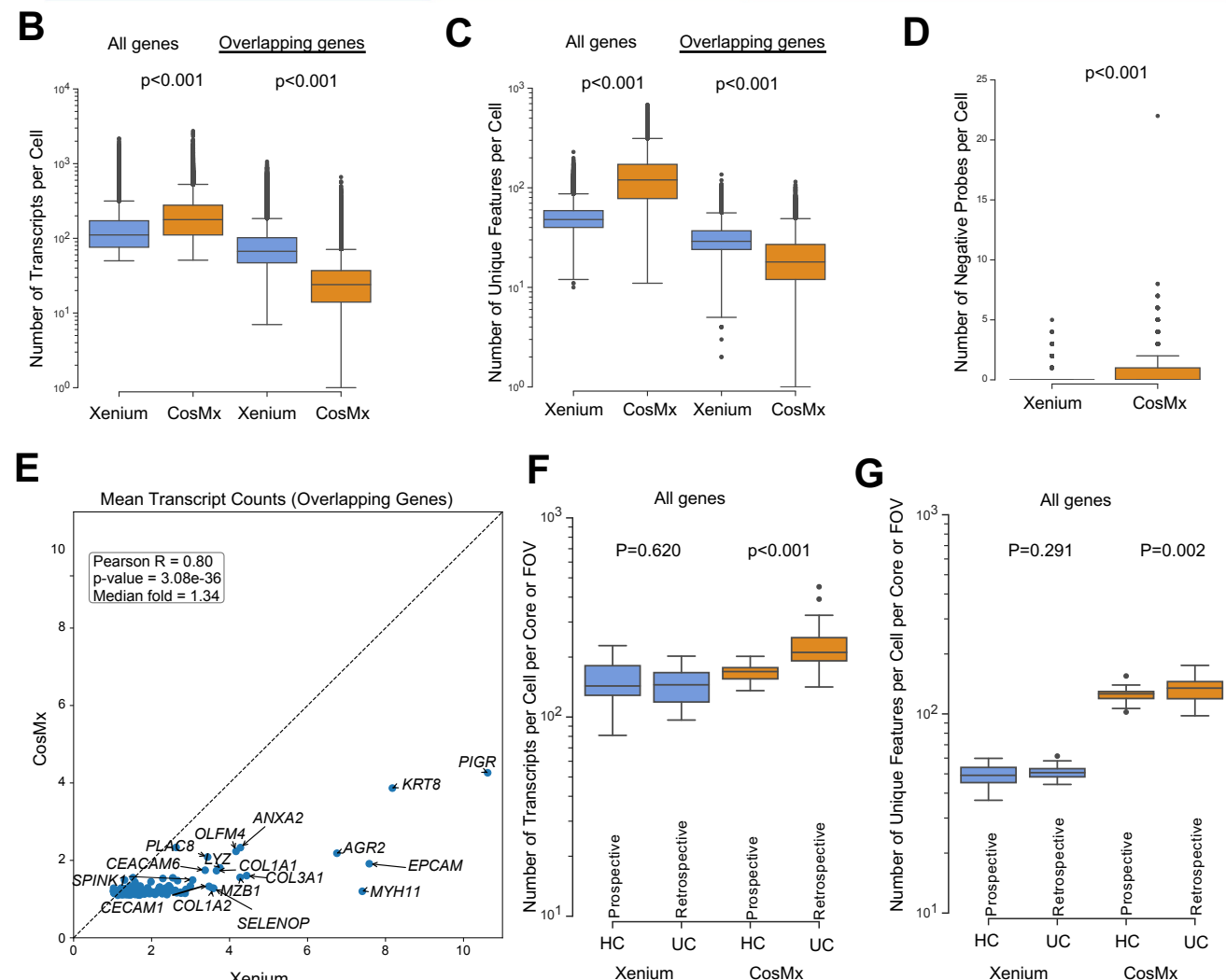
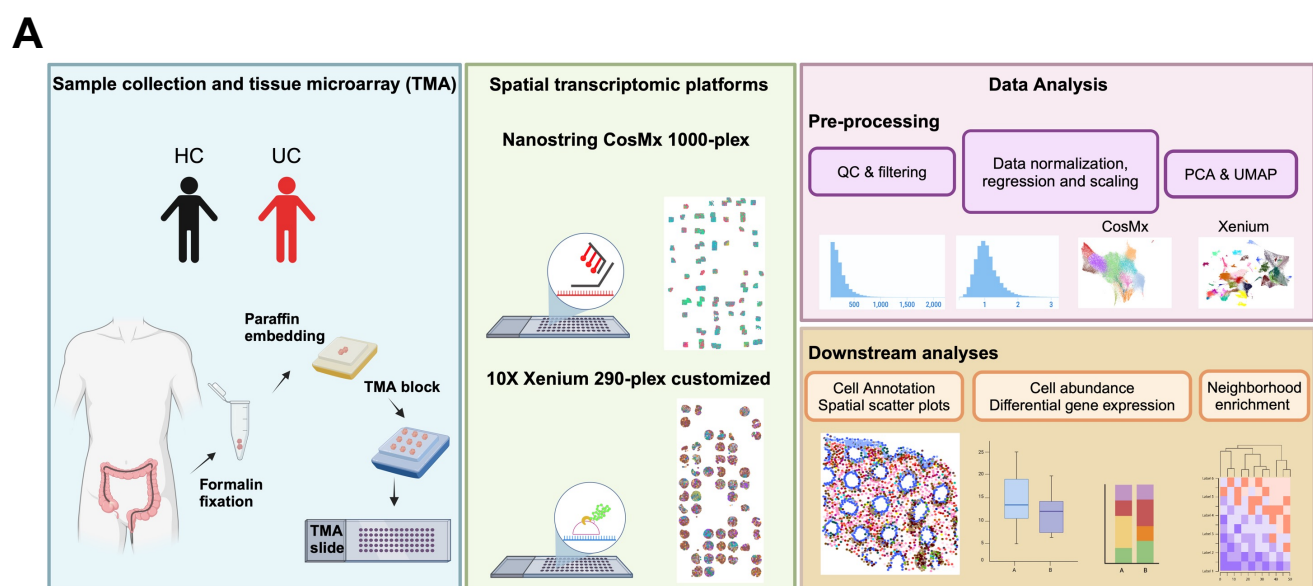


Fig. 1 | Schematic of study design and technical performance comparison between Xenium and CosMx platforms. (A) Schematic of study design. Created with BioRender.com **(B,C)** Number of **(B)** transcripts and **(C)** unique features detected per cell within the Xenium and CosMx datasets, calculated using the complete gene panel for each platform (Xenium, 290 genes; CosMx, 1,000 genes; left) and limited to the 159 overlapping genes across both panels (right). **(D)** Number of negative probes detected per cell within the Xenium and CosMx (Xenium mean=0.03 and CosMx mean=0.37). **(E)** Correlation between average transcript counts in Xenium and CosMx for the 159 overlapping genes. **(F,G)** Number of **(F)** transcripts and **(G)** unique features detected per cell per core or FOV within the Xenium and CosMx datasets split by prospectively collected HC and retrospectively collected UC. For panels **B, C, D, F** and **G** box and whisker plots, the band indicates the median, the box indicates the first and third quartiles, and the whiskers indicate minimum and maximum value within the upper/lower fence (upper fence=Q3+1.5xIQR and lower fence= Q1-1.5xIQR), only outlier points are shown. Mann-Whitney, two-tailed tests, p-values are indicated.

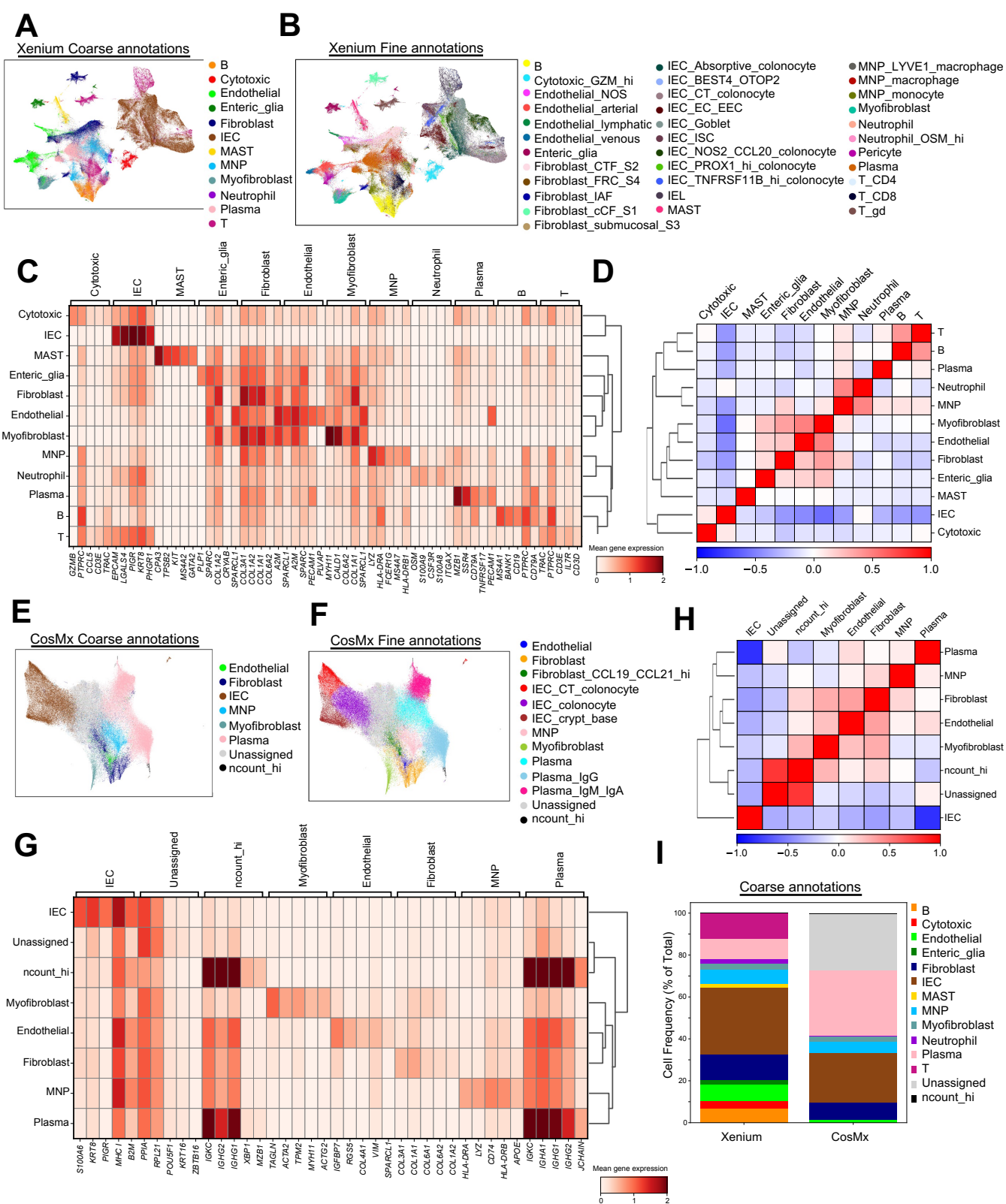


Fig. 2 | Cell type recovery across spatial transcriptomics platforms. (A,B) UMAP visualization of Xenium dataset (313,940 cells), colored by coarse (A) and fine (B) annotations. **(C)** Heatmap displaying gene expression of the top 5 landmark genes for each coarse annotation cell type within the Xenium dataset. **(D)** Correlation matrix displaying the correlation between coarse annotation cell types identified for Xenium. **(E,F)** UMAP visualization of CosMx dataset (126,368 cells), colored by coarse (E) and fine (F) annotations. **(G)** Heatmap displaying gene expression of the top 5 landmark genes for each coarse annotation cell type within the CosMx dataset. **(H)** Correlation matrix displaying the correlation between coarse annotation cell types identified for CosMx. **(I)** Stacked bar plots for coarse annotation displaying cell frequency (percent of total) for Xenium and CosMx.

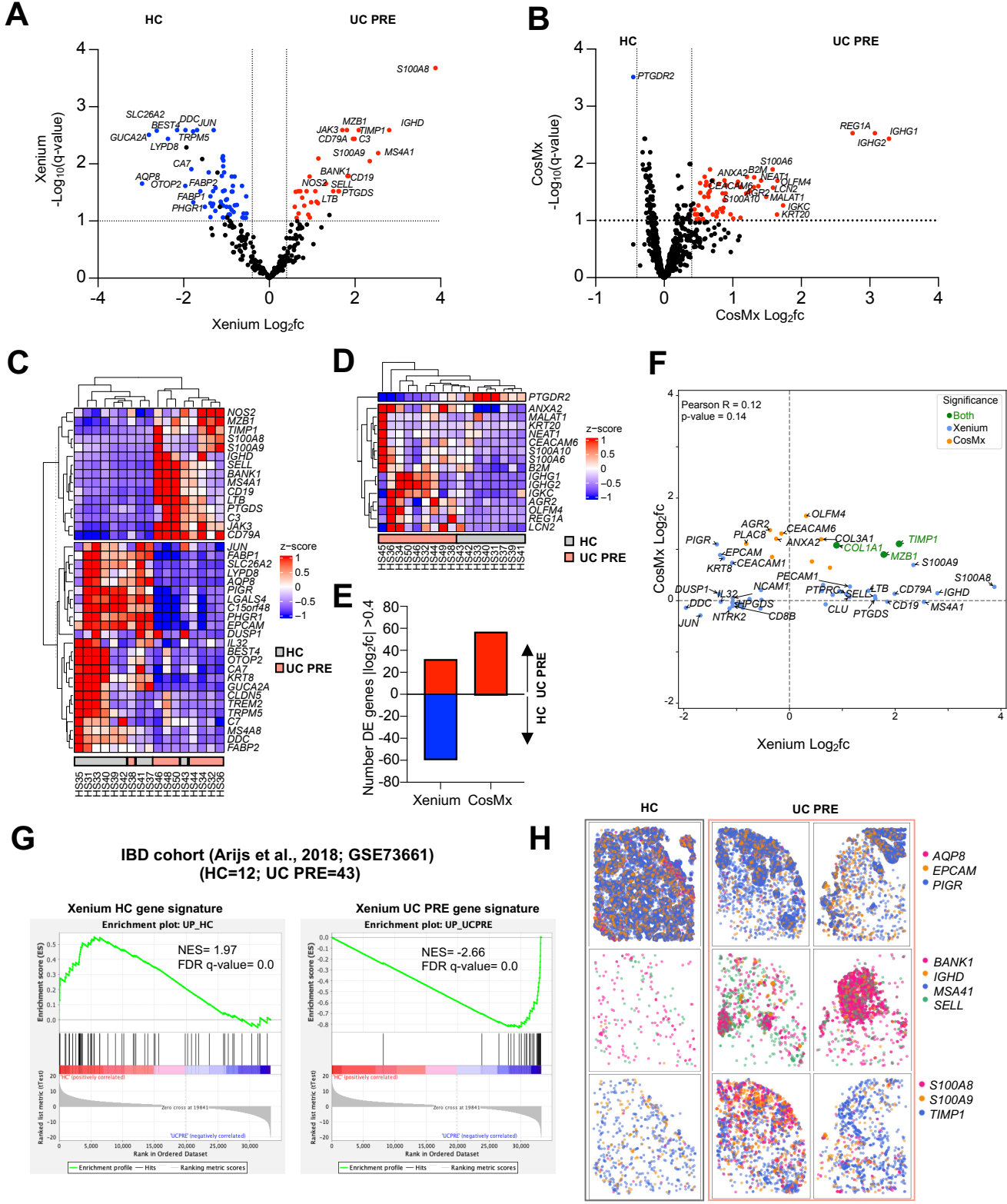


Fig. 3| Pseudobulk DE gene analysis comparing UC PRE versus HC in both platforms and gene set enrichment analysis (GSEA) of an external, publicly available, bulk transcriptomic dataset using Xenium transcriptomic signatures. (A) Volcano plot of pseudobulk DE genes identified by DESeq2 with $\log_2fc > 0.4$ or < -0.4 and $q < 0.1$ in UC PRE vs HC for Xenium dataset. **(B)** Volcano plot of pseudobulk DE genes identified by DESeq2 with $\log_2fc > 0.4$ or < -0.4 and $q < 0.1$ in UC PRE vs HC for CosMx dataset. **(C)** Heatmap of expression z-scores for the indicated genes in UC PRE (Up/Down) relative to HC for Xenium dataset. **(D)** Heatmap of expression z-scores for the indicated genes in UC PRE (Up/Down) relative to HC for CosMx dataset. **(E)** Number of pseudobulk DE genes in the indicated platform with $\log_2fc > 0.4$ or < -0.4 in UC PRE relative to HC identified by DESeq2 analysis. **(F)** Volcano plot of significant overlapping genes identified by DESeq2 with $\log_2fc > 0.4$ or < -0.4 for Xenium and CosMx; genes are color coded (green, significant in both panels; blue, significant in Xenium panel only; orange, significant in CosMx panel only). **(G)** GSEA of Xenium HC and UC PRE spatial gene signatures in an external cohort of patients and relative Normalized Enrichment Scores (NES). **(H)** Representative spatial transcript scatter plots highlighting a subset of genes relatively increased in HC and UC PRE in Xenium dataset. For panels **B** and **D**, some genes are off-scale for visualization purposes, z-score set from -1 to 1.

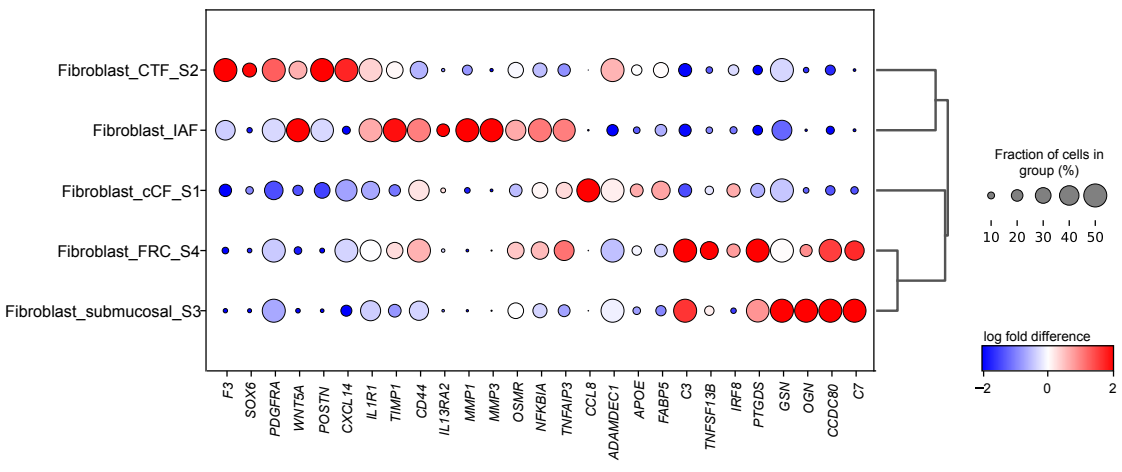
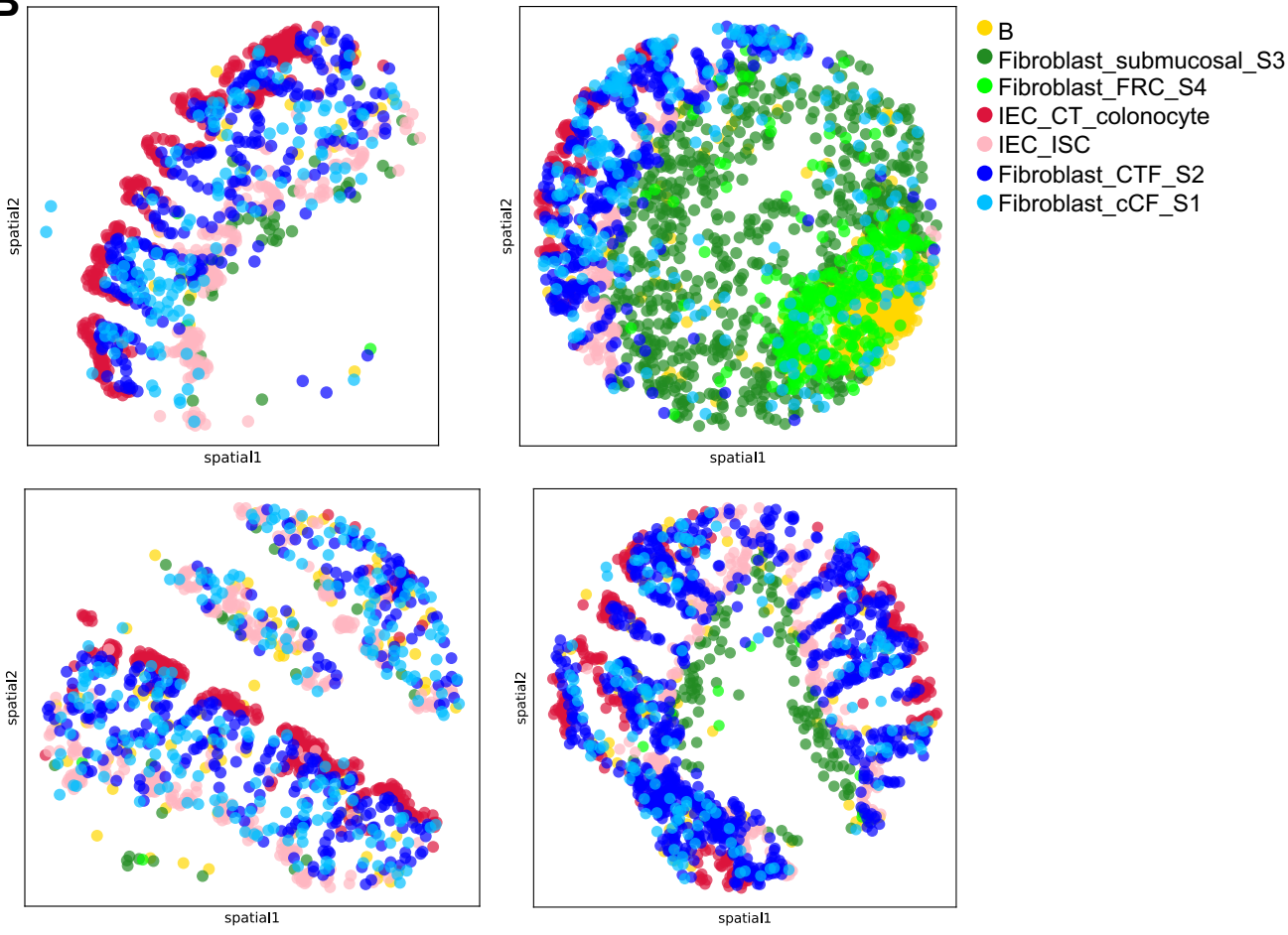
A**B**

Fig. 4| Xenium enabled identification and spatial localization of distinct fibroblast subsets in colon mucosal biopsies and identified increased myeloid and stromal cell subsets in UC. (A) Dot plot representation of landmark genes for the indicated subsets. (B) Transcriptionally distinct fibroblast subsets identified by relative spatial localization in colon tissue from representative cores for the indicated cell subsets

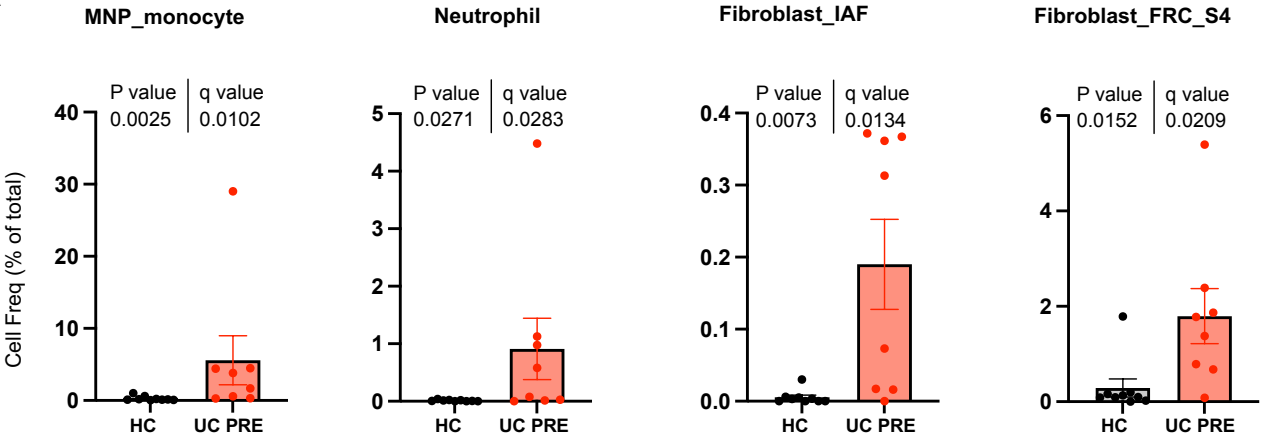
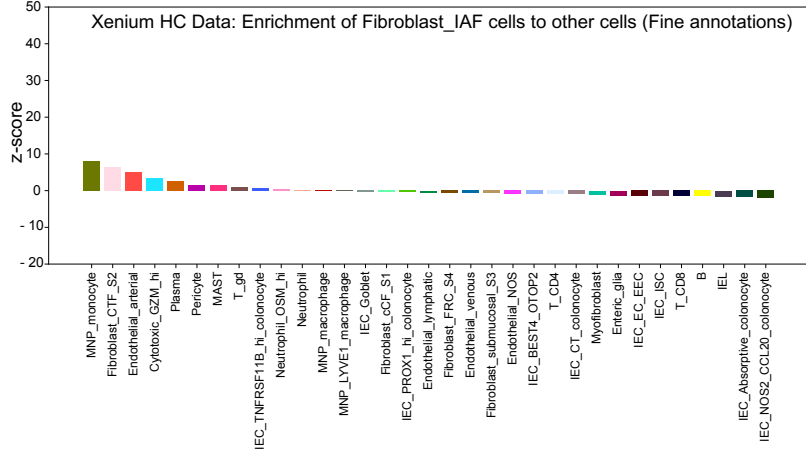
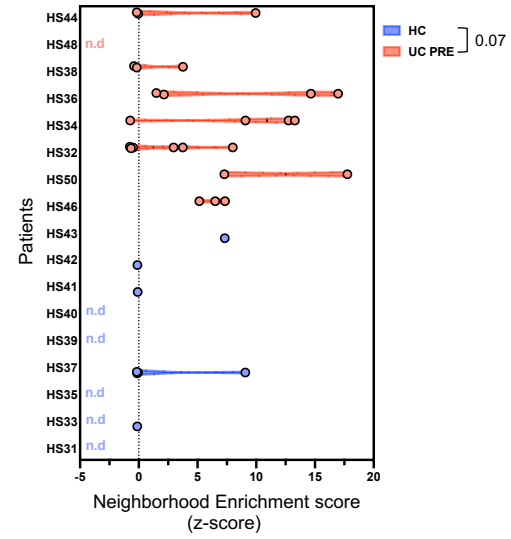
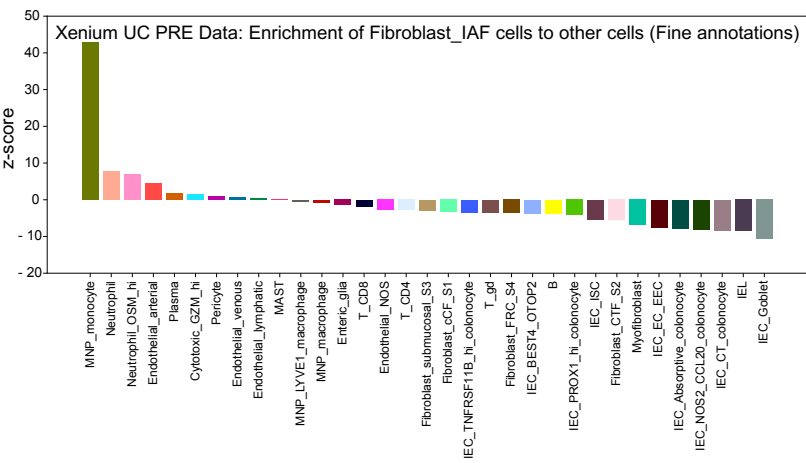
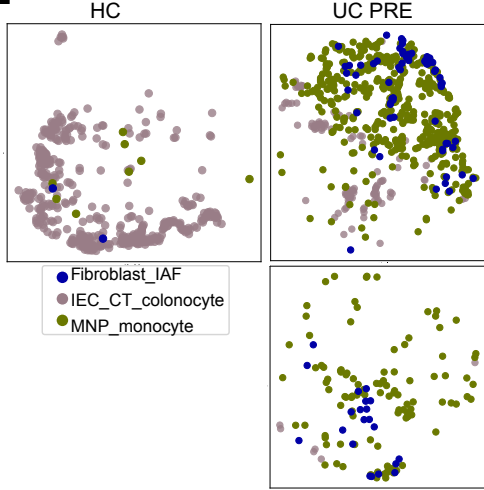
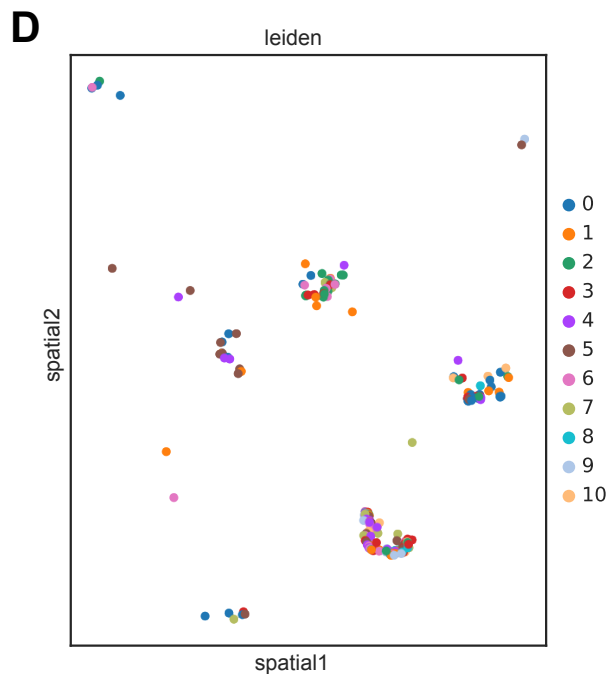
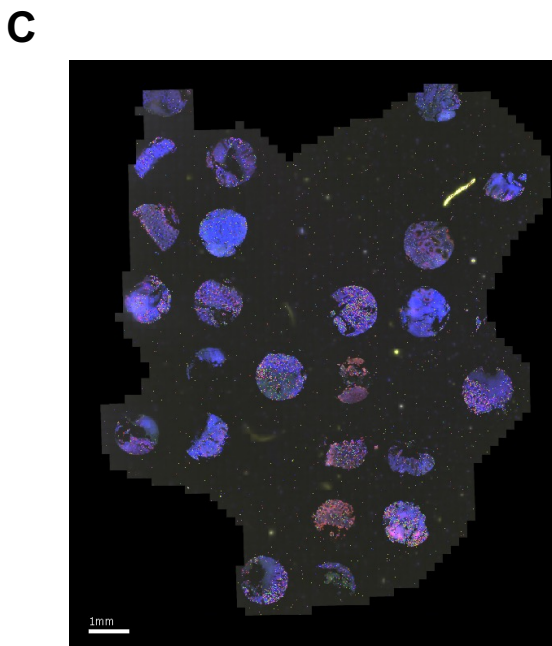
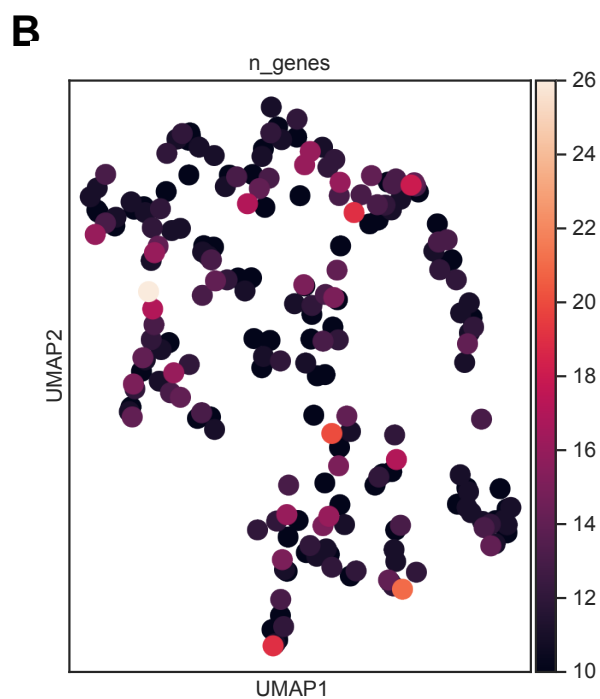
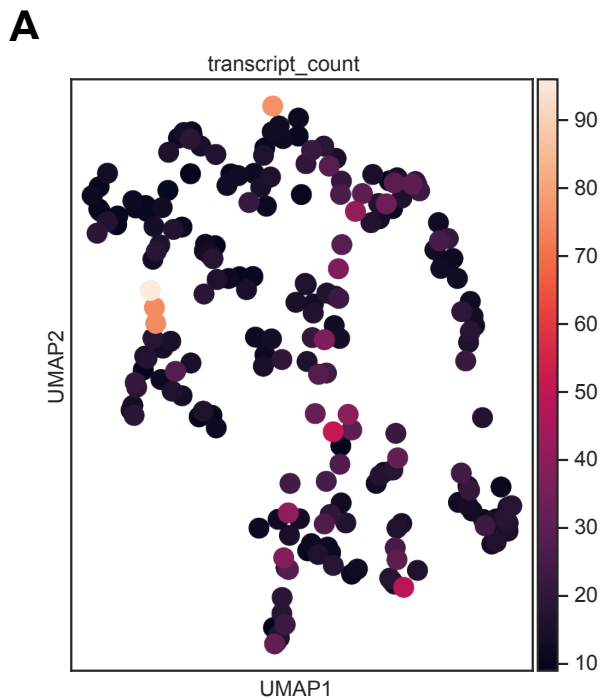
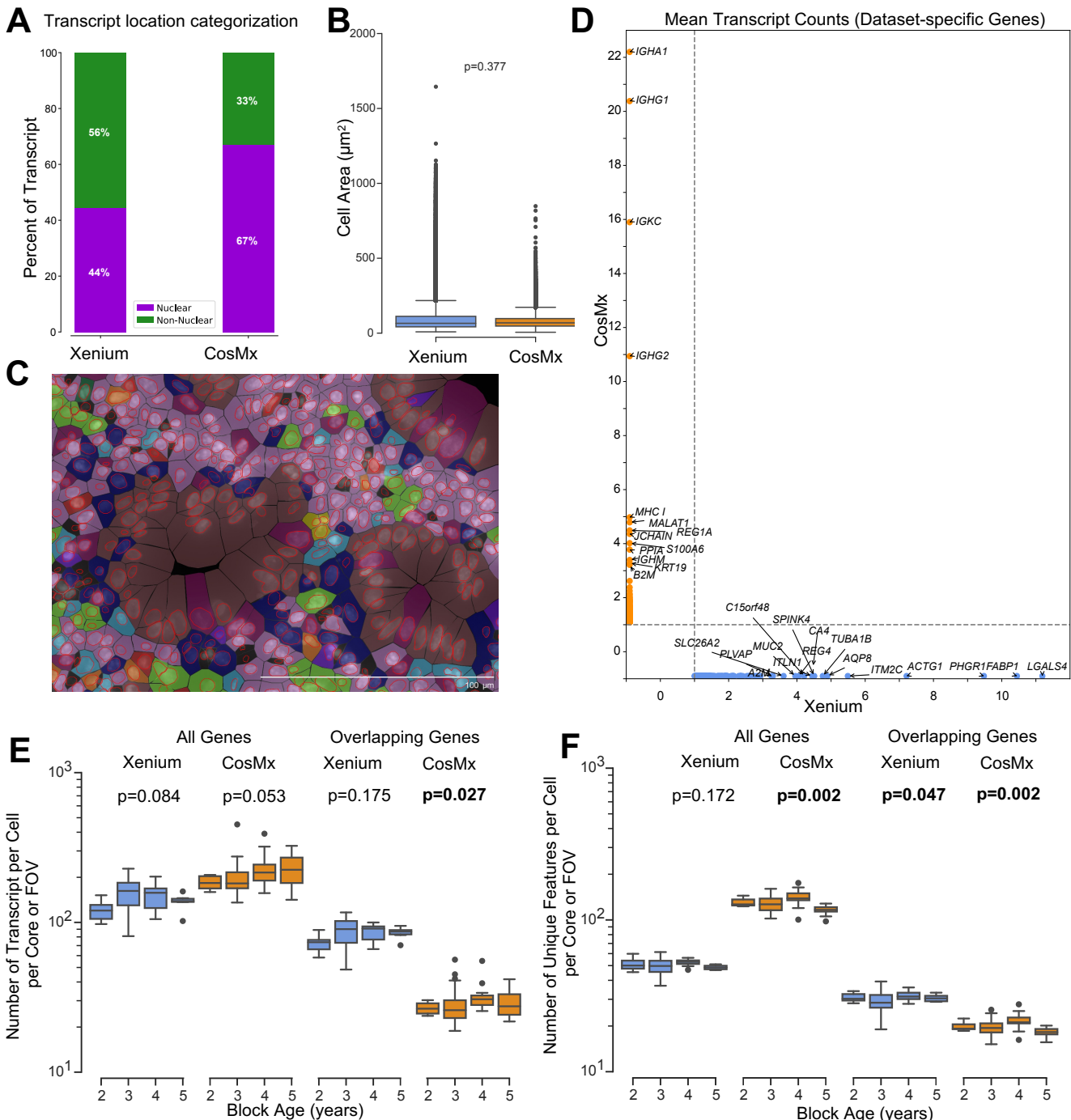
A**B****D****C****E**

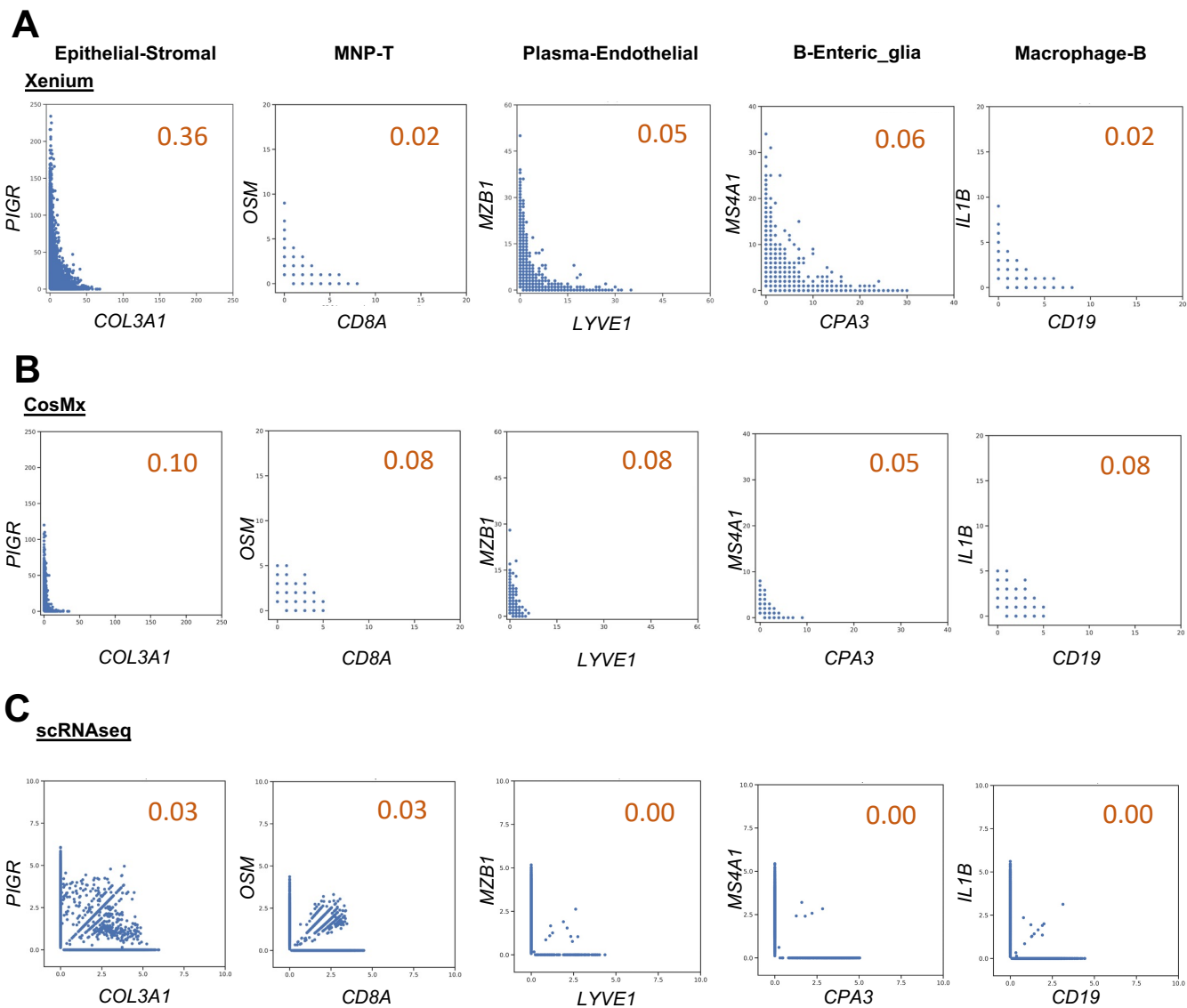
Fig. 5 | Neighborhood enrichment analysis of Xenium dataset reveals higher proximity of IAFs and monocytes in UC PRE biopsies. (A) Cell frequencies of selected subsets comparing HC and UC PRE, each dot represents one patient; Mann-Whitney, two-tailed test with FDR correction; $q < 0.1$ threshold for discovery, exact p-value and q-value are shown. Spatial enrichment of IAFs cells to all other cell types in **(B)** HC and **(C)** UC PRE biopsies. **(D)** Violin plots comparing the spatial enrichment of IAFs and monocytes by patient, each dot represents a core; nd, not defined. **(E)** Spatial scatter plot of representative cores highlighting IAF, crypt top (CT) colonocytes, and monocytes in HC and UC PRE biopsies. For panel **D**, Mann-Whitney test, p-value is indicated.



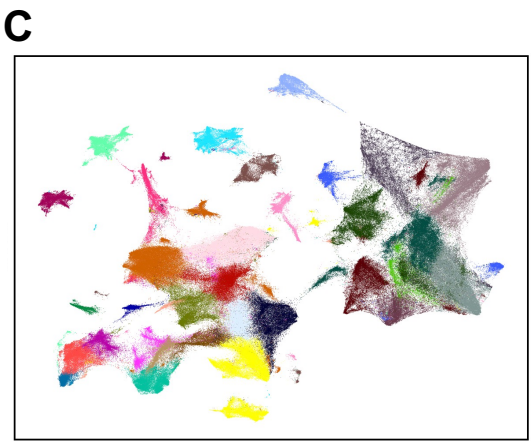
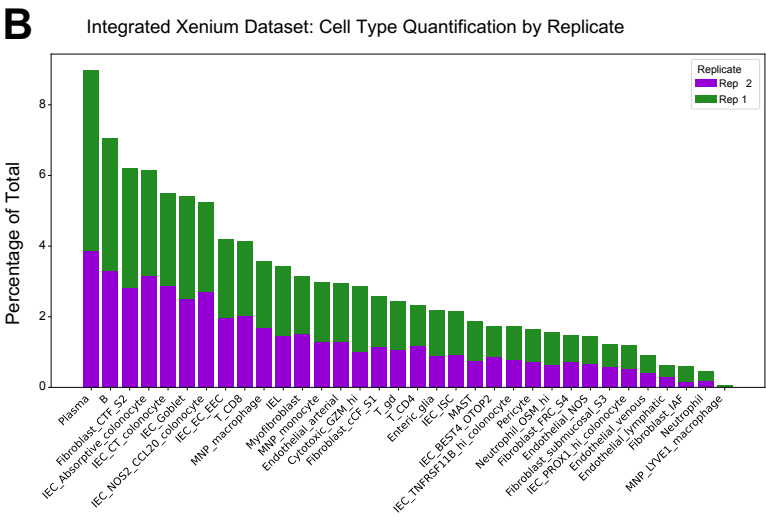
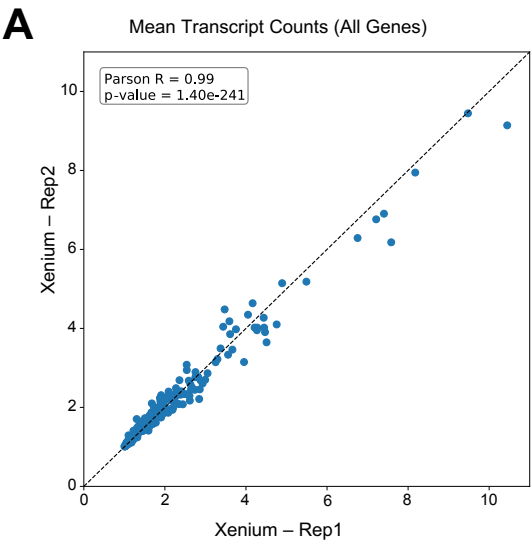
Supplemental Fig. 1| MERSCOPE dataset analysis. (A,B) UMAP visualization of MERSCOPE dataset (212 cells), highlighting **(A)** transcript count per cell, **(B)** number of genes per cell, and **(C)** area of TMA scanned showing DAPI and detected transcripts **(D)** spatial scatter plot depicting the spatial location of cells in the MERSCOPE dataset in relation to the TMA slide, colored based on leiden clustering.



Supplemental Fig. 2 | Xenium and CosMx dataset quality control and cell segmentation-related metrics. (A) Bar plot comparing the percentage of nuclear versus non-nuclear transcripts within the Xenium and CosMx datasets. **(B)** Cell area plotted in μm^2 for each cell within the Xenium and CosMx dataset. **(C)** Representative Xenium cell segmentation visualization, displaying DAPI nuclei (white), nuclei outlines (red), cell borders (black), cells are pseudocolored by Xenium fine annotation labels. **(D)** Scatter plot of average transcript count per cell for genes specific to either the Xenium or CosMx (blue for Xenium, and orange for CosMx). **(E,F)** Number of **(E)** transcripts and **(F)** unique features detected per cell per Core or FOV within the Xenium and CosMx datasets, calculated using the complete gene panel for each platform (Xenium, 290 genes; CosMx, 1,000 genes; left) and limited to the 159 overlapping genes across both panels (right). Plotted points are categorized based on the age of FFPE blocks from which they originated. For panels **B**, **E**, and **F**, box and whisker plots, the band indicates the median, the box indicates the first and third quartiles, and the whiskers indicate minimum and maximum value within the upper/lower fence (upper fence= $Q3+1.5 \times IQR$ and lower fence= $Q1-1.5 \times IQR$), only outlier points are shown; Mann-Whitney, two-tailed tests. Panels **E** and **F** compared the difference in population medians between 2-, 3-, 4-, and 5-year-old samples, averaged by core or FOV, with Kruskal-Wallis rank sum statistic (h -statistic) indicated.

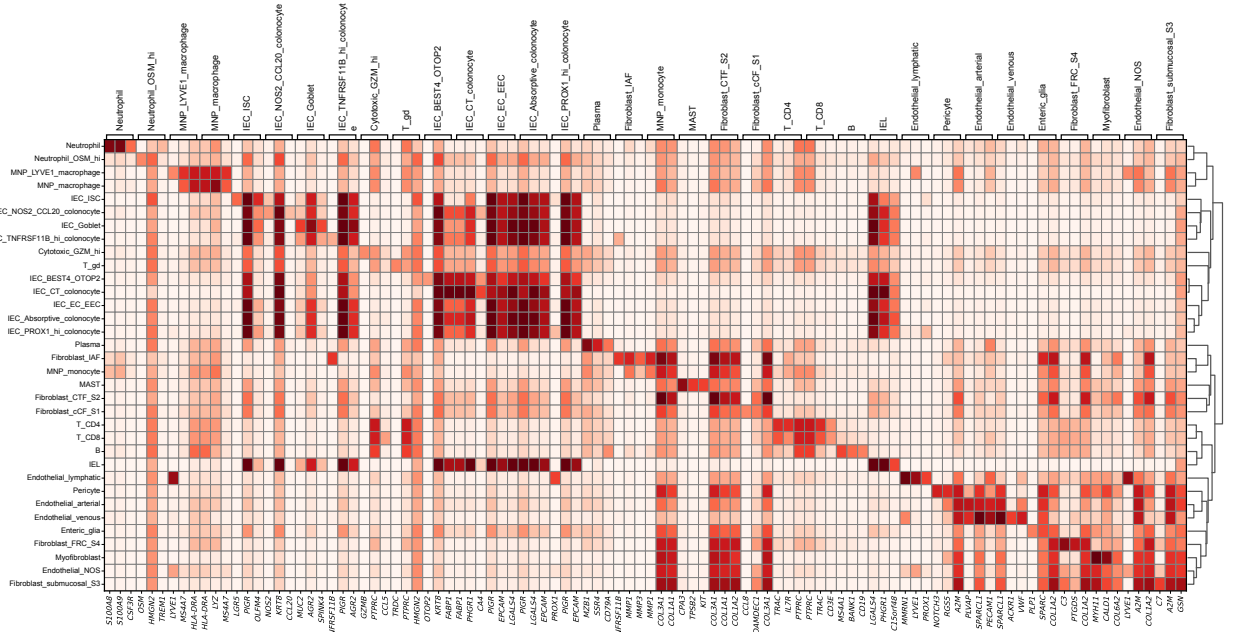
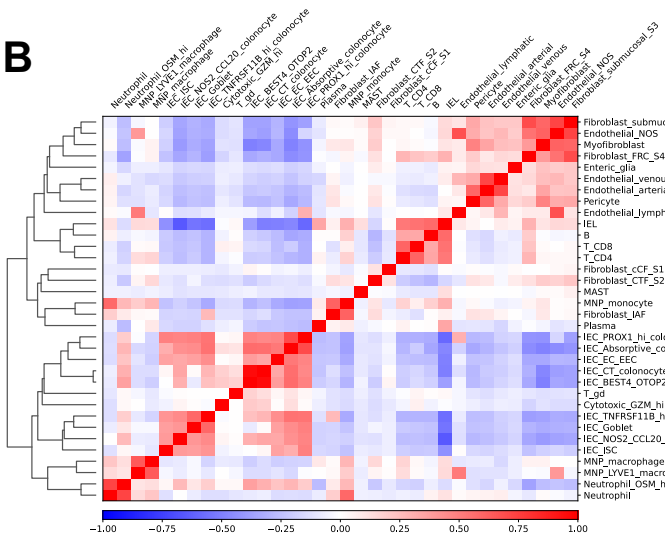
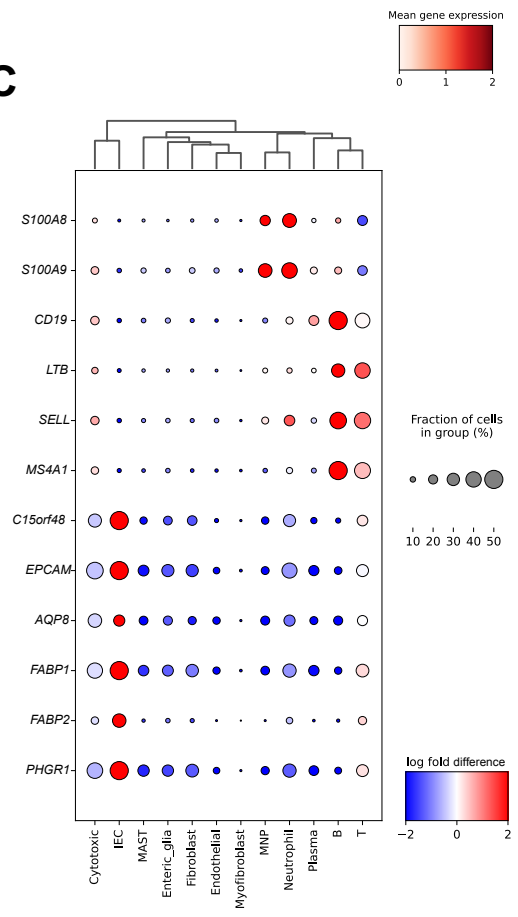


Supplemental Fig. 3 | Using mutually exclusive genes to evaluate platform specificity. (A-C) Scatter plots of gene expression level (transcript counts per cell) for two representative mutually exclusive lineage-specific genes within **(A)** Xenium, **(B)** CosMx, and **(C)** scRNA-seq datasets generated from colon biopsies collected from HC and UC patients (GSE250487). Genes were selected based on cell types of interest and the overlapping genes between Xenium and CosMx panels. The mutually exclusive co-expression rate (MECR) value is listed for each scatter plot, with lower rates corresponding to greater technology specificity.



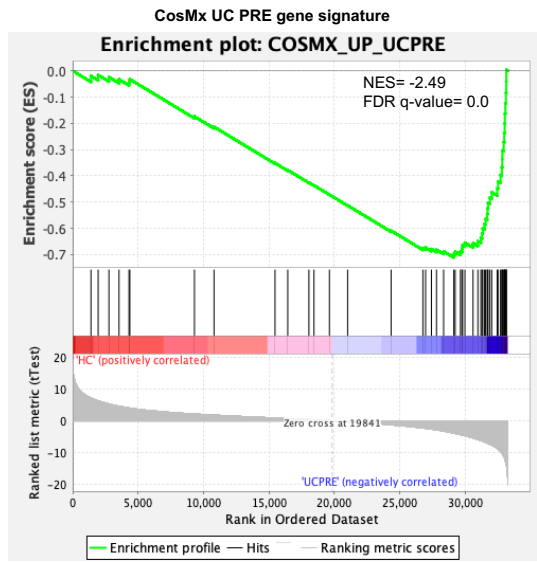
- Fine annotations
- B
 - IEC_Absorptive_colonocyte
 - MNP_LYVE1_macrophage
 - Cytotoxic_GZM_hi
 - IEC_BEST4_OTOP2
 - MNP_macrophage
 - Endothelial_NOS
 - IEC_CT_colonocyte
 - MNP_monocyte
 - Endothelial_arterial
 - IEC_EC_EEC
 - Myofibroblast
 - Endothelial_lymphatic
 - IEC_Goblet
 - Neutrophil
 - Endothelial_venous
 - IEC_ISC
 - Neutrophil_OSM_hi
 - Enteric_glia
 - IEC_NOS2_CCL20_colonocyte
 - Pericyte
 - Fibroblast_CTF_S2
 - IEC_PROX1_hi_colonocyte
 - Plasma
 - Fibroblast_FRC_S4
 - IEC_TNFRSF11B_hi_colonocyte
 - T_CD4
 - Fibroblast_IAF
 - IEL
 - T_CD8
 - Fibroblast_cCF_S1
 - MAST
 - T_gd
 - Fibroblast_submucosal_S3

Supplemental Fig. 4| Reproducibility of Xenium replicates. (A) Scatter plot showing the gene expression level (transcript counts per cell) for all genes between Xenium replicates. (B) Cell frequency as a percent of dataset total for fine annotations within Xenium replicates. (C) UMAP visualization of two integrated Xenium replicate runs, colored by fine annotations (582,188 total cells: 313,940 from replicate 1 and 268,248 from replicate 2). Xenium replicate data were obtained from different runs of different sections from same TMA block.

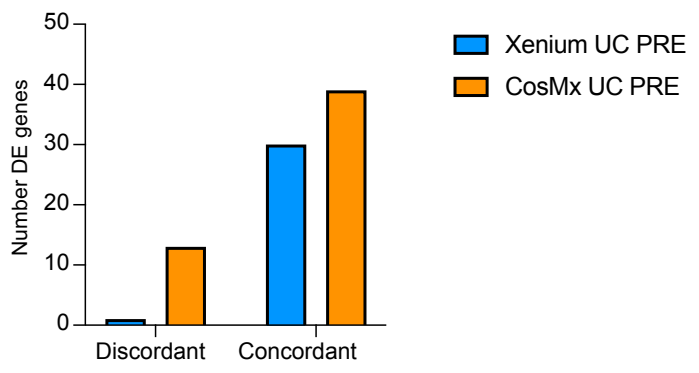
A**B****C**

Supplemental Fig. 5] Xenium dataset landmark gene heatmap and correlation matrix for fine annotations, and DEGs between UC and HC. (A,B) Fine cell annotation (A) heatmap displaying gene expression of the top 3 landmark genes and (B) correlation matrix in Xenium replicate 1. (C) Dot plot representation of a subset of genes from pseudobulk DEG analysis by coarse annotations.

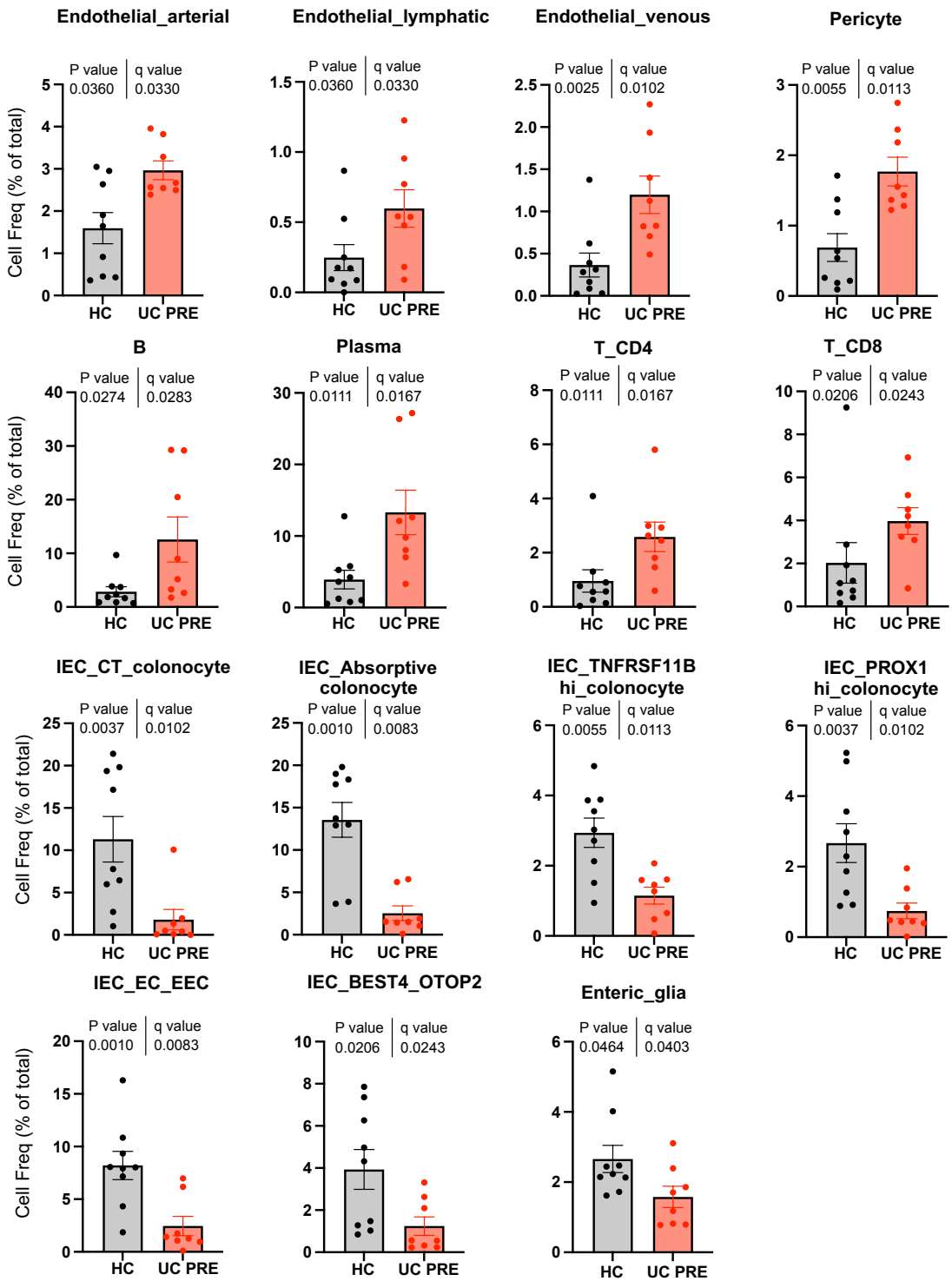
A IBD cohort (Arijs et al., 2018; GSE73661)
(HC=12; UC PRE=43)



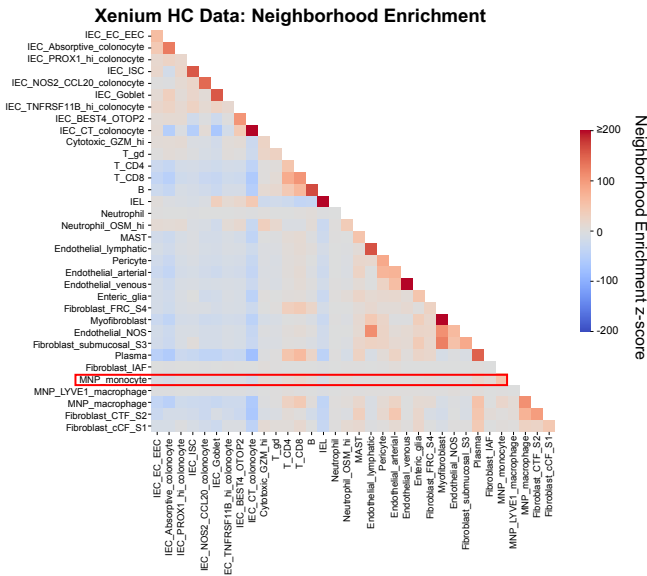
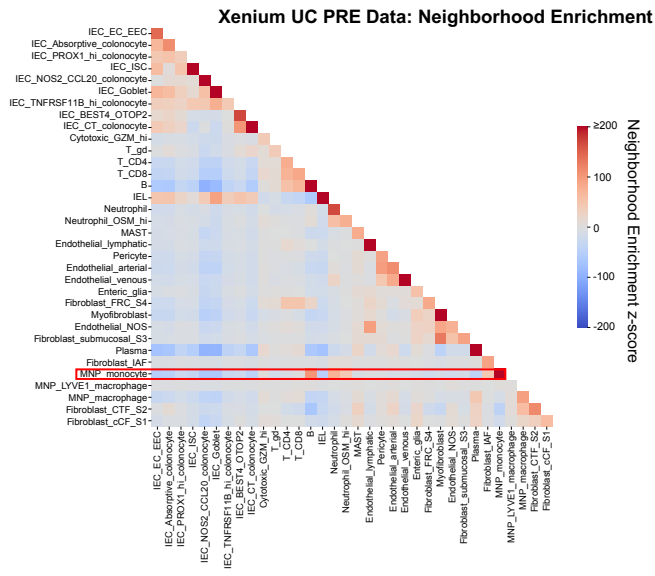
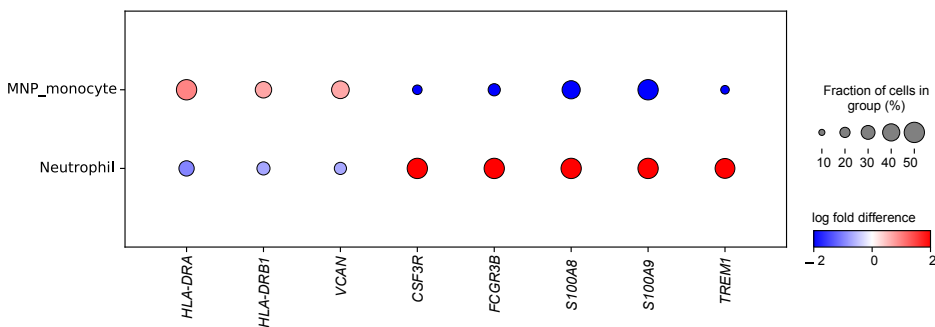
B



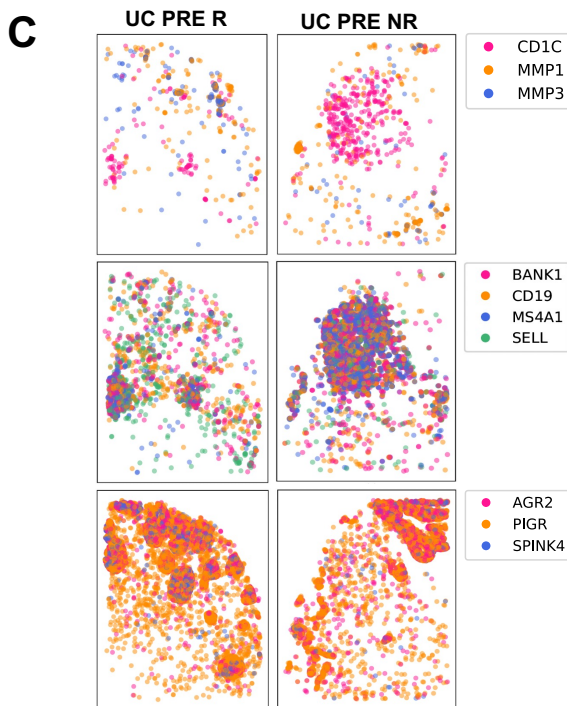
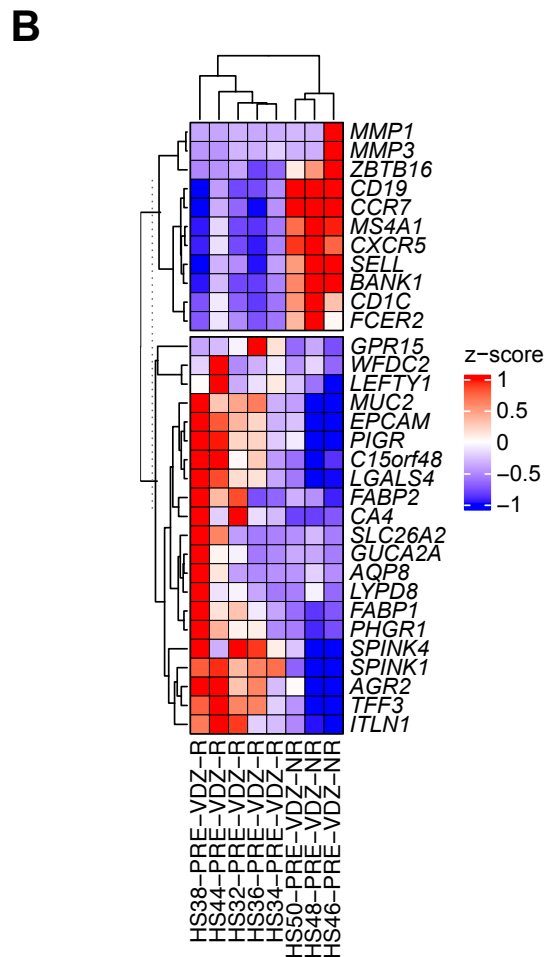
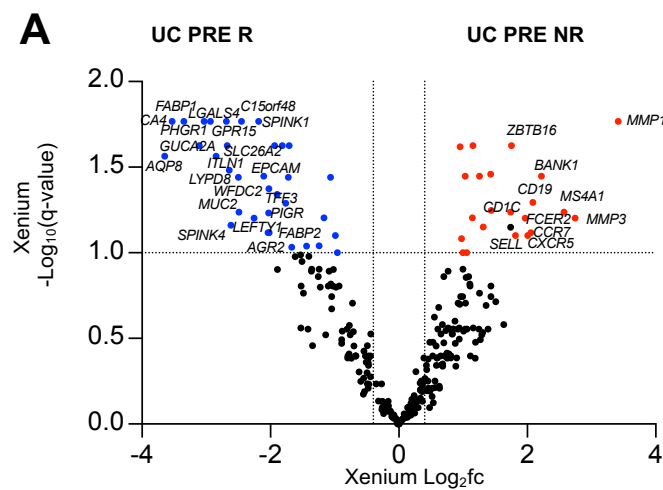
Supplemental Fig. 6| GSEA of an external, publicly-available, bulk transcriptomic dataset using a CosMx transcriptomic signature associated with UC PRE biopsies. (A) GSEA of CosMx UC PRE spatial gene signature in an external cohort of patients and relative NES. **(B)** Number of DE genes in the UC PRE signature for Xenium and CosMx that are concordantly or discordantly expressed to the UC PRE patients from the publicly available dataset.



Supplemental Fig. 7] Quantitation of differential cell abundance in the Xenium integrated dataset. Cell frequencies of the indicated subsets comparing HC and UC PRE, each dot represents one patient; Mann–Whitney, two-tailed test with FDR correction; $q < 0.1$ threshold for discovery. Only statistically significant cell subsets are shown with exact p-value and q-value displayed.

A**B****C**

Supplemental Fig. 8] Unsupervised Neighborhood enrichment analysis in Xenium FFPE colon biopsies and dot plot of neutrophil versus monocyte landmark genes. (A,B) Heatmaps displaying neighborhood enrichment z-scores for fine annotation cell pairs within (A) HC and (B) UC PRE biopsies. (C) Dot plot representation of landmark genes for the indicated subsets. For panels A and B, several values exceed the scale for visualization purposes (values greater than 200).



D

Xenium Gene Signature	NES	FDR q-value	Significance
UC PRE R	-2.02	0	yes
UC PRE NR	0.88	0.6	no
IAF-monocyte-neutrophil	1.88	0	yes
GALT-B-DC-S4_fibroblast	0.57	0.96	no

Supplemental Fig. 9| Pseudobulk DE gene analysis comparing UC PRE Non-Responders (UC PRE NR) versus UC PRE Responders (UC PRE R) in the Xenium dataset. (A) Volcano plot of pseudobulk DE genes identified by DESeq2 with $\log_2fc > 0.4$ or < -0.4 and $q < 0.1$ in UC PRE NR vs UC PRE R. **(B)** Heatmap of expression z-scores for the indicated genes in UC PRE NR (Up/Down) relative to UC PRE R. **(C)** Representative spatial transcript scatter plots highlighting a subset of genes relatively increased in UC PRE R (left) and UC PRE NR (right). **(D)** GSEA of Xenium signatures in external cohort of patients pre-VDZ stratified by UC PRE NR and UC PRE R with relative Normalized Enrichment Scores (NES) and FDR q-value. For panel B, some genes are off-scale for visualization purposes, z-score set from -1 to 1.

Patient ID	Age (y)	Sex	Disease status	UC Medication	Disease duration (y)	Duration VDZ (mo)	Prior anti-TNF exposure	Montreal classification	Mayo Endoscopic subscore	Responder to VDZ
HS31	60-69	F	HC	None	n/a	n/a	No	n/a	0	n/a
HS33	30-39	M	HC	None	n/a	n/a	No	n/a	0	n/a
HS35	20-29	F	HC	None	n/a	n/a	No	n/a	0	n/a
HS37	20-29	M	HC	None	n/a	n/a	No	n/a	0	n/a
HS39	20-29	F	HC	None	n/a	n/a	No	n/a	0	n/a
HS40	60-69	M	HC	None	n/a	n/a	No	n/a	0	n/a
HS41	50-59	M	HC	None	n/a	n/a	No	n/a	0	n/a
HS42	40-49	M	HC	None	n/a	n/a	No	n/a	0	n/a
HS43	50-59	M	HC	None	n/a	n/a	No	n/a	0	n/a
HS32	20-29	F	UC	VDZ	2	4	No	E2	pre 2 ; post 0	Yes
HS34	30-39	F	UC	VDZ	1	6	No	E1	pre 2; post 0	Yes
HS36	40-49	M	UC	VDZ	3	2	Yes	E2	pre 3; post 0	Yes
HS38	50-59	M	UC	VDZ	25	7	Yes	E3	pre 2; post 0	Yes
HS44	30-39	F	UC	VDZ	2	2	No	E1	pre 1	Yes
HS45	40-49	M	UC	VDZ	14	19	Yes	E2	pre 1; post 3	No
HS46	40-49	n/a	UC	VDZ	21	2	Yes	E2	pre 3; post 3	No
HS47	30-39	M	UC	VDZ	11	5	Yes	E2	post 3	No
HS48	70-79	M	UC	VDZ	8	6	Yes	E3	pre 2; post 2	No
HS49	30-39	F	UC	VDZ	2	3	Yes	E2	pre 2; post 3	No
HS50	20-29	M	UC	VDZ	0	5	Yes	E2	pre 2; post 2	No
					3 (2-14)					
p-value	ns	ns	p<0.0001	p<0.0001	n/a	n/a	p=0.0010	ns	pre, ns; post, p=0.0016	

Supplementary Table 1. Baseline demographic and clinical data for study participants. Categorical variables were analyzed by Chi-square test and continuous variables were compared using one-way ANOVA with FDR correction or Mann-Whitney test where appropriate. ns, not significant; n/a, not applicable; pre, pre-VDZ treatment; post, post-VDZ treatment. VDZ-vedolizumab.

Assay type	Target	Vendor
Xenium 290-plex custom panel	ACM	10x Genomics
	ABCC9	10x Genomics
	ACKR1	10x Genomics
	ACTG1	10x Genomics
	ADAMDEC1	10x Genomics
	ADGRB3	10x Genomics
	AGRP	10x Genomics
	ALOX5	10x Genomics
	ALOX5AP	10x Genomics
	ANKK2	10x Genomics
	APOE	10x Genomics
	APP	10x Genomics
	AQP8	10x Genomics
	ASCL2	10x Genomics
	ASPM	10x Genomics
	BANK1	10x Genomics
	BASP1	10x Genomics
	BATF	10x Genomics
	BEST1	10x Genomics
	C15orf48	10x Genomics
	C1QA	10x Genomics
	C1QB	10x Genomics
	C1QC	10x Genomics
	C3	10x Genomics
	C7	10x Genomics
	CA4	10x Genomics
	CA7	10x Genomics
	CACNA1A	10x Genomics
	CALD1	10x Genomics
	CAV1	10x Genomics
	CCDC80	10x Genomics
	CCL20	10x Genomics
	CCL23	10x Genomics
	CCL4	10x Genomics
	CCL5	10x Genomics
	CCL8	10x Genomics
	CCR6	10x Genomics
	CCR7	10x Genomics
	CCSER1	10x Genomics
	CD14	10x Genomics
	CD19	10x Genomics
	CD1C	10x Genomics
	CD1D	10x Genomics
	CD209	10x Genomics
	CD28	10x Genomics
	CD3D	10x Genomics
	CD3E	10x Genomics
	CD4	10x Genomics
	CD40	10x Genomics
	CD44	10x Genomics
	CD59	10x Genomics
	CD69	10x Genomics
	CD7	10x Genomics
	CD79A	10x Genomics
	CD80	10x Genomics
	CD86	10x Genomics
	CD8A	10x Genomics
	CD8B	10x Genomics
	CDH5	10x Genomics
	CEACAM1	10x Genomics
	CEACAM6	10x Genomics
	CLDN5	10x Genomics
	CLEC10A	10x Genomics
	CLEC3A	10x Genomics
	CLU	10x Genomics
	COL1A1	10x Genomics
	COL1A2	10x Genomics
	COL3A1	10x Genomics
	COL6A2	10x Genomics
	CPA3	10x Genomics
	CPE	10x Genomics
	CRYAB	10x Genomics
	CSP3R	10x Genomics
	CSPG4	10x Genomics
	CST3	10x Genomics
	CTLA4	10x Genomics
	CTSL	10x Genomics
	CXCL14	10x Genomics
	CXCR1	10x Genomics
	CXCR5	10x Genomics
	CYTH1	10x Genomics
	DDC	10x Genomics
	DUSP1	10x Genomics
	DUSP23	10x Genomics
	EPCAM	10x Genomics
	F3	10x Genomics
	FABP1	10x Genomics
	FABP2	10x Genomics
	FABP5	10x Genomics
	FCER1A	10x Genomics
	FCER1G	10x Genomics
	FCER2	10x Genomics
	FCGR3A	10x Genomics
	FCGR3B	10x Genomics
	FCN1	10x Genomics
	FLT3	10x Genomics
	FOLR3	10x Genomics
	FOXP3	10x Genomics
	FXYD5	10x Genomics
	FYB1	10x Genomics
GATA2	10x Genomics	
GATA3	10x Genomics	
GLIS3	10x Genomics	
GPR115	10x Genomics	
GSN	10x Genomics	
GUCA2A	10x Genomics	
GZMA	10x Genomics	
GZMB	10x Genomics	
GZMK	10x Genomics	
HAND2	10x Genomics	
HLA-DRA	10x Genomics	
HLA-DRB1	10x Genomics	
HMG2	10x Genomics	
HMG2	10x Genomics	
HRGDS	10x Genomics	
ICOS	10x Genomics	
IFITM2	10x Genomics	
IFNG	10x Genomics	
IGHA2	10x Genomics	
IGHD	10x Genomics	
IGHH	10x Genomics	
IL10	10x Genomics	
IL10RA	10x Genomics	
IL13RA2	10x Genomics	
IL18R1	10x Genomics	
IL1B	10x Genomics	
IL1R1	10x Genomics	
IL1R2	10x Genomics	
IL1RL1	10x Genomics	
IL32	10x Genomics	
IL3RA	10x Genomics	
IL7R	10x Genomics	
INAVA	10x Genomics	
INSM1	10x Genomics	
IRF1	10x Genomics	
IRF8	10x Genomics	
ITGAX	10x Genomics	
ITLN1	10x Genomics	
ITM2C	10x Genomics	
JAK1	10x Genomics	
JAK2	10x Genomics	
JAK3	10x Genomics	
JUN	10x Genomics	
KCNK18	10x Genomics	
KIT	10x Genomics	
KLF2	10x Genomics	

KLRB1	10x Genomics	
KLRC2	10x Genomics	
KLRF1	10x Genomics	
KRT8	10x Genomics	
LAMP3	10x Genomics	
LEF1	10x Genomics	
LEFTY1	10x Genomics	
LGALS4	10x Genomics	
LGR5	10x Genomics	
LILRA4	10x Genomics	
LST1	10x Genomics	
LTA	10x Genomics	
LTB	10x Genomics	
LTBR	10x Genomics	
LYPD8	10x Genomics	
LVE1	10x Genomics	
LVZ	10x Genomics	
MAF	10x Genomics	
MCAM	10x Genomics	
MEF2C	10x Genomics	
MGLL	10x Genomics	
MKI67	10x Genomics	
MMP1	10x Genomics	
MMP3	10x Genomics	
MIRN1	10x Genomics	
MRC1	10x Genomics	
MSA1	10x Genomics	
MSA2	10x Genomics	
MSA7	10x Genomics	
MSA8	10x Genomics	
MT1G	10x Genomics	
MUC1	10x Genomics	
MUC2	10x Genomics	
MTH11	10x Genomics	
MZB1	10x Genomics	
NCAM1	10x Genomics	
NEUROD1	10x Genomics	
NFBIA	10x Genomics	
NG2	10x Genomics	
NOS2	10x Genomics	
NOTCH3	10x Genomics	
NOTCH4	10x Genomics	
NPC2	10x Genomics	
NTRK2	10x Genomics	
NUPR1	10x Genomics	
OGN	10x Genomics	
OLFM4	10x Genomics	
OSM	10x Genomics	
OSMR	10x Genomics	
OTOP2	10x Genomics	
PDGFRA	10x Genomics	
PECAM1	10x Genomics	
PHGR1	10x Genomics	
PHLDA2	10x Genomics	
PGR	10x Genomics	
PLAC8	10x Genomics	
PLP1	10x Genomics	
PLVAP	10x Genomics	
POSTN	10x Genomics	
PRDX1	10x Genomics	
PTGS2	10x Genomics	
PTPRC	10x Genomics	
PYY	10x Genomics	
QDPR	10x Genomics	
RGS4	10x Genomics	
RGCC	10x Genomics	
RGSS	10x Genomics	
RORC	10x Genomics	
RTRN2	10x Genomics	
S100A11	10x Genomics	
S100A12	10x Genomics	
S100A16	10x Genomics	
S100A4	10x Genomics	
S100B	10x Genomics	
S100A9	10x Genomics	
S100B	10x Genomics	
S100P	10x Genomics	
S1PR1	10x Genomics	
S1PR5	10x Genomics	
SEC61B	10x Genomics	
SELENOP	10x Genomics	
SELL	10x Genomics	
SERPINF1	10x Genomics	
SH2D6	10x Genomics	
SLC26A2	10x Genomics	
SOX6	10x Genomics	
SOX9	10x Genomics	
SOX9	10x Genomics	
SPARC	10x Genomics	
SPARCL1	10x Genomics	
SPINK1	10x Genomics	
SPINK4	10x Genomics	
SSR4	10x Genomics	
STAT4	10x Genomics	
STMN1	10x Genomics	
TCF4	10x Genomics	
TFE3	10x Genomics	
TGFB1	10x Genomics	
TGFB1	10x Genomics	
TGFB1	10x Genomics	
TGFB2	10x Genomics	
TGIF1	10x Genomics	
TIMP1	10x Genomics	
TINAGL1	10x Genomics	
TLE4	10x Genomics	
TM6SF1	10x Genomics	
TMEM176A	10x Genomics	
TMEM176B	10x Genomics	
TNF	10x Genomics	
TNFAIP3	10x Genomics	
TNFRSF11A	10x Genomics	
TNFRSF11B	10x Genomics	
TNFRSF13B	10x Genomics	
TNFRSF17	10x Genomics	
TNFRSF1A	10x Genomics	
TNFRSF1B	10x Genomics	
TNFRSF13B	10x Genomics	
TNFRSF15	10x Genomics	
TNFRSF9	10x Genomics	
TOP2A	10x Genomics	
TPH1	10x Genomics	
TPSAB1	10x Genomics	
TPS2	10x Genomics	
TRAC	10x Genomics	
TRAV1-2	10x Genomics	
TRDC	10x Genomics	
TRDV2	10x Genomics	
TREM1	10x Genomics	
TREM2	10x Genomics	
TRGC1	10x Genomics	
TRGC2	10x Genomics	
TRGV9	10x Genomics	
TRPM5	10x Genomics	
TUBA1B	10x Genomics	
TUBB	10x Genomics	
TYK2	10x Genomics	
TYROBP	10x Genomics	
UBE2C	10x Genomics	
VCAN	10x Genomics	
VWF	10x Genomics	
WDC2	10x Genomics	
WNT5A	10x Genomics	
XCR1	10x Genomics	
ZBTB16	10x Genomics	
ZFP98L1	10x Genomics	
MIRSCOPE	TMEM176A	Vizgen
280-plex	CP4	Vizgen
panel	TNFRSF17	Vizgen

TRPM5 Vezgen
TNFRSF1A Vezgen
CEACAM6 Vezgen
OSM Vezgen
GZMB Vezgen
NFKBIA Vezgen
TIMP1 Vezgen
OLFM4 Vezgen
MMP2 Vezgen
AQP9 Vezgen
TGFB1 Vezgen
CD73A Vezgen
NKG7 Vezgen
SEC61B Vezgen
COL1A1 Vezgen
NFKB1 Vezgen
IL10RA Vezgen
CD69 Vezgen
LTBR Vezgen
IFNG Vezgen
KLRB1 Vezgen
GZMK Vezgen
IL18R1 Vezgen
SELL Vezgen
TNFAIP3 Vezgen
ADGRB3 Vezgen
KCNJ8 Vezgen
FLT3 Vezgen
IL13RA2 Vezgen
TREM1 Vezgen
SOX9 Vezgen
TNFSF9 Vezgen
CCR7 Vezgen
KLF2 Vezgen
TPH1 Vezgen
APOE Vezgen
PLVAP Vezgen
SEPPIN1 Vezgen
CLEC10A Vezgen
LYVE1 Vezgen
ADAMDEC1 Vezgen
REG4 Vezgen
PDGFRA Vezgen
ABCC9 Vezgen
LYZ Vezgen
VWF Vezgen
PROX1 Vezgen
TNFRSF13B Vezgen
TYROBP Vezgen
IL1B Vezgen
NOTCH3 Vezgen
CD44 Vezgen
MCAM Vezgen
MMRN1 Vezgen
LAMP3 Vezgen
LGR5 Vezgen
ITGAX Vezgen
IRF8 Vezgen
IFNAR1 Vezgen
TM6GL1 Vezgen
S100A11 Vezgen
LEFTY1 Vezgen
FABP2 Vezgen
OSMR Vezgen
G2MA Vezgen
QDPR Vezgen
GPR15 Vezgen
SLC26A2 Vezgen
BATF Vezgen
KIT Vezgen
FCER1G Vezgen
IL10RB Vezgen
S100B Vezgen
IL1RA4 Vezgen
CXCR5 Vezgen
SOX8 Vezgen
NEUROD1 Vezgen
HRGDS Vezgen
CXCR1 Vezgen
TGFB2 Vezgen
CTLA4 Vezgen
OPAS Vezgen
S100P Vezgen
SPINK1 Vezgen
COL1A2 Vezgen
TNFRSF11B Vezgen
MMP3 Vezgen
MSA48 Vezgen
NOD2 Vezgen
CD3D Vezgen
CA4 Vezgen
MEB1 Vezgen
IL7R Vezgen
COL3A1 Vezgen
S1PR1 Vezgen
TM6SF1 Vezgen
CSFG4 Vezgen
XCR1 Vezgen
INSM1 Vezgen
IL1RL1 Vezgen
CD7 Vezgen
C7 Vezgen
NOS2 Vezgen
RGSS Vezgen
PHLD42 Vezgen
MMP1 Vezgen
CD209 Vezgen
ICOS Vezgen
SOX9 Vezgen
WCAM1 Vezgen
AZM Vezgen
BASP1 Vezgen
DUOX2 Vezgen
CD28 Vezgen
NLRP12 Vezgen
GLIS3 Vezgen
CD19 Vezgen
ITLN1 Vezgen
TMEM176B Vezgen
CD86 Vezgen
IL3RA Vezgen
ASCL2 Vezgen
OTOP2 Vezgen
F3 Vezgen
ZBTB16 Vezgen
IL21R Vezgen
CAT Vezgen
CTSL Vezgen
GATA2 Vezgen
CDH5 Vezgen
CCR6 Vezgen
JAK1 Vezgen
VCAN Vezgen
FCER2 Vezgen
APP Vezgen
IL23R Vezgen
PTPRC Vezgen
FYB1 Vezgen
CDBA Vezgen
CLEC9A Vezgen
UBE2C Vezgen
RORC Vezgen
MSA47 Vezgen
CCL20 Vezgen
HAND2 Vezgen
NTRK2 Vezgen
HLA-DRB1 Vezgen

CYTH1	Vzgen
MUC2	Vzgen
CSF3R	Vzgen
CD3E	Vzgen
CALD1	Vzgen
INAVA	Vzgen
IFNGR1	Vzgen
DUSP23	Vzgen
FCER1A	Vzgen
ACKR1	Vzgen
CD1C	Vzgen
CD1D	Vzgen
IL6R	Vzgen
MKG67	Vzgen
S100A16	Vzgen
S100A4	Vzgen
S100A8	Vzgen
S100A12	Vzgen
S100A9	Vzgen
JUN	Vzgen
PTGDS	Vzgen
FCN1	Vzgen
BEST4	Vzgen
CD40	Vzgen
MMP9	Vzgen
WFDC2	Vzgen
TREM2	Vzgen
RTKN2	Vzgen
TNFSF15	Vzgen
STMN1	Vzgen
ALOX5	Vzgen
C1QC	Vzgen
TGFBF1	Vzgen
NOTCH4	Vzgen
ASPN	Vzgen
OGN	Vzgen
TNFSF13B	Vzgen
FOXO3	Vzgen
TNFRSF1B	Vzgen
TLE4	Vzgen
GATA3	Vzgen
RGCC	Vzgen
SPRN4	Vzgen
IL2RA	Vzgen
ALOX5AP	Vzgen
JAK2	Vzgen
IFNAR2	Vzgen
TGIT	Vzgen
TRDV2	Vzgen
TRDC	Vzgen
IGHF	Vzgen
IGHD	Vzgen
CD8B	Vzgen
NLRP3	Vzgen
FXR1	Vzgen
STAT4	Vzgen
MAF	Vzgen
IL1R2	Vzgen
CCL8	Vzgen
HLA-DRA	Vzgen
NUPR1	Vzgen
CD59	Vzgen
FABP5	Vzgen
IRF7	Vzgen
MCLL	Vzgen
IFITM2	Vzgen
CD14	Vzgen
NLR4	Vzgen
C1QA	Vzgen
CRE	Vzgen
CEACAM1	Vzgen
CLU	Vzgen
CAV1	Vzgen
IFNGR2	Vzgen
IL1R1	Vzgen
PLAC8	Vzgen
LTA	Vzgen
ALGR2	Vzgen
TOP2A	Vzgen
IL10	Vzgen
LTB	Vzgen
FCGR3A	Vzgen
LST1	Vzgen
HMG2	Vzgen
CCDC80	Vzgen
ZFP38L1	Vzgen
TRG1	Vzgen
DDC	Vzgen
BANK1	Vzgen
TRGV9	Vzgen
TNF	Vzgen
JAK3	Vzgen
WNT5A	Vzgen
CD80	Vzgen
MUC1	Vzgen
LEF1	Vzgen
CCSER1	Vzgen
C1QB	Vzgen
CXCL14	Vzgen
SELENP	Vzgen
TYK2	Vzgen
CRYAB	Vzgen
IL32	Vzgen
MS4A1	Vzgen
POSTN	Vzgen
NPC2	Vzgen
PECAM1	Vzgen
MRC1	Vzgen
ACTG1	Vzgen
TNFRSF11A	Vzgen
CACNA1A	Vzgen
LYPD8	Vzgen
PYY	Vzgen
C3	Vzgen
CCL5	Vzgen
DUOX2	Vzgen
TRAC	Vzgen
GCLA	Vzgen
FCGR3B	Vzgen
CCL23	Vzgen
CCL18	Vzgen
IKBK6	Vzgen
MS4A2	Vzgen
S1PR5	Vzgen
KLRP1	Vzgen
CLDN5	Vzgen
ALP1	Vzgen
TCF4	Vzgen
MEF2C	Vzgen
SH2D6	Vzgen

Supplementary Table 2. Gene panels for the different spatial transcriptomic platforms.

Run		Xenium	CosMx
Panel size (Num. genes; num. neg probes)		290; 20	1000; 10
		(Custom panel)	(Pre-designed panel)
Overlapping genes across panels		159	
Percent of cells that passed QC		72%	78%
Mean transcripts per cell (Sensitivity)	All genes	148	219
	Overlapping genes	85	29
Mean unique genes counted per cell (Genomic Breadth)	All genes	51	132
	Overlapping genes	31	20
Mean expression of each gene within cells	All genes	2	1.33
	Overlapping genes	2	1.3
Mean negative probe counts per cell		0.034	0.37
Mean signal detected per cell above background		59	4

Supplementary Table 3. Summarized QC results.

	baseMean	log2FoldChange	lfcSE	stat	pvalue	padj	-log10 (padj) Significance	
S100A8	1912.86507	3.877071757	0.78254345	-4.9544492	7.25E-07	0.00021035	3.67705129	yes
IGHD	555.955821	2.7995075	0.696344	-4.0202939	5.81E-05	0.00255326	2.59290428	yes
MS4A1	5393.16287	2.541605012	0.7152485	-3.5534573	0.0003802	0.00648581	2.18803551	yes
S100A9	3473.14706	2.344474824	0.69231803	-3.3868464	0.00070701	0.00891447	2.04990452	yes
TIMP1	4973.32528	2.086217495	0.52557312	-3.9694144	7.20E-05	0.00255326	2.59290428	yes
CD79A	6817.54988	1.988670369	0.53065281	-3.7475923	0.00017854	0.00363757	2.43918912	yes
C3	8969.74854	1.95141288	0.52254809	-3.7344178	0.00018815	0.00363757	2.43918912	yes
CD19	3401.9927	1.850081789	0.59046468	-3.1332641	0.00172874	0.01630356	1.78771753	yes
BANK1	4178.99064	1.823652303	0.58247153	-3.1308866	0.00174279	0.01630356	1.78771753	yes
MZB1	15536.3626	1.812298856	0.45136199	-4.0151783	5.94E-05	0.00255326	2.59290428	yes
JAK3	4521.55009	1.703751567	0.43113513	-3.9517809	7.76E-05	0.00255326	2.59290428	yes
PTGDS	7751.66236	1.625414177	0.58242248	-2.790782	0.00525809	0.03002352	1.52253846	yes
SELL	2560.14415	1.616523274	0.56725529	-2.849728	0.00437566	0.03002352	1.52253846	yes
LTB	1866.54329	1.493209523	0.53337272	-2.7995611	0.00511721	0.03002352	1.52253846	yes
S100A12	414.708353	1.403679815	0.62201356	-2.2566708	0.02402865	0.07829562	1.10626256	no
NOS2	4415.26132	1.321676825	0.44145556	-2.9939068	0.0027543	0.02218742	1.65389322	yes
IL1B	1957.75188	1.214190665	0.62098928	-1.9552522	0.05055331	0.12973858	0.86693086	no
PECAM1	9946.17504	1.142853852	0.33090956	-3.4536743	0.00055301	0.00801857	2.09590313	yes
CLU	5555.10391	1.133578759	0.44529262	-2.545694	0.01090608	0.04893374	1.3103916	yes
SSR4	10887.252	1.099170797	0.42466536	-2.5883222	0.00964447	0.04585076	1.33865343	yes
PTPRC	13970.3792	1.074416383	0.38313502	-2.8042761	0.00504297	0.03002352	1.52253846	yes
REG4	15966.2714	1.02886571	0.67728103	-1.5191119	0.12873432	0.25396567	0.59522499	no
IL7R	6618.94046	0.974229392	0.37835684	-2.5748957	0.01002703	0.0468846	1.3289698	yes
TRAC	6948.11474	0.945210701	0.43059747	-2.1951144	0.02815539	0.08675302	1.06171539	yes
BASP1	4239.58352	0.940309996	0.30325814	-3.1006917	0.00193069	0.01662429	1.77925689	yes
COL1A1	27985.0535	0.90730443	0.40001618	-2.2681693	0.02331889	0.07723413	1.11219073	yes
TNFRSF17	2792.8458	0.87596328	0.42961753	-2.0389375	0.04145627	0.11559921	0.93704514	no
ALOX5	3354.62151	0.867041813	0.30673357	-2.8266936	0.00470313	0.03002352	1.52253846	yes
MRC1	3356.91078	0.816368591	0.33015494	-2.4726832	0.0134103	0.05401369	1.26749616	yes
SPINK4	10731.9425	0.790681008	0.72035586	-1.0976256	0.27236802	0.44126663	0.35529892	no
TCF4	2331.13703	0.767445287	0.28785708	-2.6660636	0.00767452	0.03904579	1.4084258	yes
COL1A2	24033.8077	0.765825491	0.39521009	-1.9377681	0.05265152	0.13162881	0.88064905	no
HLA-DRB1	9531.98169	0.756374509	0.45318256	-1.6690283	0.09511178	0.20121698	0.69633538	no
SEC61B	2324.72837	0.747724586	0.3799327	-1.9680448	0.04906288	0.12703782	0.89606698	no
FYB1	3987.67501	0.736294259	0.37231454	-1.9776135	0.04797232	0.12647249	0.89800393	no
FCER1G	6285.04915	0.72922225	0.37980601	-1.9199861	0.05485966	0.13482458	0.87023092	no
SERPINF1	6266.924	0.721190193	0.2585434	-2.7894357	0.00528	0.03002352	1.52253846	yes
FCGR3A	1237.8205	0.710101793	0.4076122	-1.7421014	0.0814907	0.18462737	0.73370392	no
S100A11	10790.127	0.709428326	0.34734401	-2.0424372	0.04110818	0.11559921	0.93704514	no
CCL20	1862.03197	0.698841203	0.36016724	-1.9403242	0.05234031	0.13162881	0.88064905	no
CCR7	1745.05622	0.683942802	0.59985592	-1.1401785	0.25421196	0.42290132	0.37376096	no
VWF	2640.62439	0.683547581	0.29572971	-2.311393	0.02081116	0.07357857	1.13324868	yes
CD1D	1611.36803	0.676243014	0.24119119	-2.8037633	0.005051	0.03002352	1.52253846	yes
CD3D	2876.52694	0.66733552	0.34928375	-1.9105828	0.05605822	0.13661246	0.86450969	no
SPARC	16800.0698	0.666501158	0.43245795	-1.541193	0.12326982	0.24653964	0.60811324	no
IL10RA	5656.27472	0.65260346	0.30879271	-2.113403	0.03456629	0.10024223	0.99894928	no
MLP3	518.286632	0.642093989	0.58123327	-1.1047096	0.26928543	0.43883121	0.35770249	no
CD44	22491.6212	0.635630985	0.29248921	-2.1731776	0.02976696	0.08808589	1.05509365	yes
HLA-DRA	16413.3057	0.627693207	0.37933941	-1.6547008	0.09798522	0.20296937	0.69256949	no
FCER2	1164.9854	0.626284012	0.56105117	-1.116269	0.26430702	0.43550589	0.36100597	no
ITGAX	3566.65599	0.625895494	0.38019082	-1.6462667	0.09970886	0.20507495	0.68808738	no
OSMR	2661.85795	0.616225186	0.22295788	-2.7638637	0.00571214	0.03067631	1.51319695	yes
VCAN	4267.30924	0.615826417	0.34688374	-1.7753107	0.0758466	0.17596411	0.75457591	no
COL3A1	35487.2811	0.598611296	0.40345989	-1.4836947	0.13788994	0.26658722	0.57416068	no
MEF2C	3166.64943	0.595413511	0.24323126	-2.4479317	0.01436789	0.05630659	1.24944081	yes
S100P	5597.95965	0.594878565	0.60142623	-0.9891131	0.32260781	0.49500669	0.30538893	no
CTLA4	1716.01122	0.576267846	0.42670238	-1.3505147	0.17685093	0.32255831	0.49139177	no
C1QB	2214.65925	0.57351651	0.39973295	-1.4347492	0.15135859	0.28318704	0.54792662	no
CXCR5	1502.46352	0.554916287	0.60895445	-0.9112608	0.362158	0.52776794	0.277557	no
CD40	2964.34461	0.55178545	0.33124179	-1.6658087	0.09575153	0.20121698	0.69633538	no
COL6A2	9314.92282	0.523772485	0.43920322	-1.1925516	0.23304505	0.40298668	0.39470931	no
NOTCH3	2021.86666	0.51846979	0.2550454	-2.0328529	0.04206738	0.11618611	0.93484579	no
CD1C	870.394762	0.500083519	0.49480352	-1.0106709	0.31217397	0.4859094	0.3134447	no
TNFRSF1B	5545.37429	0.492326925	0.26504261	-1.8575387	0.06323454	0.15155387	0.81943298	no
ICOS	712.35705	0.488258905	0.33857912	-1.4420821	0.1492792	0.28312927	0.54801523	no
IL1R1	6092.98725	0.481839517	0.28669859	-1.6806484	0.09283124	0.20090342	0.69701267	no
ALOX5AP	1967.02909	0.468476406	0.33076371	-1.4163477	0.15667374	0.29125247	0.53573038	no
CCDC80	3139.17565	0.456909155	0.46904628	-0.9741238	0.32999506	0.5008332	0.30030689	no
C1QA	3218.33667	0.431689435	0.34505197	-1.2510853	0.21090337	0.36844565	0.43362657	no
CD28	1851.17888	0.43024337	0.38951666	-1.1045571	0.26935157	0.43883121	0.35770249	no
NFKBIA	6678.05303	0.430112392	0.3294757	-1.305445	0.19174138	0.34324074	0.46440117	no
LYZ	27013.2345	0.42383674	0.43430122	-0.975905	0.32911154	0.5008332	0.30030689	no
TNFRSF13B	1217.16313	0.412392961	0.39341779	-1.0482316	0.29453192	0.47190196	0.32614822	no
RGCC	1611.68025	0.40234956	0.23813367	-1.6895761	0.09110909	0.19865891	0.70189195	no
CAV1	3118.44421	0.384585441	0.32277211	-1.1915077	0.23345435	0.40298668	0.39470931	no
SPARCL1	10113.9213	0.369652816	0.38072271	-0.970924	0.33158612	0.5008332	0.30030689	no
CCR6	1063.59855	0.362211737	0.41738856	-0.8678047	0.38550128	0.55071611	0.25907222	no
WNT5A	3349.41961	0.349187366	0.44121659	-0.7914194	0.4286993	0.60000541	0.22184484	no
CD4	3278.25061	0.34617996	0.24901295	-1.3902087	0.16446552	0.30186709	0.52018423	no
CD80	589.995259	0.343685733	0.37686656	-0.911956	0.36179186	0.52776794	0.277557	no
ZFP36L1	12275.9423	0.343468865	0.39226995	-0.8755931	0.38125127	0.54734093	0.26174207	no
CD11	12046.6369	0.335531377	0.42235337	-0.7944328	0.4269435	0.60000541	0.22184484	no
TGFB2	7579.67825	0.333138574	0.28998669	-1.1488064	0.2506358	0.4221352	0.37454844	no
OLFM4	25435.5281	0.314916332	0.63090143	-0.499153	0.61767161	0.7311215	0.13601045	no
GPR15	3900.81575	0.309105497	0.58515506	-0.5282454	0.59732899	0.72177253	0.14159965	no
LST1	515.700859	0.307866377	0.30134352	-1.0216459	0.30694851	0.48116253	0.3177082	no
IL3RA	870.508283	0.307005814	0.30448954	-1.0082639	0.31332779	0.4859094	0.3134447	no
C1QC	4069.13535	0.306134287	0.39341742	-0.7781412	0.43648581	0.60276611	0.21985117	no
CTSL	5683.08235	0.295792977	0.31727063	-0.9323049	0.35117896	0.51941117	0.28448872	no
F3	7352.51271	0.292489392	0.45251801	-0.6463597	0.51804645	0.65891873	0.18116814	no
CD69	1516.25797	0.286078531	0.36403299	-0.7858588	0.43195021	0.60000541	0.22184484	no
IL18R1	1253.08496	0.276143106	0.24269664	-1.1378118	0.25519907	0.42290132	0.37370696	no
TNFSF13B	1863.35862	0.272824023	0.27245712	-1.0013466	0.31665925	0.48846374	0.31116767	no
RG55	5353.96751	0.272693261	0.331521	-0.822552	0.41076281	0.58392752	0.23364106	no
FCGR3B	2307.78612	0.258865367	0.48620922	-0.5324156	0.5944382	0.72128484	0.1418932	no
CD3E	3772.72142	0.25585611	0.3414956	-0.7492223	0.45372324	0.61774526	0.20919058	no
IL1R2	177.225688	0.254478739	0.49926909	-0.5097026	0.61025985	0.72605935	0.13902788	no
JAK2	5120.8998	0.249018248	0.21399918	-1.1636411	0.24456948	0.41564604	0.38127635	no

MMP1	1314.51458	0.244594878	0.38533706	-0.6347557	0.52558779	0.66269765	0.17868457	no
MAF	9653.17113	0.241740252	0.25578591	-0.9450882	0.34461384	0.51250264	0.29030389	no
TNFAIP3	7131.71415	0.229911582	0.26169584	-0.878545	0.37964801	0.54734093	0.26174207	no
KLRB1	1985.69773	0.215872798	0.29544362	-0.7306734	0.46497865	0.62482141	0.2042441	no
MMRN1	1987.36669	0.209470394	0.35410667	-0.591546	0.55415462	0.68095272	0.16688304	no
MKI67	7800.26954	0.207285928	0.29121312	-0.7118015	0.47658772	0.63628163	0.19635061	no
ABCC9	636.055213	0.206281516	0.30954416	-0.6664042	0.5051528	0.65399247	0.18442725	no
GZMK	1222.45935	0.199227499	0.44570975	-0.4469893	0.65488277	0.76433939	0.11671376	no
MCAM	3740.74407	0.182268832	0.28161011	-0.6472382	0.51747777	0.65891873	0.18116814	no
TGFB1	20332.6947	0.165467989	0.44300208	-0.3735151	0.70876507	0.80035742	0.09671603	no
JAK1	11059.4691	0.159933609	0.28179863	-0.5675457	0.57034346	0.69788863	0.15621388	no
TYK2	5738.73775	0.130997963	0.21334874	-0.6140086	0.53920964	0.67111193	0.17320027	no
NRG7	583.09906	0.128220446	0.38985349	-0.3288939	0.74223587	0.82294613	0.08462859	no
TGFBFR1	4446.9934	0.115757565	0.1854311	-0.6242619	0.53245563	0.66573551	0.17669828	no
CD59	17776.8393	0.114739025	0.36018975	-0.3185516	0.75006655	0.82542311	0.08332337	no
LAMP3	3485.7638	0.111537098	0.2172795	-0.5133347	0.60771725	0.72605935	0.13902788	no
PLVAP	5503.58908	0.100715693	0.29239391	-0.3444521	0.73050632	0.81679119	0.08788896	no
IFITM2	2616.48229	0.099663191	0.25482371	-0.3911064	0.69571856	0.79746397	0.09828893	no
MUC1	8206.29814	0.094807607	0.39581826	-0.2395231	0.81070001	0.87075186	0.06010559	no
LYVE1	1537.22231	0.094490719	0.43618356	-0.2166306	0.82849621	0.88008755	0.05547412	no
IRF8	4519.44282	0.091292825	0.25308109	-0.3607256	0.7183046	0.80739664	0.09291306	no
CD8A	1127.59325	0.089263831	0.33926602	-0.2631087	0.79246682	0.86170569	0.06464104	no
FXYD5	5369.07009	0.077229423	0.23600515	-0.3272362	0.74348926	0.82294613	0.08462859	no
TUBB	8071.50028	0.072557631	0.19160592	-0.3786816	0.70492434	0.80035742	0.09671603	no
TNF	1069.46083	0.068719602	0.41367144	-0.1661212	0.86806156	0.91209367	0.03996056	no
KLF2	1876.11788	0.067079451	0.2926839	-0.2291874	0.81872329	0.87612456	0.05743415	no
CYTH1	4619.9569	0.063904798	0.28387189	-0.2251184	0.82188713	0.87627672	0.05735872	no
A2M	18885.8881	0.060866797	0.42583506	-0.1429351	0.8663414	0.92460074	0.03404576	no
S100A4	1685.74879	0.05850637	0.23621184	-0.247686	0.80437735	0.86717261	0.06189445	no
PDGFRA	6603.12943	0.051086071	0.28465802	-0.1794647	0.85757282	0.90434952	0.04366369	no
NPC2	5980.98134	0.050343408	0.19638699	-0.256348	0.79768215	0.86316352	0.06390692	no
SPINK1	10616.1579	0.04361875	0.47363258	-0.0920941	0.9266233	0.94619985	0.02401712	no
ACKR1	1261.60761	0.03260274	0.34354704	-0.0949004	0.92439396	0.94619985	0.02401712	no
STMN1	7112.84912	0.03235154	0.29810948	-0.1085223	0.91358135	0.94284197	0.02556109	no
ZBTB16	709.078541	0.022426795	0.43009456	-0.0521439	0.95841406	0.96506971	0.01544132	no
TPSB2	1488.32088	0.021534502	0.3587389	-0.0600283	0.95213306	0.96506971	0.01544132	no
CD209	3280.26477	0.003264054	0.24106837	-0.01354	0.98919701	0.98919701	0.0047172	no
CDH5	2144.0873	-0.004045773	0.25734635	0.01572112	0.98745688	0.98919701	0.0047172	no
HMG2	7935.80976	-0.016049411	0.29463083	0.05447295	0.96555836	0.96506971	0.01544132	no
KIT	2108.29862	-0.029515672	0.26991548	0.10935153	0.91292367	0.94284197	0.02556109	no
CSF3R	1189.80923	-0.034883345	0.57737823	0.0604168	0.95182368	0.96506971	0.01544132	no
CD7	46.6169971	-0.037133241	0.33447304	0.11102013	0.91160038	0.94284197	0.02556109	no
S1PR1	1096.0719	-0.037891277	0.37594074	0.10079056	0.91971672	0.94580798	0.02419703	no
BATF	409.524264	-0.045188924	0.21545566	0.20973654	0.8338733	0.88256664	0.05425249	no
CD14	5297.90012	-0.045593991	0.2981742	0.15291058	0.87846879	0.91969657	0.03635544	no
TLE4	3245.07062	-0.053038496	0.20247918	0.26194543	0.79336351	0.86170569	0.06464104	no
STAT4	1540.00042	-0.095074739	0.23952759	0.39692605	0.69142199	0.79568404	0.09925935	no
LEF1	3583.37577	-0.109466333	0.24323861	0.45003683	0.65268389	0.76433939	0.11671376	no
GZMA	1227.09625	-0.121277875	0.32529856	0.37282021	0.70928226	0.80035742	0.09671603	no
TOP2A	3752.54684	-0.132913266	0.24951889	0.53267818	0.59425638	0.72128484	0.1418932	no
CCL4	2162.1315	-0.139184019	0.37279479	0.37335291	0.7088858	0.80035742	0.09671603	no
NOTCH4	739.349007	-0.142234533	0.32222474	0.44141406	0.65891326	0.76433939	0.11671376	no
CPA3	3586.24516	-0.146333261	0.24320614	0.60168408	0.54738445	0.67838243	0.16852541	no
TNFRSF11B	1085.42105	-0.150590658	0.33871685	0.44459157	0.65661494	0.76433939	0.11671376	no
UBE2C	1475.25515	-0.153055307	0.24525749	0.62405966	0.53258841	0.66573551	0.17669828	no
CEACAM6	23845.8847	-0.154245261	0.49276587	0.31301937	0.75426595	0.82542311	0.08332337	no
TPSAB1	676.972831	-0.154742995	0.48903784	0.31642336	0.75168119	0.82542311	0.08332337	no
IGHA2	769.55433	-0.172278342	0.36303966	0.47454414	0.63511193	0.74870919	0.12568864	no
GZMB	859.258529	-0.185799038	0.4353451	0.42678564	0.66953546	0.77356687	0.11150214	no
TMEM176A	12356.3759	-0.194352895	0.29780004	0.65262884	0.51399559	0.65891873	0.18116814	no
TIGIT	2064.10891	-0.196532574	0.38319932	0.51287298	0.60804018	0.72605935	0.13902788	no
MS4A7	5283.47913	-0.212709637	0.22244176	0.95624867	0.33894662	0.50929802	0.29302801	no
MYH11	20743.4326	-0.214850742	0.62808348	0.34207354	0.73229555	0.81679119	0.08788896	no
CLEC10A	1867.66406	-0.217331768	0.31241281	0.69565574	0.48664445	0.6428948	0.19186008	no
TMEM176B	19200.2275	-0.229330042	0.33047035	0.69395042	0.4877133	0.6428948	0.19186008	no
POSTN	6799.184	-0.241187528	0.37975855	0.63510757	0.52535826	0.66269765	0.17868457	no
CD86	2135.88046	-0.248732818	0.3168324	0.78506119	0.43241769	0.60000541	0.22184484	no
TUBA1B	57892.879	-0.249738573	0.3243354	0.77000098	0.44129931	0.60652512	0.21715121	no
ANXA2	51690.1993	-0.251112634	0.35416556	0.70902613	0.47830826	0.63628163	0.19635061	no
GATA3	338.898803	-0.256220104	0.34931743	0.7334879	0.46326091	0.62482141	0.2042441	no
APOE	2353.41664	-0.276739333	0.37908991	0.73000976	0.46538422	0.62482141	0.2042441	no
CXCL14	8732.76611	-0.277760178	0.46516198	0.59712571	0.55042346	0.67924597	0.16797293	no
TM4SF1	4506.98939	-0.290386777	0.42434747	0.68431368	0.49377711	0.64794281	0.18846332	no
TNFRSF1A	6989.81671	-0.294922097	0.31154763	0.94663567	0.34382446	0.51250264	0.29030389	no
FOXO3	506.931456	-0.296153861	0.44051069	0.67229665	0.50139486	0.65203816	0.18572698	no
SELENOP	34314.8266	-0.3299702	0.37567706	0.87833472	0.3797621	0.54734093	0.26174207	no
MUC2	12916.4213	-0.334779382	0.65797631	0.50880157	0.61089132	0.72605935	0.13902788	no
LTBR	4714.62655	-0.33737116	0.3301577	1.02184852	0.3068526	0.48116253	0.3177082	no
FCN1	684.105916	-0.347226043	0.45306938	0.76638602	0.44344665	0.60660154	0.21709649	no
ACTG1	105448.403	-0.357071893	0.2771673	1.28829013	0.19764499	0.35067859	0.45509075	no
AGR2	47284.3389	-0.369422326	0.57093239	0.64705092	0.51759899	0.65891873	0.18116814	no
QDPR	2915.60647	-0.369851475	0.21519058	1.71871593	0.08566611	0.19110132	0.71873631	no
DUSP23	915.194974	-0.387868082	0.26902734	1.44174225	0.1493751	0.28312927	0.54801523	no
OSM	540.695673	-0.38869551	0.57151941	0.68010902	0.49643543	0.64849674	0.18809221	no
TYROBP	1596.51563	-0.394821971	0.33967168	1.16236351	0.24508784	0.41564604	0.38127635	no
IFNG	487.783311	-0.395817413	0.37889083	1.04467405	0.29617364	0.47192503	0.32612698	no
TNFSF15	451.778802	-0.426436468	0.37213241	1.14592671	0.25182548	0.4221352	0.37454844	no
S100A16	8527.96765	-0.42647993	0.45902871	0.92909206	0.35284138	0.51941117	0.28448872	no
PROX1	1646.78975	-0.43845515	0.2816277	1.5668609	0.11950352	0.2406668	0.61858381	no
LEFTY1	3988.95609	-0.500070209	0.6139855	0.81446583	0.41537814	0.5876081	0.23091222	no
KLRK1	670.003887	-0.51090705	0.28489865	1.79329404	0.07292592	0.17193916	0.7646252	no
S100B	1431.59288	-0.530535892	0.23046795	2.30199424	0.0213355	0.07365826	1.13277853	yes
HMG2	3212.0311	-0.538534208	0.20022304	2.68967156	0.00715224	0.03703837	1.43134811	yes
CRYAB	2098.64151	-0.543559278	0.32490441	1.67298214	0.09433081	0.20121698	0.69633538	no
RTKN2	1858.83013	-0.547455394	0.31950076	1.71347134	0.08662586	0.19176717	0.71722573	no
IL1RL1	1153.38695	-0.549690879	0.25264318	2.17575983	0.02957322	0.08808589	1.05509365	yes
FLT3	867.918626	-0.566636898	0.36853436	1.51040707	0.13093959	0.25657081	0.59079275	no
KCNJ8	882.613362	-0.566022534	0.40292067	1.40479896	0.16008107	0.29569115	0.52916168	no
XCR1	582.639676	-0.568342817	0.35167409	1.61610658	0.10607127	0.21662443	0.66429257	no

MS4A2	1147.41002	-0.589241169	0.27041282	2.179043	0.02932847	0.08808589	1.05509365	yes
ASPN	1211.93258	-0.596651486	0.40157785	1.48576791	0.13734052	0.26658722	0.57416068	no
TRGC2	1582.5655	-0.601106693	0.26056558	2.30693053	0.02105869	0.07357857	1.13324868	yes
APP	28138.247	-0.616961251	0.35868978	1.72004135	0.08542493	0.19110132	0.71873631	no
IL13RA2	854.347269	-0.621057006	0.52444508	1.18421744	0.236327	0.40553154	0.39197537	no
CS73	10473.5316	-0.63099466	0.28715909	2.19736958	0.02799406	0.08675302	1.06171539	yes
HAND2	636.828897	-0.632897053	0.38077529	1.66212744	0.09648722	0.20130428	0.69614699	no
LILRA4	1838.12172	-0.635626594	0.21497609	2.95673165	0.00310919	0.02422279	1.61577591	yes
TREM1	1611.896	-0.639966607	0.61534959	1.04000493	0.29833761	0.47277545	0.32534509	no
INSM1	994.016817	-0.64477586	0.40269384	1.6011565	0.10934226	0.22174305	0.65414999	no
CPE	2511.08592	-0.647535058	0.34588864	1.87209112	0.061194	0.1478855	0.83007441	no
GSN	26004.6796	-0.64997153	0.37230866	1.74578675	0.08084802	0.18461358	0.73373636	no
IRF7	100.856079	-0.655020781	0.35584164	1.84076484	0.06565603	0.15606761	0.80668723	no
TFF3	10832.0483	-0.664245276	0.50813307	1.30722701	0.19113563	0.34324074	0.46440117	no
CXCR1	657.025772	-0.670383819	0.63427229	1.05693379	0.29054181	0.46809513	0.32966588	no
CCL5	3433.52566	-0.670668446	0.33106816	2.02577149	0.04278821	0.11695823	0.93196923	no
OGN	1294.86949	-0.691371608	0.51448883	1.34380295	0.17901211	0.32445946	0.48883956	no
ADAMDEC1	10264.2272	-0.693748814	0.47111741	1.4725561	0.14087077	0.27054651	0.56775806	no
PYY	288.419992	-0.695341775	0.40813538	1.70370375	0.08843645	0.19429219	0.71154465	no
TNFRSF11A	7263.14539	-0.719036375	0.43020082	1.67139704	0.09464328	0.20121698	0.69633538	no
NUPR1	5388.12845	-0.756354225	0.30258011	2.49968257	0.01243046	0.05224398	1.28196379	yes
LTA	791.260317	-0.771573334	0.53706366	1.43665154	0.15081703	0.28318704	0.54792662	no
KLRC2	1351.28228	-0.808269276	0.32462583	2.48984893	0.01277974	0.05294464	1.27617801	yes
SOX6	1718.78727	-0.8100739	0.26147542	3.09808816	0.00194774	0.01662429	1.77925689	yes
PLAC8	26890.5595	-0.819407735	0.41563114	1.97147823	0.0486692	0.12703782	0.89606698	no
Wfdc2	1460.19394	-0.82854165	0.64409398	1.28636764	0.19831479	0.35067859	0.45509075	no
TRGC1	907.388359	-0.831968936	0.35601342	2.33690332	0.01944421	0.06961508	1.15729668	yes
ITLN1	13676.6227	-0.841688292	0.65713417	1.28084695	0.20024743	0.35195003	0.45351899	no
SOX8	492.621655	-0.850512269	0.42612964	1.99590028	0.04594478	0.12253574	0.91173722	no
CCSER1	2486.56767	-0.851418043	0.28903669	2.94570926	0.00322215	0.02422279	1.61577591	yes
ITM2C	59915.0621	-0.862029806	0.44197187	1.95041779	0.05112634	0.13005824	0.88586212	no
TRDC	982.418259	-0.86215405	0.3107555	2.77438066	0.00553069	0.03047716	1.51602555	yes
S1PR5	221.729939	-0.863489115	0.56294302	1.53388367	0.12505827	0.24840342	0.60484243	no
NEUROD1	791.465371	-0.878235624	0.43429266	2.02222074	0.04315355	0.11695823	0.93196923	no
GLIS3	1096.79648	-0.878573281	0.31693667	2.77207833	0.00556996	0.03047716	1.51602555	yes
FABP5	12212.1062	-0.879388743	0.28386724	3.09788739	0.00194906	0.01662429	1.77925689	yes
ADGRB3	556.980907	-0.8804005	0.37013578	2.37858797	0.01737909	0.06379666	1.19520207	yes
ASCL2	1023.18462	-0.896728423	0.42958023	2.08745271	0.03684723	0.10579898	0.97551852	no
TNFSF9	233.517645	-0.920825108	0.43441774	2.11967657	0.03403333	0.09969359	1.00133275	no
CSPG4	2330.574	-0.920839821	0.40632897	2.2662421	0.02343656	0.07723413	1.11219073	yes
CCL8	795.427419	-0.92668492	0.3822066	2.42456543	0.01532672	0.05698396	1.24424735	yes
SOX9	4574.56688	-0.928899879	0.4656432	1.99487479	0.04605654	0.12253574	0.91173722	no
INAVA	4294.78486	-0.93599246	0.41195267	2.27208739	0.02308123	0.07723413	1.11219073	yes
TPH1	2162.42886	-0.95446585	0.42009332	2.27203293	0.02308452	0.07723413	1.11219073	yes
TRAV1-2	415.503525	-0.979896722	0.44623069	2.19594204	0.02809609	0.08675302	1.06171539	no
TINAGL1	3562.7049	-0.988860877	0.37468292	2.6391939	0.00831034	0.04155172	1.38141102	yes
FCER1A	1467.9427	-0.996139113	0.40953658	2.43235685	0.01500092	0.05649697	1.24797484	yes
IL10	695.611225	-0.998995837	0.45218367	2.20927007	0.02715586	0.08654066	1.0627798	yes
CLEC9A	681.956717	-1.01077522	0.38547552	2.62215753	0.0087375	0.04294705	1.36706665	yes
FOLR3	190.086772	-1.028690102	0.58152192	1.76896186	0.07690024	0.17699262	0.75204485	no
LGR5	1818.8912	-1.038843835	0.50935902	2.03951202	0.04139895	0.11559921	0.93704514	no
MGLL	6414.94017	-1.040525273	0.36287338	2.86746101	0.0041378	0.02926735	1.5336166	yes
CCL23	584.543271	-1.055967304	0.32774724	3.22189537	0.00127346	0.01407847	1.85144466	yes
NCAM1	1040.62283	-1.072975749	0.31516595	3.40447861	0.00066291	0.00873829	2.05857345	yes
RORC	2441.77639	-1.076352143	0.32447686	3.31719228	0.00090927	0.01098702	1.95912028	yes
CD8B	1926.92698	-1.076930465	0.43470723	2.47736957	0.01323548	0.05401369	1.26749616	yes
HPGDS	935.045685	-1.081433936	0.30848182	3.5056651	0.00045547	0.00733809	2.13441673	yes
CEACAM1	21259.322	-1.083730291	0.49452612	2.19145209	0.02841909	0.08675302	1.06171539	yes
TRGV9	716.779404	-1.083847352	0.38261772	2.83271603	0.00461544	0.03002352	1.52253846	yes
GATA2	2043.52493	-1.09515286	0.31568336	3.46922079	0.00052197	0.00796692	2.09870982	yes
PLP1	686.667114	-1.110634786	0.35401713	3.13723458	0.0017055	0.01630356	1.78771753	yes
CACNA1A	960.236156	-1.12006772	0.44448851	2.51990252	0.01173873	0.05039473	1.2976149	yes
NTRK2	1115.41481	-1.134323876	0.43789356	2.59041006	0.00958617	0.04585076	1.33865343	yes
TRDV2	198.094352	-1.154833903	0.47369223	2.4379414	0.01477117	0.05649697	1.24797484	no
PHLDA2	358.524149	-1.21110305	0.37835647	3.20095766	0.00136972	0.01418635	1.84812933	yes
KRT8	97907.0904	-1.255598483	0.43175457	2.90813017	0.00363597	0.02636078	1.57904176	yes
C7	2206.58325	-1.259853661	0.53363456	2.36089218	0.01823103	0.06608748	1.17988078	yes
IL32	5750.57097	-1.301140683	0.32410249	4.01459635	5.95E-05	0.00255326	2.59290428	yes
EPCAM	57971.1687	-1.312016935	0.52085126	2.51898584	0.01176934	0.05039473	1.2976149	yes
MS4A8	1287.98924	-1.313573162	0.4702177	2.79354257	0.00521342	0.03002352	1.52253846	yes
C15orf48	26739.1836	-1.314316204	0.52205713	2.51757161	0.0118167	0.05039473	1.2976149	yes
IGHE	97.0412267	-1.326356501	0.74521104	1.77984011	0.07510213	0.17564208	0.75537142	no
DUSP1	7987.84709	-1.334020115	0.54240834	2.4594388	0.01391544	0.05528052	1.25742785	yes
CA4	10499.4036	-1.355132063	0.70416733	1.92444609	0.05429869	0.1345865	0.8709985	no
TREM2	853.424568	-1.374656617	0.51063852	2.69203472	0.00710176	0.03703837	1.43134811	yes
PIGR	117128.085	-1.374798454	0.54046775	2.54371966	0.01096791	0.04893374	1.3103916	yes
LGALS4	94777.0134	-1.376957257	0.62043026	2.21935866	0.02646233	0.08526752	1.06921636	yes
CLDN5	889.083778	-1.413466752	0.43983701	3.21361484	0.00131075	0.01407847	1.85144466	yes
PHGR1	74019.8639	-1.506143806	0.61823876	2.43618471	0.0148431	0.05649697	1.24797484	yes
SH2D6	207.044499	-1.565720391	0.45609034	3.43291721	0.00059712	0.008246	2.08375646	no
FABP2	5896.1976	-1.61008423	0.56715757	2.83886579	0.00452742	0.03002352	1.52253846	yes
JUN	13975.4846	-1.68586719	0.40952534	4.11663711	3.84E-05	0.00255326	2.59290428	yes
FABP1	63313.6438	-1.777128568	0.69163101	2.56947498	0.01018528	0.0468846	1.3289698	yes
TRPM5	803.841932	-1.778431142	0.45782584	3.8845146	0.00010254	0.00270318	2.56812455	yes
CA7	1298.27157	-1.821126865	0.55630216	3.273629	0.00106176	0.01231641	1.909516	no
MTG1	237.253781	-1.935739452	0.53328129	3.62986566	0.00028357	0.00513968	2.28906358	yes
DDC	5190.05703	-1.958693357	0.49628768	3.94668944	7.92E-05	0.00255326	2.59290428	yes
OTOP2	738.768648	-1.964202761	0.66756758	2.94232798	0.00325755	0.02422279	1.61577591	yes
BEST4	551.312459	-2.154949713	0.53770077	4.00771177	6.13E-05	0.00255326	2.59290428	yes
LYPD8	8786.16714	-2.365349345	0.6323874	3.74034861	0.00018377	0.00363757	2.43918912	yes
SLC26A2	20711.8808	-2.627487213	0.67124898	3.91432583	9.07E-05	0.00262906	2.5802	yes
GUCA2A	1260.16858	-2.809367372	0.73362335	3.82944106	0.00012844	0.00310384	2.50810109	yes
AQP8	10362.8134	-2.971248595	0.99182156	2.99574914	0.00273772	0.02218742	1.65389322	yes

Supplementary Table 4. Pseudobulk DE gene analysis of Xenium data comparing colon biopsies in UC PRE versus HC. Significance was set as log2fc >0.4 or <-0.4, p-adj < 0.1 and baseMean >500.

AFAP3 56239889 -0.04726639 0.14651106 0.3043732 0.7698666 0.9819682 0.06848021 0.00000000
PF0016 44147311 -0.04270071 -0.06192379 0.6920007 0.4484944 0.9047515 0.0207462 0.15686822
DMTA 49187515 -0.04134884 0.02963746 0.7292145 0.4893929 0.8912032 0.19034808 0.00000000
GATA4 34514474 -0.04084454 0.02963746 0.7292145 0.4893929 0.8912032 0.19034808 0.00000000
GATA 49189337 -0.04084454 0.02963746 0.7292145 0.4893929 0.8912032 0.19034808 0.00000000
CSTF 48035930 -0.04084454 0.02963746 0.7292145 0.4893929 0.8912032 0.19034808 0.00000000
E 38338764 -0.04084454 0.02963746 0.7292145 0.4893929 0.8912032 0.19034808 0.00000000
RSB 07726812 -0.04084454 0.02963746 0.7292145 0.4893929 0.8912032 0.19034808 0.00000000
AD0906 37479474 -0.04084454 0.02963746 0.7292145 0.4893929 0.8912032 0.19034808 0.00000000
LEP 36356828 -0.04078601 0.02963746 0.7292145 0.4893929 0.8912032 0.19034808 0.00000000
BST1 23844452 -0.04073772 0.02963746 0.7292145 0.4893929 0.8912032 0.19034808 0.00000000
WPI1 40413963 -0.04073772 0.02963746 0.7292145 0.4893929 0.8912032 0.19034808 0.00000000
WPI2 30104875 -0.04073772 0.02963746 0.7292145 0.4893929 0.8912032 0.19034808 0.00000000
CLZD1 46424164 -0.04068061 0.02963746 0.7292145 0.4893929 0.8912032 0.19034808 0.00000000
GPIK 48048737 -0.04068061 0.02963746 0.7292145 0.4893929 0.8912032 0.19034808 0.00000000
AD093 56838444 -0.04064345 0.02963746 0.7292145 0.4893929 0.8912032 0.19034808 0.00000000
TUT1 41817844 -0.04059427 0.02963746 0.7292145 0.4893929 0.8912032 0.19034808 0.00000000
FMS2 66811981 -0.04044475 0.02963746 0.7292145 0.4893929 0.8912032 0.19034808 0.00000000
CSTF 26968603 -0.04039556 0.02963746 0.7292145 0.4893929 0.8912032 0.19034808 0.00000000
TCTF 38452645 -0.04034627 0.02963746 0.7292145 0.4893929 0.8912032 0.19034808 0.00000000
SST 51555113 -0.04029698 0.02963746 0.7292145 0.4893929 0.8912032 0.19034808 0.00000000
CHEK2 25430021 -0.04024769 0.02963746 0.7292145 0.4893929 0.8912032 0.19034808 0.00000000
CDY 41442867 -0.04019840 0.02963746 0.7292145 0.4893929 0.8912032 0.19034808 0.00000000
FTV5 15252162 -0.04014911 0.02963746 0.7292145 0.4893929 0.8912032 0.19034808 0.00000000
SCLRA 32488844 -0.04009982 0.02963746 0.7292145 0.4893929 0.8912032 0.19034808 0.00000000
ITD4 46452174 -0.04005053 0.02963746 0.7292145 0.4893929 0.8912032 0.19034808 0.00000000
DORR 70248478 -0.04000124 0.02963746 0.7292145 0.4893929 0.8912032 0.19034808 0.00000000
ELN1B 36844837 -0.03995195 0.02963746 0.7292145 0.4893929 0.8912032 0.19034808 0.00000000
FOGFB 38659767 -0.03990266 0.02963746 0.7292145 0.4893929 0.8912032 0.19034808 0.00000000
CCIL 39818573 -0.03985337 0.02963746 0.7292145 0.4893929 0.8912032 0.19034808 0.00000000
OPB3 27818484 -0.03980408 0.02963746 0.7292145 0.4893929 0.8912032 0.19034808 0.00000000
CYTOR 10333679 -0.03975479 0.02963746 0.7292145 0.4893929 0.8912032 0.19034808 0.00000000
CDM 48732636 -0.03970550 0.02963746 0.7292145 0.4893929 0.8912032 0.19034808 0.00000000
FCOR3AB 60925607 -0.03965621 0.02963746 0.7292145 0.4893929 0.8912032 0.19034808 0.00000000
DORR 48732636 -0.03960692 0.02963746 0.7292145 0.4893929 0.8912032 0.19034808 0.00000000
TFUSF8 47324016 -0.03955762 0.02963746 0.7292145 0.4893929 0.8912032 0.19034808 0.00000000
CLZD2 38818174 -0.03950833 0.02963746 0.7292145 0.4893929 0.8912032 0.19034808 0.00000000
WPI1 50173847 -0.03945904 0.02963746 0.7292145 0.4893929 0.8912032 0.19034808 0.00000000
JUNB 92057929 -0.03940975 0.02963746 0.7292145 0.4893929 0.8912032 0.19034808 0.00000000
FPI1 66570497 -0.03936046 0.02963746 0.7292145 0.4893929 0.8912032 0.19034808 0.00000000
CLC1Y 47850104 -0.03931117 0.02963746 0.7292145 0.4893929 0.8912032 0.19034808 0.00000000
ZDN6 38835845 -0.03926188 0.02963746 0.7292145 0.4893929 0.8912032 0.19034808 0.00000000
ATD2 46155849 -0.03921259 0.02963746 0.7292145 0.4893929 0.8912032 0.19034808 0.00000000
MDC1 55482629 -0.03916330 0.02963746 0.7292145 0.4893929 0.8912032 0.19034808 0.00000000
MIFP9 20774635 -0.03911401 0.02963746 0.7292145 0.4893929 0.8912032 0.19034808 0.00000000
MIFP10 37551811 -0.03906472 0.02963746 0.7292145 0.4893929 0.8912032 0.19034808 0.00000000
SMAD2 47574621 -0.03901543 0.02963746 0.7292145 0.4893929 0.8912032 0.19034808 0.00000000
E1 47274073 -0.03896614 0.02963746 0.7292145 0.4893929 0.8912032 0.19034808 0.00000000
E1 47274073 -0.03891685 0.02963746 0.7292145 0.4893929 0.8912032 0.19034808 0.00000000
E1 47274073 -0.03886756 0.02963746 0.7292145 0.4893929 0.8912032 0.19034808 0.00000000
E1 47274073 -0.03881827 0.02963746 0.7292145 0.4893929 0.8912032 0.19034808 0.00000000
E1 47274073 -0.03876898 0.02963746 0.7292145 0.4893929 0.8912032 0.19034808 0.00000000
E1 47274073 -0.03871969 0.02963746 0.7292145 0.4893929 0.8912032 0.19034808 0.00000000
E1 47274073 -0.03867040 0.02963746 0.7292145 0.4893929 0.8912032 0.19034808 0.00000000
E1 47274073 -0.03862111 0.02963746 0.7292145 0.4893929 0.8912032 0.19034808 0.00000000
E1 47274073 -0.03857182 0.02963746 0.7292145 0.4893929 0.8912032 0.19034808 0.00000000
E1 47274073 -0.03852253 0.02963746 0.7292145 0.4893929 0.8912032 0.19034808 0.00000000
E1 47274073 -0.03847324 0.02963746 0.7292145 0.4893929 0.8912032 0.19034808 0.00000000
E1 47274073 -0.03842395 0.02963746 0.7292145 0.4893929 0.8912032 0.19034808 0.00000000
E1 47274073 -0.03837466 0.02963746 0.7292145 0.4893929 0.8912032 0.19034808 0.00000000
E1 47274073 -0.03832537 0.02963746 0.7292145 0.4893929 0.8912032 0.19034808 0.00000000
E1 47274073 -0.03827608 0.02963746 0.7292145 0.4893929 0.8912032 0.19034808 0.00000000
E1 47274073 -0.03822679 0.02963746 0.7292145 0.4893929 0.8912032 0.19034808 0.00000000
E1 47274073 -0.03817750 0.02963746 0.7292145 0.4893929 0.8912032 0.19034808 0.00000000
E1 47274073 -0.03812821 0.02963746 0.7292145 0.4893929 0.8912032 0.19034808 0.00000000
E1 47274073 -0.03807892 0.02963746 0.7292145 0.4893929 0.8912032 0.19034808 0.00000000
E1 47274073 -0.03802963 0.02963746 0.7292145 0.4893929 0.8912032 0.19034808 0.00000000
E1 47274073 -0.03798034 0.02963746 0.7292145 0.4893929 0.8912032 0.19034808 0.00000000
E1 47274073 -0.03793105 0.02963746 0.7292145 0.4893929 0.8912032 0.19034808 0.00000000
E1 47274073 -0.03788176 0.02963746 0.7292145 0.4893929 0.8912032 0.19034808 0.00000000
E1 47274073 -0.03783247 0.02963746 0.7292145 0.4893929 0.8912032 0.19034808 0.00000000
E1 47274073 -0.03778318 0.02963746 0.7292145 0.4893929 0.8912032 0.19034808 0.00000000
E1 47274073 -0.03773389 0.02963746 0.7292145 0.4893929 0.8912032 0.19034808 0.00000000
E1 47274073 -0.03768460 0.02963746 0.7292145 0.4893929 0.8912032 0.19034808 0.00000000
E1 47274073 -0.03763531 0.02963746 0.7292145 0.4893929 0.8912032 0.19034808 0.00000000
E1 47274073 -0.03758602 0.02963746 0.7292145 0.4893929 0.8912032 0.19034808 0.00000000
E1 47274073 -0.03753673 0.02963746 0.7292145 0.4893929 0.8912032 0.19034808 0.00000000
E1 47274073 -0.03748744 0.02963746 0.7292145 0.4893929 0.8912032 0.19034808 0.00000000
E1 47274073 -0.03743815 0.02963746 0.7292145 0.4893929 0.8912032 0.19034808 0.00000000
E1 47274073 -0.03738886 0.02963746 0.7292145 0.4893929 0.8912032 0.19034808 0.00000000
E1 47274073 -0.03733957 0.02963746 0.7292145 0.4893929 0.8912032 0.19034808 0.00000000
E1 47274073 -0.03729028 0.02963746 0.7292145 0.4893929 0.8912032 0.19034808 0.00000000
E1 47274073 -0.03724099 0.02963746 0.7292145 0.4893929 0.8912032 0.19034808 0.00000000
E1 47274073 -0.03719170 0.02963746 0.7292145 0.4893929 0.8912032 0.19034808 0.00000000
E1 47274073 -0.03714241 0.02963746 0.7292145 0.4893929 0.8912032 0.19034808 0.00000000
E1 47274073 -0.03709312 0.02963746 0.7292145 0.4893929 0.8912032 0.19034808 0.00000000
E1 47274073 -0.03704383 0.02963746 0.7292145 0.4893929 0.8912032 0.19034808 0.00000000
E1 47274073 -0.03699454 0.02963746 0.7292145 0.4893929 0.8912032 0.19034808 0.00000000
E1 47274073 -0.03694525 0.02963746 0.7292145 0.4893929 0.8912032 0.19034808 0.00000000
E1 47274073 -0.03689596 0.02963746 0.7292145 0.4893929 0.8912032 0.19034808 0.00000000
E1 47274073 -0.03684667 0.02963746 0.7292145 0.4893929 0.8912032 0.19034808 0.00000000
E1 47274073 -0.03679738 0.02963746 0.7292145 0.4893929 0.8912032 0.19034808 0.00000000
E1 47274073 -0.03674809 0.02963746 0.7292145 0.4893929 0.8912032 0.19034808 0.00000000
E1 47274073 -0.03669880 0.02963746 0.7292145 0.4893929 0.8912032 0.19034808 0.00000000
E1 47274073 -0.03664951 0.02963746 0.7292145 0.4893929 0.8912032 0.19034808 0.00000000
E1 47274073 -0.03660022 0.02963746 0.7292145 0.4893929 0.8912032 0.19034808 0.00000000
E1 47274073 -0.03655093 0.02963746 0.7292145 0.4893929 0.8912032 0.19034808 0.00000000
E1 47274073 -0.03650164 0.02963746 0.7292145 0.4893929 0.8912032 0.19034808 0.00000000
E1 47274073 -0.03645235 0.02963746 0.7292145 0.4893929 0.8912032 0.19034808 0.00000000
E1 47274073 -0.03640306 0.02963746 0.7292145 0.4893929 0.8912032 0.19034808 0.00000000
E1 47274073 -0.03635377 0.02963746 0.7292145 0.4893929 0.8912032 0.19034808 0.00000000
E1 47274073 -0.03630448 0.02963746 0.7292145 0.4893929 0.8912032 0.19034808 0.00000000
E1 47274073 -0.03625519 0.02963746 0.7292145 0.4893929 0.8912032 0.19034808 0.00000000
E1 47274073 -0.03620590 0.02963746 0.7292145 0.4893929 0.8912032 0.19034808 0.00000000
E1 47274073 -0.03615661 0.02963746 0.7292145 0.4893929 0.8912032 0.19034808 0.00000000
E1 47274073 -0.03610732 0.02963746 0.7292145 0.4893929 0.8912032 0.19034808 0.00000000
E1 47274073 -0.03605803 0.02963746 0.7292145 0.4893929 0.8912032 0.19034808 0.00000000
E1 47274073 -0.03600874 0.02963746 0.7292145 0.4893929 0.8912032 0.19034808 0.00000000
E1 47274073 -0.03595945 0.02963746 0.7292145 0.4893929 0.8912032 0.19034808 0.00000000
E1 47274073 -0.03591016 0.02963746 0.7292145 0.4893929 0.8912032 0.19034808 0.00000000
E1 47274073 -0.03586087 0.02963746 0.7292145 0.4893929 0.8912032 0.19034808 0.00000000
E1 47274073 -0.03581158 0.02963746 0.7292145 0.4893929 0.8912032 0.19034808 0.00000000
E1 47274073 -0.03576229 0.02963746 0.7292145 0.4893929 0.8912032 0.19034808 0.00000000
E1 47274073 -0.03571300 0.02963746 0.7292145 0.4893929 0.8912032 0.19034808 0.00000000
E1 47274073 -0.03566371 0.02963746 0.7292145 0.4893929 0.8912032 0.19034808 0.00000000
E1 47274073 -0.03561442 0.02963746 0.7292145 0.4893929 0.8912032 0.19034808 0.00000000
E1 47274073 -0.03556513 0.02963746 0.7292145 0.4893929 0.8912032 0.19034808 0.00000000
E1 47274073 -0.03551584 0.02963746 0.7292145 0.4893929 0.8912032 0.19034808 0.00000000
E1 47274073 -0.03546655 0.02963746 0.7292145 0.4893929 0.8912032 0.19034808 0.00000000
E1 47274073 -0.03541726 0.02963746 0.7292145 0.4893929 0.8912032 0.19034808 0.00000000
E1 47274073 -0.03536797 0.02963746 0.7292145 0.4893929 0.8912032 0.19034808 0.00000000
E1 47274073 -0.03531868 0.02963746 0.7292145 0.4893929 0.8912032 0.19034808 0.00000000
E1 47274073 -0.03526939 0.02963746 0.7292145 0.4893929 0.8912032 0.19034808 0.00000000
E1 47274073 -0.03522010 0.02963746 0.7292145 0.4893929 0.8912032 0.19034808 0.00000000
E1 47274073 -0.03517081 0.02963746 0.7292145 0.4893929 0.8912032 0.19034808 0.00000000
E1 47274073 -0.03512152 0.02963746 0.7292145 0.4893929 0.8912032 0.19034808 0.00000000
E1 47274073 -0.03507223 0.02963746 0.7292145 0.4893929 0.8912032 0.19034808 0.00000000
E1 47274073 -0.03502294 0.02963746 0.7292145 0.4893929 0.8912032 0.19034808 0.00000000
E1 47274073 -0.03497365 0.02963746 0.7292145 0.4893929 0.8912032 0.19034808 0.00000000
E1 47274073 -0.03492436 0.02963746 0.7292145 0.4893929 0.8912032 0.19034808 0.00000000
E1 47274073 -0.03487507 0.02963746 0.7292145 0.4893929 0.8912032 0.19034808 0.00000000
E1 47274073 -0.03482578 0.02963746 0.7292145 0.4893929 0.8912032 0.19034808 0.00000000
E1 47274073 -0.03477649 0.02963746 0.7292145 0.4893929 0.8912032 0.19034808 0.00000000
E1 47274073 -0.03472720 0.02963746 0.7292145 0.4893929 0.8912032 0.19034808 0.00000000
E1 47274073 -0.03467791 0.02963746 0.7292145 0.4893929 0.8912032 0.19034808 0.00000000
E1 47274073 -0.03462862 0.02963746 0.7292145 0.4893929 0.8912032 0.19034808 0.00000000
E1 47274073 -0.03457933 0.02963746 0.7292145 0.4893929 0.8912032 0.19034808 0.00000000
E1 47274073 -0.03453004 0.02963746 0.7292145 0.4893929 0.8912032 0.19034808 0.00000000
E1 47274073 -0.03448075 0.02963746 0.7292145 0.4893929 0.8912032 0.19034808 0.00000000
E1 47274073 -0.03443146 0.02963746 0

BTSM	438.28034	-0.1921855	0.0927747	1.7056493	0.0970068	0.2791989	0.5529046	no
BCSA	434.52041	-0.1915349	0.0771288	1.6945453	0.1059952	0.3092053	0.5729582	no
PF26	421.85338	-0.1946157	0.0644165	1.8545495	0.0636562	0.2829194	0.6499888	no
ELPBA	407.62747	-0.1951028	0.0749645	1.4825254	0.0717650	0.1892744	0.5470958	no
FFN	347.55617	-0.1996877	0.0735173	1.6277916	0.1015689	0.3036074	0.5173284	no
AEY	355.55997	-0.1204722	0.0546925	1.5948176	0.0713629	0.1824202	0.5202651	no
PHARD	548.58147	-0.1213665	0.0711351	1.7051247	0.0878848	0.2791989	0.5530345	no
TN0A8	614.04837	-0.1219981	0.0695241	1.4810571	0.0720275	0.1892744	0.5470958	no
CLC22	390.39429	-0.1222589	0.0739707	1.6252003	0.0841433	0.2944664	0.4705333	no
MMZL	360.69683	-0.1232054	0.0642659	1.3072044	0.1089962	0.2422137	0.3794276	no
REFR8	437.77904	-0.1246841	0.0691622	1.2864706	0.0988323	0.1792287	0.3749749	no
NAME	338.28242	-0.1242268	0.0691432	1.7901484	0.0724271	0.2474234	0.6070209	no
IC41	588.70745	-0.1244447	0.0749448	1.6514445	0.0872761	0.2474234	0.5326582	no
AL4	440.02084	-0.1246324	0.0623264	1.2007892	0.0444724	0.1024496	0.1769122	no
CLC81	474.42023	-0.1250433	0.0526462	1.0713947	0.0729862	0.1892744	0.5470958	no
FLAC	440.94732	-0.1256718	0.0738738	1.7011488	0.0981768	0.2813861	0.5569947	no
LE4	524.69643	-0.1259276	0.0762958	1.7591922	0.0810151	0.1492268	0.3251028	no
EFNA5	419.19943	-0.1262034	0.0714855	1.7814974	0.0779754	0.2544924	0.5943204	no
COLB4	255.26204	-0.1262042	0.0723976	1.7412304	0.0814444	0.2627738	0.5825207	no
TEP1	566.62627	-0.1262984	0.0724888	1.7366252	0.0824741	0.1407191	0.3524148	no
KJK	431.07888	-0.1264745	0.0520233	1.4875305	0.1386780	0.3612087	0.4421861	no
CS05	585.89892	-0.1265407	0.0733468	1.6832658	0.0928755	0.2320703	0.5429786	no
RKX	538.62916	-0.1262870	0.0677493	1.908726	0.0595637	0.2142203	0.6691370	no
NDF42.2	470.24524	-0.1266478	0.0574845	1.5335545	0.0917193	0.1121528	0.4946943	no
NLRC4	387.88186	-0.1289200	0.0589422	1.2871485	0.0288848	0.1478719	0.3304117	no
COE2	355.91918	-0.1295107	0.0494463	1.5428165	0.1734071	0.142252	0.3841281	no
RFZ	419.91515	-0.1297144	0.0818833	1.8886717	0.1120781	0.312615	0.4926329	no
BEK	448.70305	-0.1311248	0.0816833	1.8823962	0.1348178	0.3832357	0.4484628	no
TNFRF14	665.07723	-0.1323261	0.107033	1.2867765	0.1220781	0.4822135	0.6451629	no
TNFRF24	509.18427	-0.1323246	0.0694732	1.9058946	0.0917887	0.2142203	0.6691370	no
LEW	314.78229	-0.1327662	0.0707351	1.3052163	0.1759815	0.3077568	0.3969903	no
TNFRF14	670.31241	-0.1324754	0.0909126	1.3884774	0.1802404	0.4136034	0.3841281	no
APC21	670.81892	-0.1328724	0.0654466	1.5548776	0.1169153	0.3387762	0.4700819	no
EFNA2	331.12378	-0.1329129	0.0507313	1.4189122	0.1561015	0.1807386	0.4969938	no
TNFRF12	548.5125	-0.1314473	0.0811288	1.5491963	0.1221241	0.4060066	0.4877432	no
TEP2	517.76962	-0.1347818	0.0816222	1.992691	0.1717427	0.2691198	0.4882916	no
PGF14	530.29681	-0.1349566	0.1004201	1.6006512	0.1932346	0.442137	0.3724762	no
TLM	330.52369	-0.13698105	0.0747107	1.8622084	0.062474	0.2688877	0.6410741	no
DOC	584.71737	-0.1362854	0.0846744	1.6848488	0.0926927	0.2069074	0.5241183	no
FLN	535.55057	-0.1365448	0.0589251	1.4869349	0.0142828	0.1085716	0.5472982	no
WRG5	565.11970	-0.1391255	0.0579238	1.2555336	0.0843463	0.178477	0.4441173	no
FALB3	1650.44138	-0.1397265	0.0785208	1.7793488	0.0751765	0.230032	0.6020074	no
HNK4	586.96154	-0.1407433	0.0695111	1.3247898	0.0811006	0.1424664	0.4907303	no
COL3A3	445.97371	-0.1420757	0.0794368	1.7760427	0.0737227	0.2520302	0.6020074	no
NKX2	402.94207	-0.1420989	0.0794368	1.7760427	0.0737227	0.2520302	0.6020074	no
FAM2P	412.34473	-0.14118673	0.0794368	1.7760427	0.0737227	0.2520302	0.6020074	no
ITAC1	489.87048	-0.1418164	0.0696847	1.2027134	0.0242668	0.1324484	0.3173208	no
MFH9	527.51678	-0.1423573	0.0707041	1.2027134	0.0448815	0.1917681	0.3173208	no
AL17A	475.61481	-0.1430949	0.0739972	1.9513248	0.0512256	0.2044201	0.6889176	no
ICM21	621.74248	-0.1444774	0.0742974	1.8915031	0.0469463	0.0632324	0.7622329	no
AAT4	478.85868	-0.1446478	0.0596972	1.5983919	0.0042870	0.0781093	1.0732166	no
ICL12	608.22556	-0.1441180	0.0748625	1.6254243	0.0417821	0.2148111	0.6737033	no
HLB2	402.3433	-0.1476208	0.0643297	1.7784887	0.0757915	0.2520302	0.6020074	no
DJF9	587.82035	-0.1465847	0.0695111	1.3247898	0.0811006	0.1424664	0.4907303	no
AMR2	621.92849	-0.1490242	0.0742023	1.4007008	0.0901884	0.0781093	1.0732166	no
ICD9F	578.79242	-0.1493181	0.081864	1.4248599	0.011327	0.0781093	1.0732166	no
MTM1	573.29207	-0.1495148	0.0814456	1.8381874	0.0813346	0.2324335	0.6307251	no
BCR4	488.89384	-0.1512141	0.0837204	1.2119116	0.0209993	0.1443303	0.8466292	no
TFB2	474.47171	-0.1515237	0.0262964	1.2681825	0.0488817	0.0444156	1.2618971	no
FRF2	588.85781	-0.1517129	0.0713481	1.8789257	0.0328929	0.1711549	0.7491654	no
MLL12	371.54133	-0.1521222	0.0807133	1.8731823	0.082027	0.0881328	0.5446258	no
NLRC4	397.88186	-0.1522833	0.0589251	1.2871485	0.0288848	0.1478719	0.3304117	no
BT1	477.23307	-0.1538816	0.0696277	1.1023897	0.0855151	0.1498179	0.8209465	no
IL1RL1	282.15151	-0.1538833	0.0736629	1.9068454	0.0465009	0.1633324	0.7622329	no
IL1RL2	324.49077	-0.1540928	0.0736629	1.9068454	0.0465009	0.1633324	0.7622329	no
TNFRF3	370.34451	-0.15399152	0.089513	1.2332713	0.0253331	0.180179	0.8806492	no
WRG18	565.74828	-0.1543397	0.0491176	1.1714225	0.0916281	0.0340486	1.0529242	no
RSK1	399.91865	-0.1547409	0.0545219	1.815249	0.0718617	0.2413191	0.6174738	no
MLK1	467.2328	-0.1569278	0.0840524	1.4307765	0.015096	0.0696642	1.0122847	no
ABL1	483.88816	-0.1569289	0.0840524	1.4307765	0.015096	0.0696642	1.0122847	no
EFNA6	434.01338	-0.1593028	0.0797562	1.2526712	0.0242674	0.1334484	0.8743704	no
PLTAL2	448.07778	-0.1598813	0.0759144	1.0719668	0.0715481	0.1791368	0.7491654	no
NLRC4	397.88186	-0.1598813	0.0759144	1.0719668	0.0715481	0.1791368	0.7491654	no
NR1H2	246.21481	-0.1600824	0.0788628	1.2039815	0.0437020	0.1917581	0.7171808	no
SPRY3	403.47028	-0.1605783	0.0813521	1.8464586	0.0821313	0.2207344	0.6482369	no
FZD5	714.71084	-0.1610522	0.1292134	1.4402014	0.0211694	0.4405309	0.3024077	no
EFNA8	488.49986	-0.1622881	0.0814671	1.7734453	0.0811881	0.2020398	0.6174687	no
CELSR2	447.02791	-0.1625734	0.0913229	1.5745465	0.0103102	0.0603174	1.0982253	no
LYN	507.86222	-0.1631177	0.0642314	1.4200666	0.0107079	0.085716	1.0478262	no
LEP11	717.52181	-0.1644258	0.1492617	1.259186	0.282661	0.6881777	0.3024077	no
HEY1	503.87102	-0.16514813	0.0592993	1.7782891	0.0758884	0.2020398	0.6174687	no
AEY	355.55997	-0.1651838	0.0592993	1.7782891	0.0758884	0.2020398	0.6174687	no
APC21	670.81892	-0.1658363	0.0785208	1.7793488	0.0833969	0.2819121	0.5503348	no
AGE	389.91939	-0.1668710	0.0202787	1.6033165	0.0717823	0.1798207	1.1327463	no
EFNA6	434.01338	-0.1688712	0.0640346	1.6058197	0.0081191	0.0781093	1.0732166	no
FNY1A	520.59978	-0.1698179	0.0728222	1.9994421	0.0512989	0.0781093	1.0732166	no
CSDEA	296.79017	-0.1678642	0.0284141	1.8038797	0.0738275	0.2413191	0.6174738	no
ROP	578.84223	-0.1684194	0.0826232	1.4248599	0.011327	0.0781093	1.0732166	no
SPRY3	403.47028	-0.1685734	0.0813521	1.8464586	0.0821313	0.2207344	0.6482369	no
CELSR2	447.02791	-0.1692574	0.0913229	1.5745465	0.0103102	0.0603174	1.0982253	no
LYN	507.86222	-0.1631177	0.0642314	1.4200666	0.0107079	0.085716	1.0478262	no
LEP11	717.52181	-0.1644258	0.1492617	1.259186	0.282661	0.6881777	0.3024077	no
HEY1	503.87102	-0.16514813	0.0592993	1.7782891	0.0758884	0.2020398	0.6174687	no
AEY	355.55997	-0.1651838	0.0592993	1.7782891	0.0758884	0.2020398	0.6174687	no
APC21	670.81892	-0.1658363	0.0785208	1.7793488	0.0833969	0.2819121	0.5503348	no
AGE	389.91939	-0.1668710	0.0202787	1.6033165	0.0717823	0.1798207	1.1327463	no
EFNA6	434.01338	-0.1688712	0.0640346	1.6058197	0.0081191	0.0781093	1.0732166	no
FNY1A	520.59978	-0.1698179	0.0728222	1.9994421	0.0512989	0.0781093	1.0732166	no
CSDEA	296.79017	-0.1678642	0.0284141	1.8038797	0.0738275	0.2413191	0.6174738	no
ROP	578.84223	-0.1684194	0.0826232	1.4248599	0.011327	0.0781093	1.0732166	no
SPRY3	403.47028	-0.1685734	0.0813521	1.8464586	0.0821313	0.2207344	0.6482369	no
CELSR2	447.02791	-0.1692574	0.0913229	1.5745465	0.0103102	0.0603174	1.0982253	no
LYN	507.86222	-0.1631177	0.0642314	1.4200666	0.0107079	0.085716	1.0478262	no
LEP11	717.52181	-0.1644258	0.1492617	1.259186	0.282661	0.6881777	0.3024077	no
HEY1	503.87102	-0.16514813	0.0592993	1.7782891	0.0758884	0.2020398	0.6174687	no
AEY	355.55							

	baseMean	log2FoldChange	lfcSE	stat	pvalue	padj	$-\log_{10}(q\text{-value})$	Significance
MMP1	4356.24289	3.41523231	0.97080174	3.51795035	0.00043489	0.01709684	1.76708418	yes
MMP3	1673.18929	2.74233559	1.04598916	2.6217632	0.00874762	0.0626411	1.20314041	yes
MS4A1	5393.16287	2.57076258	0.95200461	2.70036778	0.00692629	0.05783023	1.23784507	yes
BANK1	4178.99064	2.22221574	0.74315608	2.99024095	0.00278757	0.03562572	1.4482364	yes
CD19	3401.9927	2.08618451	0.74763838	2.79036573	0.00526485	0.05089358	1.29333699	yes
CCR7	1745.05622	2.05465648	0.81784489	2.51228136	0.01199534	0.076209	1.11799376	yes
CXCR5	1502.46352	2.00830911	0.81341173	2.46899454	0.01354933	0.07918847	1.10133805	yes
FCCR2	1164.9854	1.96605834	0.74627599	2.63449228	0.00842632	0.06264113	1.20314041	yes
SELL	2560.14415	1.81666133	0.73396255	2.47514171	0.01331833	0.07918847	1.10133805	yes
ZBTB16	709.078541	1.7551234	0.53162473	3.30143296	0.00096192	0.02363953	1.62636116	yes
CD1C	870.394762	1.73887084	0.64302203	2.7042166	0.00684656	0.05783023	1.23784507	yes
IL1R2	177.225688	1.73802411	0.68142389	2.55057703	0.01075448	0.07088177	1.14946544	no
IGHD	555.95821	1.63342091	0.96545353	1.69186902	0.09067095	0.26282945	0.58032587	no
OSM	540.695673	1.51049856	0.80321953	1.88055507	0.06003247	0.19343795	0.71345831	no
CCR6	1063.59855	1.43849137	0.52601261	2.73470892	0.00624355	0.05658214	1.24732067	yes
LTB	1866.54329	1.43458494	0.70964458	2.02155414	0.04322243	0.15657365	0.80528132	no
LTA	791.260317	1.43269229	0.74761231	1.91635728	0.05531963	0.18025499	0.7441127	no
CD89	1516.25796	1.43060727	0.4711908	3.03615282	0.00239618	0.03474459	1.45911277	yes
TREM1	1611.896	1.39068068	0.85440512	1.62765957	0.10359709	0.27861496	0.55499557	no
DUSP1	7987.84709	1.35970994	0.74104759	1.83484835	0.06652816	0.20308597	0.69232008	no
SPR1	1096.07189	1.31159152	0.51232586	2.56007283	0.01046502	0.07057806	1.15133027	yes
PTGDS	7751.66235	1.30609567	0.84667142	1.54262402	0.12292203	0.2921917	0.53433212	no
FOLR3	190.086772	1.2929175	0.86339402	1.49748258	0.13426774	0.3018422	0.52022005	no
S100A12	414.708353	1.26764323	0.87080574	1.45571299	0.14547198	0.32128204	0.49311355	no
CLU	5555.10391	1.25462836	0.64012069	1.95998721	0.04999729	0.17201781	0.7644266	no
ALOX5AP	1967.02909	1.25363105	0.42166159	2.97307384	0.00294834	0.03562572	1.4482364	yes
C3	8969.74854	1.24566561	0.76643811	1.62526574	0.10410595	0.27861496	0.55499557	no
SPR5	221.729939	1.19289581	0.8343949	1.42965377	0.15281642	0.33300625	0.47754761	no
S100A8	1912.86507	1.18893337	1.01388688	1.17264894	0.24093662	0.41344153	0.3835859	no
TRDV2	198.094352	1.15827169	0.70533365	1.64216139	0.10055656	0.27510757	0.56049745	no
IL3RA	870.508282	1.15489548	0.35083364	3.2918607	0.00099527	0.02363953	1.62636116	yes
ICOS	712.357049	1.14549785	0.43328483	2.64375248	0.00819926	0.06257329	1.203611	yes
CXCR1	657.025771	1.11373192	0.89532389	1.24394305	0.21352052	0.40050485	0.39739222	no
CTLA4	1716.01121	1.10990554	0.54576565	2.03366689	0.04198519	0.15657365	0.80528132	no
CD28	1851.17888	1.10502101	0.53587772	2.0620768	0.03920042	0.1525121	0.8166957	no
FLT3	867.918626	1.08780692	0.51245277	2.12274569	0.03377517	0.13773601	0.86095251	no
IL10	695.611225	1.06027296	0.66311524	1.59892715	0.10983679	0.27861496	0.55499557	no
CD7	46.6169971	1.05645492	0.45127521	2.34104353	0.01922993	0.09962906	1.00161399	no
HAND2	636.828897	1.04846807	0.49761037	2.10700608	0.03511705	0.1395061	0.85540681	no
TNF	1069.46083	1.03661032	0.55798183	1.85778509	0.06319954	0.19713568	0.70523476	no
ITGAX	3566.65599	1.03480904	0.34736542	2.97902146	0.00289171	0.03562572	1.4482364	yes
TNFSF9	233.517645	1.03395086	0.64472639	1.60370489	0.10877912	0.27861496	0.55499557	no
GZMK	1222.45935	1.00616956	0.64451838	1.56111849	0.1184958	0.28636484	0.54308031	no
ABCC9	636.055213	0.99795395	0.42726247	2.33569301	0.01950725	0.09962906	1.00161399	yes
CD80	589.995259	0.99615144	0.45187814	2.20446922	0.02749136	0.12457024	0.90458571	no
IL7R	6618.94046	0.99241457	0.51755142	1.9175188	0.05517206	0.18025499	0.7441127	no
KLF2	1876.11788	0.97479619	0.39898545	2.44318732	0.01455818	0.0827818	1.08206513	yes
GATA3	338.898803	0.96339833	0.50006999	1.92650897	0.05404085	0.18025499	0.7441127	no
IL18R1	1253.08496	0.95463137	0.29733514	3.21062405	0.00132447	0.04006003	1.61967957	yes
PTPRC	13970.3792	0.94880185	0.51384207	1.84648536	0.06482176	0.19998204	0.69900901	no
CDB8	1926.92689	0.93983684	0.64191522	1.46411364	0.1431629	0.31936339	0.49571487	no
TNFRSF13B	1217.16313	0.93819237	0.56730659	1.65376602	0.09817506	0.27510757	0.56049745	no
ACKR1	1261.60761	0.92205745	0.49366497	1.86777978	0.06179277	0.19692202	0.70570571	no
JAK3	4521.55009	0.9179017	0.57851788	1.58664362	0.11259338	0.27907762	0.554275	no
TREM2	853.42568	0.89808523	0.75314965	1.19243929	0.23308904	0.41144595	0.38568721	no
IL1B	1957.75188	0.8847266	0.82825214	1.06818511	0.28543702	0.45987076	0.33736421	no
TRAC	6948.11473	0.87758204	0.62512999	1.40383393	0.16036671	0.3384902	0.4704539	no
TNFSF15	451.778802	0.87166786	0.50703726	1.71913967	0.08558894	0.25071509	0.60081953	no
CCL4	2162.1315	0.85204854	0.53312085	1.59822775	0.1099923	0.27861496	0.55499557	no
TIGIT	2064.10891	0.84057996	0.52106889	1.61318394	0.10670455	0.27861496	0.55499557	no
IFNG	487.783311	0.83190631	0.54705245	1.52070665	0.12833347	0.29773365	0.52617208	no
ADGRB3	556.980907	0.83071509	0.54559302	1.5225911	0.12786104	0.29773365	0.52617208	no
FCN1	684.105916	0.81193855	0.64093968	1.26679401	0.20522895	0.40050485	0.39739222	no
MMRN1	1987.36669	0.80819908	0.50039553	1.61512049	0.10628461	0.27861496	0.55499557	no
TRAV1-2	415.503525	0.80491034	0.66661089	1.20746653	0.22725253	0.41144595	0.38568721	no
KCNJ8	882.613362	0.78018257	0.60164458	1.29674995	0.19471724	0.38915281	0.40987983	no
SERPINF1	6266.924	0.76678158	0.35341939	2.16960813	0.03003655	0.12810694	0.89242734	no
NOTCH4	739.349007	0.76655003	0.46664964	1.64266713	0.10045182	0.27510757	0.56049745	no
CCDC80	3139.17565	0.76099121	0.64354512	1.1824986	0.23700792	0.41144595	0.38568721	no
SOX8	492.621655	0.75053481	0.63652724	1.1791087	0.23835489	0.41144595	0.38568721	no
CLEC9A	681.956717	0.74862995	0.57308031	1.30632642	0.19144157	0.38554206	0.41392824	no
RTKN2	1858.83013	0.73032349	0.46440622	1.57259627	0.11581233	0.28462353	0.5457292	no
LYVE1	1537.22231	0.70698892	0.56229526	1.25732683	0.20863531	0.40050485	0.39739222	no
CD3E	3772.72142	0.7020892	0.49637746	1.41442604	0.15723685	0.33528446	0.47458658	no
STAT4	1540.00042	0.69899308	0.33006453	2.11774669	0.03419653	0.13773601	0.86095251	no
PYY	288.419992	0.68242214	0.61560274	1.10854304	0.26762736	0.4460456	0.35062074	no
NTRK2	1115.41481	0.68076118	0.63520649	1.07171636	0.28384745	0.45986458	0.33737004	no
BASP1	4239.58352	0.67774494	0.40166368	1.68734437	0.09153715	0.26282945	0.58032597	no
CSPG4	2330.574	0.66435397	0.604946	1.09820376	0.27211553	0.4509343	0.34588673	no
CD40	2964.34461	0.6577479	0.43156979	1.52408234	0.12748814	0.29773365	0.52617208	no
FYB1	3987.67501	0.65261179	0.53160444	1.22762668	0.21958714	0.40050485	0.39739222	no
MT1G	237.253781	0.63545611	0.80697033	0.78745907	0.43101318	0.61765959	0.20925081	no
TIMP1	4973.32528	0.62874391	0.77036966	0.81615871	0.41440937	0.60089358	0.22120243	no
IRF8	4519.44282	0.61888905	0.34025876	1.81887763	0.0689301	0.20822635	0.68146431	no
CDH5	2144.0873	0.60618286	0.37617423	1.61144178	0.10708347	0.27861496	0.55499557	no
XCR1	582.639676	0.5999356	0.50622852	1.18510826	0.23597465	0.41144595	0.38568721	no
CD3D	2876.52694	0.59369513	0.50158145	1.18364651	0.23655302	0.41144595	0.38568721	no
TRGC1	907.388359	0.5845915	0.53969721	1.08318422	0.27872666	0.45410523	0.34284349	no
CD86	2135.89046	0.58200204	0.42572694	1.36707823	0.17160079	0.35054231	0.45537107	no
SH2D6	207.044499	0.56380102	0.70582219	0.7987862	0.42441439	0.61233917	0.21300796	no
NEUROD1	791.465371	0.56028891	0.62252389	0.90002796	0.36810537	0.56184504	0.25038345	no
FXYD5	5369.07009	0.55419012	0.31682914	1.74917659	0.0802605	0.23750556	0.62432622	no
S100A9	3473.14706	0.53585536	0.96858096	0.55323756	0.58010075	0.75007895	0.12489302	no
NOTCH3	2021.86666	0.52916021	0.37108326	1.42598783	0.15387185	0.33300625	0.47754761	no
KLRF1	670.003887	0.52592936	0.41736479	1.26011913	0.20762639	0.40050485	0.39739222	no
CLDN5	889.083778	0.52139784	0.67144331	0.77653293	0.43743439	0.61880962	0.20844294	no
CSF3R	1189.80923	0.51914081	0.78815178	0.65868126	0.51010047	0.69125764	0.16036005	no
LEF1	3583.37577	0.48364171	0.34012302	1.42196113	0.15503754	0.3330436	0.47749891	no

CACNA1A	960.236156	0.48163638	0.65663091	0.73349636	0.46325575	0.64279505	0.19192747	no
IGHE	97.0412267	0.47857994	1.06351777	0.44999713	0.65271251	0.80206198	0.09579207	no
TRGV9	716.779404	0.45828269	0.58639262	0.78152875	0.43449158	0.61765959	0.20925081	no
TNFSF13B	1863.35862	0.4570269	0.39421808	1.15932508	0.2463237	0.41774195	0.37909191	no
MRC1	3356.91078	0.45282759	0.50084353	0.90412987	0.36592654	0.56147459	0.25066989	no
ZFP36L1	12275.9423	0.43886158	0.59282452	0.74028917	0.45912455	0.64012557	0.19373482	no
CRYAB	2098.64151	0.43353543	0.41901327	1.034658	0.30082866	0.48199067	0.31696137	no
TRGC2	1582.5655	0.42894772	0.39474646	1.0866411	0.27719545	0.45410523	0.34284349	no
IL1R1	6092.98725	0.40521105	0.43358735	0.93455458	0.3500179	0.5428085	0.26535336	no
OSMR	2661.85795	0.39047101	0.3266134	1.19551433	0.23188614	0.41144595	0.38568721	no
CCSER1	2486.56767	0.37726307	0.42810619	0.88123713	0.37818948	0.5712237	0.24319378	no
VWF	2640.62439	0.36738076	0.4452452	0.82512008	0.40930342	0.59647232	0.2244097	no
FOXP3	506.931456	0.36732149	0.63264665	0.58061082	0.56150278	0.73622147	0.13299152	no
CCL23	584.543271	0.36214927	0.50250257	0.72069139	0.47109941	0.6474826	0.1887719	no
CYTH1	4619.9569	0.35658088	0.42331242	0.84235866	0.39958722	0.58525401	0.2326556	no
IL1RL1	1153.38695	0.34880068	0.38443592	0.90730512	0.36424547	0.56147459	0.25066989	no
VCAN	4267.30924	0.33719796	0.53011325	0.63608665	0.52471994	0.70776178	0.15011289	no
TGFBR2	7579.67825	0.33570305	0.44261746	0.75844965	0.44818185	0.63093561	0.20001496	no
ALOX5	3354.62151	0.33357323	0.4450963	0.74944058	0.4535917	0.63546663	0.19690725	no
TNFAIP3	7131.71415	0.32997486	0.37882781	0.87104181	0.38373132	0.5765911	0.23913206	no
CD8A	1127.59325	0.32053351	0.51971139	0.61675291	0.53739772	0.71818128	0.14376592	no
FCGR3B	2307.78612	0.29779736	0.66919248	0.44501002	0.65631251	0.8025054	0.09555204	no
NFKBIA	6678.05303	0.28819199	0.50063273	0.57565551	0.56484805	0.73622147	0.13299152	no
CD1D	1611.36803	0.26645507	0.26290255	1.01351267	0.31081535	0.49525522	0.30517094	no
TRDC	982.418259	0.2577235	0.46832779	0.5503058	0.58210965	0.75007895	0.12489302	no
CD79A	6817.54988	0.24730059	0.76989811	0.3212121	0.74804966	0.86428049	0.06334529	no
HPGDS	935.045685	0.24320181	0.45826619	0.53069989	0.59562676	0.7561008	0.1214203	no
KLRB1	1985.69773	0.24102815	0.45473205	0.53004435	0.59608118	0.7561008	0.1214203	no
TNFRSF1B	5545.37429	0.23719667	0.35329017	0.67139335	0.50196998	0.68343331	0.16530386	no
MCAM	3740.74407	0.2158931	0.41229661	0.5236354	0.60053215	0.7561008	0.1214203	no
CD4	3278.25061	0.21539046	0.37351612	0.57665641	0.56417159	0.73622147	0.13299152	no
COL1A2	24033.8077	0.21354201	0.60721746	0.35167303	0.72508349	0.84447474	0.07341333	no
GLIS3	1096.79648	0.20364274	0.48740297	0.41781186	0.67608468	0.8113261	0.09080455	no
BATF	409.524264	0.20095653	0.32287329	0.62240061	0.53367848	0.71651278	0.14477606	no
GATA2	2043.52493	0.1980654	0.48013069	0.41252393	0.67995544	0.81146946	0.09072782	no
MEF2C	3166.64943	0.19467715	0.3740221	0.52049639	0.60271764	0.7561008	0.1214203	no
C7	2206.58324	0.18843596	0.74359751	0.25341123	0.79995045	0.88760144	0.051782	no
S100B	1431.59288	0.18807367	0.35793906	0.5254349	0.5992809	0.7561008	0.1214203	no
COL1A1	27985.0535	0.18546701	0.61483639	0.30165263	0.76291689	0.86763097	0.06166495	no
FCER1G	6285.04915	0.17552422	0.5462375	0.32133316	0.74795793	0.86428049	0.06334529	no
SPARC	16800.0697	0.17186035	0.66376984	0.25891557	0.79570038	0.88760144	0.051782	no
IL10RA	5656.27472	0.16564736	0.4637217	0.35721287	0.72093245	0.84447474	0.07341333	no
LILRA4	1838.12172	0.15420247	0.33349447	0.46238389	0.64380605	0.79448406	0.09991481	no
GZMB	859.258529	0.15061619	0.59322533	0.25389373	0.79957766	0.88760144	0.051782	no
CTSL	5683.08235	0.13764451	0.44727845	0.30773786	0.75828181	0.86763097	0.06166495	no
COL6A2	9314.92282	0.13700599	0.66664261	0.20551639	0.83716869	0.90252387	0.0445413	no
LAMP3	3485.7638	0.13614552	0.30942409	0.43999651	0.65993963	0.8025054	0.09555204	no
COL3A1	35487.2811	0.13468081	0.62056665	0.21702876	0.82818593	0.90252387	0.0445413	no
TNFRSF11B	1906.35102	0.13279169	0.77956772	0.17034015	0.86474264	0.91523856	0.03846569	no
SPARCL1	10113.9213	0.12963438	0.56263457	0.23040601	0.8177763	0.90044036	0.04554505	no
APOE	2353.41664	0.12448485	0.54618643	0.22791641	0.81971122	0.90044036	0.04554505	no
OGN	1294.86949	0.1142031	0.69220798	0.1649838	0.868895674	0.91538724	0.03839515	no
FCGR3A	1237.2805	0.10894855	0.52753492	0.20652387	0.83638172	0.90252387	0.0445413	no
NKG7	583.099906	0.10144009	0.56068765	0.18092086	0.85642969	0.90976048	0.04107293	no
MAF	9653.17113	0.09874499	0.39358458	0.25088633	0.80190199	0.88760144	0.051782	no
CCL8	795.427419	0.09578607	0.59076391	0.16213934	0.87119613	0.91538724	0.03839515	no
HMGB2	7935.80976	0.09423443	0.45260241	0.20820577	0.8350683	0.90252387	0.0445413	no
TGFBR1	4446.99339	0.08257963	0.28164549	0.29320415	0.76936611	0.87154755	0.05970892	no
TYROBP	1596.51563	0.06204919	0.49520551	0.12529988	0.90028615	0.93243922	0.03037947	no
IRF7	100.856079	0.05514205	0.52970716	0.10409912	0.91709069	0.94310745	0.02543883	no
TCF4	2331.13703	0.04918573	0.44556827	0.11038877	0.91210106	0.94131426	0.02626536	no
CLEC10A	867.66406	0.04373027	0.48071185	0.09096982	0.92751657	0.95045868	0.02206676	no
ASP1	1211.93258	0.00630214	0.48591406	0.01296965	0.98965201	0.99706356	0.00127716	no
HMG2	32112.0311	-0.0016114	0.29878793	-0.0053931	0.99569694	0.99706356	0.00127716	no
KLRC2	1351.28228	-0.001848	0.50213533	-0.0036803	0.99706356	0.99706356	0.00127716	no
TYK2	5738.37775	-0.0037923	0.32210166	-0.0117737	0.99060615	0.99706356	0.00127716	no
LST1	515.700859	-0.0069104	0.40282372	-0.017155	0.98631298	0.99706356	0.00127716	no
TRPM5	803.841932	-0.0183568	0.70743955	-0.0259483	0.97929859	0.99647927	0.00153173	no
PLP1	686.667113	-0.026776	0.53483156	-0.0500643	0.96007117	0.98035436	0.00861691	no
RGCC	1611.68025	-0.0466933	0.34133816	-0.1367948	0.89119301	0.92889968	0.03203118	no
PDGFRA	6603.12943	-0.0586203	0.43855306	-0.1336674	0.89366556	0.92889968	0.03203118	no
TLE4	3245.07062	-0.0782954	0.29311465	-0.2671154	0.78938028	0.88760144	0.051782	no
TPSB2	1488.32088	-0.0801921	0.54909061	-0.1460453	0.88388559	0.92536759	0.03368572	no
NCAM1	1040.62283	-0.083402	0.43981902	-0.189628	0.84960061	0.9061102	0.04281898	no
IAK2	5120.8998	-0.0853257	0.32079826	-0.2659794	0.79025505	0.88760144	0.051782	no
GZMA	1227.09625	-0.0934198	0.49353847	-0.1892857	0.84986888	0.9061102	0.04281898	no
HLA-DRA	16413.3057	-0.1051219	0.54481295	-0.1929505	0.84699772	0.9061102	0.04281898	no
PECAM1	9946.17504	-0.1106539	0.49996844	-0.2213219	0.82484183	0.90252387	0.0445413	no
TOP2A	3752.54684	-0.1131834	0.37517189	-0.3016841	0.7628929	0.86763097	0.06166495	no
IFITM2	2616.48229	-0.1324943	0.37363635	-0.3546076	0.72288358	0.84447474	0.07341333	no
S100A4	1685.74879	-0.1386095	0.36706203	-0.3776186	0.70571394	0.83533487	0.07813939	no
MSA47	5283.47913	-0.1636338	0.34295521	-0.4771287	0.63327051	0.78482242	0.1052286	no
TUBB	8071.50028	-0.1658269	0.28901687	-0.5737619	0.56612893	0.73622147	0.13299152	no
CPA3	3586.24516	-0.177941	0.35609713	-0.499698	0.61728773	0.76829803	0.11447028	no
JAK1	11059.4691	-0.1796985	0.43143981	-0.4165089	0.67703764	0.8113261	0.09080455	no
CCL5	3433.52566	-0.1812969	0.50719924	-0.3574471	0.72075711	0.84447474	0.07341333	no
CD14	5297.90012	-0.1987213	0.45767114	-0.4342011	0.6641424	0.8025054	0.09555204	no
MSA42	1147.41002	-0.2076834	0.40140225	-0.5173947	0.60488064	0.7561008	0.1214203	no
IL13RA2	854.347269	-0.2370598	0.76736994	-0.308925	0.75737855	0.86763097	0.06166495	no
PLVAP	5503.58908	-0.2435467	0.44543707	-0.546759	0.58454429	0.75007895	0.12489302	no
CD44	22491.6211	-0.255122	0.43907643	-0.5810424	0.56121191	0.73622147	0.13299152	no
PHLDA2	358.524149	-0.2586657	0.59073371	-0.4378719	0.66147912	0.8025054	0.09555204	no
TGFBI	20332.6947	-0.266264	0.67572625	-0.3940412	0.69355064	0.82430199	0.08391365	no
QDPR	2915.60647	-0.2706092	0.31640799	-0.855254	0.39241056	0.58406564	0.23353834	no
TPH1	2162.42886	-0.3166271	0.53314998	-0.5938799	0.55259241	0.7351	0.13365358	no
CPE	2511.08592	-0.3550456	0.41644344	-0.8525661	0.39389996	0.58406564	0.23353834	no
NPC2	5980.98134	-0.4386594	0.28939611	-1.5157749	0.12957628	0.29823112	0.52544703	no
CAV1	3118.44421	-0.443147	0.46202055	-0.9591501	0.33748315	0.52902765	0.27652163	no
UBE2C	1475.25515	-0.4443065	0.35905932	-1.2374181	0.21593189	0.40050485	0.39739222	no

INSM1	994.016817	-0.4670687	0.55342088	-0.8439665	0.39868813	0.58525401	0.2326556	no
KIT	2108.29862	-0.4674724	0.38820587	-1.2041869	0.22851733	0.41144595	0.38568721	no
RORC	2441.77639	-0.4745409	0.4373544	-1.0850261	0.2779101	0.45410523	0.34284349	no
SOX6	1718.78727	-0.475219	0.38243505	-1.2426137	0.21401024	0.40050485	0.39739222	no
WNT5A	3349.41961	-0.4762339	0.60852428	-0.7826045	0.43385938	0.61765959	0.20925081	no
PROX1	1646.78975	-0.4777906	0.4259989	-1.1215772	0.26204226	0.43926159	0.35727677	no
POSTN	6799.184	-0.4916098	0.57765857	-0.8510388	0.39474781	0.58406564	0.23353834	no
CD209	3280.26477	-0.4918763	0.35589109	-1.3820978	0.16694168	0.3482956	0.45805201	no
RG55	5353.96751	-0.4959407	0.49747498	-0.9969158	0.31880538	0.50246501	0.29889418	no
TNMIN1	7112.84912	-0.5074335	0.44907573	-1.1299508	0.25849698	0.43583793	0.36067498	no
FABP5	12212.1062	-0.5161133	0.40971007	-1.2597038	0.20777625	0.40050485	0.39739222	no
MKI67	7800.26954	-0.5165899	0.41812996	-1.2354769	0.21665308	0.40050485	0.39739222	no
TPSAB1	676.972831	-0.5360763	0.74382342	-0.7207037	0.47109183	0.6474826	0.1887719	no
ACTG1	105448.403	-0.5449691	0.41089417	-1.3263003	0.18474025	0.37464806	0.42637651	no
CALD1	12046.6369	-0.5498026	0.58381599	-0.9417395	0.34632603	0.53997068	0.26762982	no
BEST4	551.312459	-0.5546551	0.80119155	-0.6922877	0.48875666	0.66858222	0.17484518	no
HLA-DRB1	9531.98169	-0.592694	0.66348814	-0.8933	0.37169654	0.564356	0.24844685	no
AZM	18885.8881	-0.618585	0.61342017	-1.0084197	0.313253	0.49641187	0.30415785	no
APP	28138.247	-0.6676403	0.53447921	-1.2491418	0.21161323	0.40050485	0.39739222	no
IGHA2	769.55433	-0.6717744	0.54433867	-1.2341112	0.21716148	0.40050485	0.39739222	no
CD59	17776.8393	-0.6730311	0.53961026	-1.247254	0.21230437	0.40050485	0.39739222	no
CCL20	1862.03197	-0.7007523	0.51243115	-1.3675052	0.17146701	0.35045231	0.45537107	no
TNFRSF1A	6989.81671	-0.7081066	0.45589296	-1.55323	0.12036819	0.28848575	0.53987564	no
DUSP23	915.194974	-0.7205409	0.38787857	-1.8576455	0.06321937	0.19713568	0.70523476	no
TM6SF1	4506.98939	-0.7409377	0.63388519	-1.1688831	0.24245074	0.41359244	0.38342741	no
S100A11	10790.127	-0.7597886	0.50691505	-1.4988481	0.13391305	0.3018422	0.52022005	no
TUBA1B	57892.8789	-0.7720671	0.4602516	-1.6774892	0.09344686	0.26568225	0.57563746	no
FCER1A	1467.9427	-0.7747403	0.59905614	-1.2932682	0.19591831	0.38915281	0.40987983	no
MZB1	15536.3626	-0.7918994	0.64361794	-1.2303874	0.21855209	0.40050485	0.39739222	no
F3	7352.51271	-0.798783	0.67128762	-1.1899265	0.23407527	0.41144595	0.38568721	no
C1QA	3218.33667	-0.8074313	0.5083546	-1.5883231	0.1122133	0.27907762	0.554275	no
SEC61B	2324.72837	-0.8806766	0.56268317	-1.5651376	0.11755066	0.28636484	0.54308031	no
PLAC8	26890.5595	-0.8917227	0.61373416	-1.4529461	0.14623872	0.32128204	0.49311355	no
ASCL2	1023.18462	-0.8928285	0.63706736	-1.4014664	0.16107465	0.3384902	0.4704539	no
IL32	5750.57097	-0.9293315	0.46063413	-2.0175047	0.04364287	0.15657365	0.80528132	no
NUPR1	5388.12845	-0.9567296	0.40986472	-2.3342571	0.01958226	0.09962906	1.00161399	yes
GSN	26004.6796	-0.9808445	0.49027272	-2.0006099	0.04543444	0.15874684	0.7992949	no
TMEM176A	12356.3759	-0.9871753	0.40027204	-2.4662609	0.01365318	0.07918847	1.10133805	yes
LTBR	4714.62655	-1.0182869	0.4645796	-2.191846	0.02839063	0.12529201	0.90236374	no
ANXA2	51690.1993	-1.0272292	0.5093755	-2.0166444	0.04373264	0.15657365	0.80528132	no
JUN	13975.4846	-1.0465046	0.54545081	-1.9186049	0.05503435	0.18025499	0.7441127	no
C1QB	2214.65925	-1.047101	0.58023684	-1.8046097	0.07113579	0.212674	0.6722856	no
TINAGL1	3562.7049	-1.0591709	0.5142761	-2.0595374	0.03944278	0.1525121	0.8166957	no
CST3	10473.5316	-1.0633765	0.36108145	-2.9449768	0.00322979	0.03624763	1.44072037	yes
MGLL	6414.94017	-1.0875673	0.50196453	-2.1666218	0.0302637	0.12810694	0.89242734	no
LYZ	27013.2345	-1.0986711	0.54005673	-2.0343623	0.04191508	0.15657365	0.80528132	no
LGR5	1818.8912	-1.1389743	0.76046295	-1.497738	0.13420133	0.3018422	0.52022005	no
TMEM176B	19200.2275	-1.1672661	0.4409675	-2.647057	0.00811957	0.06257329	1.203611	yes
SSR4	10887.252	-1.2241086	0.61043132	-2.0053175	0.04492911	0.15874684	0.7992949	no
C1QC	4069.13535	-1.2400276	0.55975488	-2.2153046	0.02673916	0.12457024	0.90458571	no
SELENOP	34314.8266	-1.2435086	0.51776171	-2.4017006	0.01631906	0.09101013	1.04091027	yes
INAVA	4294.78486	-1.2559343	0.59033848	-2.1274817	0.03338008	0.13773601	0.86095251	no
REG4	15966.2714	-1.3432509	0.97524079	-1.3773531	0.1684031	0.348835	0.45737994	no
TNFRSF17	2792.8458	-1.3586279	0.61541533	-2.2076601	0.02726798	0.12457024	0.90458571	no
MSA48	1287.98924	-1.3637374	0.63025459	-2.1637881	0.03048062	0.12810694	0.89242734	no
TNFRSF11A	7263.14539	-1.4018091	0.60910519	-2.3014236	0.0213677	0.10502768	0.97869622	no
OLFM4	25435.528	-1.4177527	0.88830737	-1.5960159	0.11048524	0.27861496	0.55499557	no
NO52	4415.26132	-1.4378824	0.6009771	-2.3925744	0.01673064	0.091545	1.03836537	yes
CA7	1298.27157	-1.4865783	0.75985711	-1.9563918	0.05041901	0.17201781	0.7644266	no
SOX9	4574.56688	-1.5105352	0.66764838	-2.2624711	0.02366831	0.11252149	0.94876452	no
MYH11	20743.4326	-1.5204588	0.75223562	-2.0212534	0.04325355	0.15657365	0.80528132	no
OTOP2	738.768648	-1.528389	0.92993831	-1.6435381	0.10027165	0.27510757	0.56049745	no
CXCL14	8732.76611	-1.5309708	0.66100733	-2.3161177	0.02055184	0.10275922	0.98817918	no
CEACAM1	21259.322	-1.6170256	0.70494001	-2.2938485	0.0217992	0.10536281	0.97731265	no
CEACAM6	23845.8847	-1.6680934	0.70067926	-2.3806804	0.0172807	0.09280374	1.03243453	yes
MUC1	8206.29814	-1.7108829	0.52490528	-3.2594127	0.00111643	0.02363953	1.62636116	yes
KRT8	97907.0904	-1.7241713	0.58818072	-2.9313632	0.00337478	0.03624763	1.44072037	yes
S100A16	8527.96765	-1.7641203	0.63524246	-2.7770818	0.00548494	0.0513107	1.28979208	yes
ITM2C	59915.0621	-1.8161916	0.56167577	-3.2335231	0.00122273	0.02363953	1.62636116	yes
S100P	5597.95965	-1.8902844	0.86298947	-2.1903911	0.02849589	0.12520921	0.90236374	no
DDC	5190.05703	-1.894338	0.6678015	-2.8366783	0.00455855	0.04558552	1.34117306	yes
ADAMDEC1	10264.2272	-1.9346004	0.57903053	-3.3411025	0.00083446	0.02363953	1.62636116	yes
FABP2	5896.1976	-2.0219118	0.80813417	-2.5019507	0.01235111	0.076209	1.11799376	yes
TFF3	10832.0483	-2.022793	0.70427139	-2.8721783	0.00407653	0.0422212	1.37446948	yes
PIGR	117128.085	-2.0292558	0.75601726	-2.6841395	0.00727168	0.05857739	1.23226999	yes
AGR2	47284.3389	-2.0361977	0.81159554	-2.5088823	0.01211138	0.076209	1.11799376	yes
EPCAM	57971.1687	-2.1039525	0.70352997	-2.9905655	0.00278461	0.03562572	1.4482364	yes
SPINK1	10616.1579	-2.1851581	0.61445418	-3.5562588	0.00037617	0.01709684	1.76708418	yes
LEFTY1	3988.95609	-2.2570835	0.86228618	-2.6175574	0.00885616	0.06264113	1.20314041	yes
C15orf48	26739.1836	-2.4489055	0.67213804	-3.6434563	0.000269	0.01709684	1.76708418	yes
MUC2	12916.4213	-2.4902386	0.92305577	-2.6978203	0.00697951	0.05783023	1.23784507	yes
WFDCC2	1460.19394	-2.4986149	0.85141237	-2.9346706	0.00333902	0.03624763	1.44072037	yes
SPINK4	10731.9425	-2.6137551	1.01448594	-2.5764331	0.00988255	0.06892715	1.16160966	yes
LYPD8	8786.16714	-2.6434257	0.86153923	-3.0682593	0.0021531	0.03286306	1.48329199	yes
SLC26A2	20711.8808	-2.6730985	0.82422152	-3.2431797	0.00118204	0.02363953	1.62636116	yes
GPR15	3900.81575	-2.6848083	0.75945183	-3.5351923	0.00040748	0.01709684	1.76708418	yes
ITLN1	13676.6227	-2.8477454	0.90704111	-3.139599	0.00169179	0.02725666	1.56452743	yes
LGALS4	94777.0134	-2.9341603	0.83920226	-3.4963685	0.00047164	0.01709684	1.76708418	yes
PHGR1	74019.8639	-3.0317675	0.81278179	-3.7301125	0.00019139	0.01709684	1.76708418	yes
GUCY2A	1260.16858	-3.1077626	0.93260398	-3.3323498	0.00086116	0.02363953	1.62636116	yes
FABP1	63313.6438	-3.3477142	0.90835847	-3.6854549	0.00022829	0.01709684	1.76708418	yes
CA4	10499.4036	-3.5330824	0.93494966	-3.7789012	0.00015752	0.01709684	1.76708418	yes
AQP8	10362.8134	-3.6448886	1.15982052	-3.1426316	0.00167436	0.02725666	1.56452743	yes

Supplementary Table 6. Pseudobulk DE gene analysis of Xenium data comparing colon biopsies in UC PRE Non-Responders versus UC PRE Responders. Significance was set as log2fc >0.4 or <-0.4, p-adj < 0.1 and baseMean >500.

Gene Signature	Gene list	Numeric ID	
Xenium_HC	<i>AQP8</i>	7994252	
	<i>GUCA2A</i>	7915404	
	<i>SLC26A2</i>	8109194	
	<i>BEST4</i>	7915598	
	<i>OTOP2</i>	8009705	
	<i>DDC</i>	8139640	
	<i>MT1G</i>	8001531	
	<i>CA7</i>	7996331	
	<i>TRPM5</i>	7945742	
	<i>FABP1</i>	8053654	
	<i>JUN</i>	7916609	
	<i>FABP2</i>	8102523	
	<i>CLDN5</i>	8074473	
	<i>LGALS4</i>	8036591	
	<i>PIGR</i>	7923929	
	<i>TREM2</i>	8126279	
	<i>DUSP1</i>	8115831	
	<i>C15ORF48</i>	7983478	
	<i>MS4A8</i>	7940323	
	<i>EPCAM</i>	8041853	
	<i>IL32</i>	7992828	
	<i>C7</i>	8105084	
	<i>KRT8</i>	7963567	
	<i>PHLDA2</i>	7945781	
	<i>NTRK2</i>	8156134	
	<i>CACNA1A</i>	8034643	
	<i>PLP1</i>	8169061	
	<i>GATA2</i>	8090469	
	<i>TRGV9</i>	8139107	
	<i>CEACAM1</i>	8037205	
	<i>HPGDS</i>	8101780	
	<i>CD8B</i>	8044154	
	<i>RORC</i>	7920082	
	<i>NCAM1</i>	7943892	
	<i>CCL23</i>	8014361	
	<i>MGLL</i>	8090433	
	<i>CLEC9A</i>	7953924	
	<i>IL10</i>	7923907	
	<i>FCER1A</i>	7906443	
	<i>TINAGL1</i>	7899627	
	<i>TPH1</i>	7946946	
	<i>INAVA</i>	7908639	
	<i>CCL8</i>	8006453	
	<i>CSPG4</i>	7990545	
	<i>TNFSF9</i>	8025053	
	<i>ADGRB3</i>	8120468	
	<i>FABP5</i>	7948420	
	<i>GLIS3</i>	8159900	
	<i>CCSER1</i>	8096425	
	<i>TRGC1</i>	8180366	
	<i>SOX6</i>	7946757	
	<i>KLRC2</i>	7961182	
	<i>NUPR1</i>	8000574	
	<i>LILRA4</i>	8039246	
	<i>CST3</i>	8065403	
	<i>TRGC2</i>	8180366	
	<i>MS4A2</i>	7940226	
	<i>IL1RL1</i>	8044021	
	<i>HMG2</i>	7899187	
	<i>S100B</i>	8071036	
	Xenium_UC_PRE	<i>S100A12</i>	7920238
		<i>LTB</i>	8124950
		<i>SELL</i>	7896687
		<i>PTGDS</i>	8159521
		<i>JAK3</i>	8035351
		<i>MZB1</i>	8114511
		<i>BANK1</i>	8096617
		<i>CD19</i>	7994487
		<i>C3</i>	8033257
<i>CD79A</i>		8029136	
<i>TIMP1</i>		8167185	
<i>S100A9</i>		7905571	
<i>MS4A1</i>		7940287	
<i>S100A8</i>		7920244	
<i>NOS2</i>		8013536	
<i>PTPRC</i>		7908553	
<i>SSR4</i>		8170775	
<i>CLU</i>		8149927	
<i>PECAM1</i>		8017599	
<i>COL1A1</i>		8016646	
<i>BASP1</i>		8104601	
<i>IL7R</i>	8104901		
<i>MRC1</i>	7926410		

	<i>ALOX5</i>	7927215
	<i>TCF4</i>	8023415
	<i>SERPINF1</i>	8003667
	<i>CD1D</i>	7906330
	<i>VWF</i>	7960464
	<i>CD44</i>	7939341
	<i>OSMR</i>	8105040
	<i>MEF2C</i>	7896727
	<i>REG1A</i>	8042986
	<i>OLFM4</i>	7969288
	<i>KRT20</i>	8015124
	<i>LCN2</i>	8158167
	<i>S100A6</i>	7920258
	<i>MALAT1</i>	7941272
	<i>AGR2</i>	8138381
	<i>B2M</i>	7983360
	<i>CEACAM6</i>	8029098
	<i>S100A10</i>	7920123
	<i>ANXA2</i>	7989335
	<i>COL3A1</i>	8046922
	<i>TIMP1</i>	8167185
	<i>PLAC8</i>	8101429
	<i>COL1A1</i>	8016646
	<i>XBP1</i>	8075182
	<i>LGALS3</i>	7974461
	<i>DMBT1</i>	7931108
	<i>SOD2</i>	8130556
	<i>MZB1</i>	8114511
	<i>CD63</i>	7963911
	<i>SH3BGRL3</i>	7899153
	<i>PFN1</i>	8011759
	<i>SELENOP</i>	8111915
	<i>EZR</i>	8130505
CosMx_UC_PRE	<i>MYL12A</i>	8019924
	<i>HSP90B1</i>	7958130
	<i>ENO1</i>	7912198
	<i>CSTB</i>	8070701
	<i>LYZ</i>	7957023
	<i>SOD1</i>	8068168
	<i>SERPINA1</i>	7981068
	<i>TPT1</i>	7971373
	<i>FAU</i>	7893603
	<i>IGFBP7</i>	8100541
	<i>ANXA4</i>	8042468
	<i>VIM</i>	7926368
	<i>COL1A2</i>	8134263
	<i>ARF1</i>	7892830
	<i>PSAP</i>	7934196
	<i>PGK1</i>	8168500
	<i>CALM3</i>	8029831
	<i>GSTP1</i>	7941936
	<i>CALM1</i>	8052010
	<i>CTNNB1</i>	8079021
	<i>COL6A3</i>	8059905
	<i>ITM2B</i>	7969003
	<i>SRGN</i>	7927964
	<i>RACK1</i>	8116520
	<i>ATP5F1E</i>	8067288
	<i>RBM47</i>	8099967
	<i>IRF4</i>	8116559
	<i>AQP8</i>	7994252
	<i>CA4</i>	8008900
	<i>FABP1</i>	8053654
	<i>GUCA2A</i>	7915404
	<i>LGALS4</i>	8036591
	<i>ITLN1</i>	7921690
	<i>GPR15</i>	8081214
	<i>SLC26A2</i>	8109194
	<i>SPINK4</i>	8154779
	<i>WFDC2</i>	8063000
	<i>MUC2</i>	7937560
	<i>C15orf48</i>	7983478
	<i>LEFTY1</i>	7924663
	<i>SPINK1</i>	8114964
	<i>EPCAM</i>	8041853
Xenium UC PRE R	<i>AGR2</i>	8138381
	<i>PIGR</i>	7923929
	<i>TFF3</i>	8070567
	<i>FABP2</i>	8102523
	<i>ADAMDEC1</i>	8145317
	<i>DDC</i>	8139640
	<i>ITM2C</i>	8048995
	<i>S100A16</i>	7920291
	<i>KRT8</i>	7963567

	<i>MUC1</i>	7920642
	<i>CEACAM6</i>	8029098
	<i>NOS2</i>	8013536
	<i>SELENOP</i>	8111915
	<i>TMEM176B</i>	8143790
	<i>CST3</i>	8065403
	<i>TMEM176A</i>	8137264
	<i>NUPR1</i>	8000574
	<i>CD1C</i>	7906348
	<i>ZBTB16</i>	7943984
	<i>SELL</i>	7896687
	<i>FCER2</i>	8033420
	<i>CXCR5</i>	7944335
	<i>CCR7</i>	8015031
	<i>CD19</i>	7994487
	<i>BANK1</i>	8096617
	<i>MS4A1</i>	7940287
	<i>MMP3</i>	7951284
Xenium UC PRE NR	<i>MMP1</i>	7951271
	<i>CCR6</i>	8123364
	<i>CD69</i>	7896693
	<i>S1PR1</i>	7903393
	<i>ALOX5AP</i>	7968344
	<i>ICOS</i>	8047702
	<i>IL3RA</i>	8165752
	<i>CD7</i>	8019478
	<i>ITGAX</i>	7995128
	<i>ABCC9</i>	7961710
	<i>KLF2</i>	8026564
	<i>IL18R1</i>	8044035
	<i>CD19</i>	7994487
	<i>MS4A1</i>	7940287
	<i>BANK1</i>	8096617
	<i>SELL</i>	7896687
	<i>CD79A</i>	8029136
	<i>CCR7</i>	8015031
	<i>LTB</i>	8124950
	<i>C3</i>	8033257
	<i>TNFSF13B</i>	7969986
	<i>IRF8</i>	7997712
	<i>PTGDS</i>	8159521
	<i>CD1C</i>	7906348
Xenium GALT B DC S4_fibroblast	<i>HLA-DRA</i>	8118548
	<i>CD86</i>	7896700
	<i>ITGAX</i>	7995128
	<i>FCER1A</i>	7906443
	<i>CLEC10A</i>	8012013
	<i>CD1D</i>	7906330
	<i>CLEC9A</i>	7953924
	<i>XCR1</i>	8086595
	<i>FLT3</i>	7970737
	<i>HLA-DRB1</i>	8125445
	<i>CD40</i>	8063156
	<i>CD209</i>	8033445
	<i>LAMP3</i>	7893231
	<i>IL1R1</i>	8043995
	<i>TIMP1</i>	8167185
	<i>CD44</i>	7939341
	<i>IL13RA2</i>	8174598
	<i>MMP1</i>	7951271
	<i>MMP3</i>	7951284
	<i>OSMR</i>	8105040
	<i>NFKBIA</i>	7978644
	<i>TNFAIP3</i>	8122265
	<i>TNFRSF11B</i>	8152512
	<i>S100A8</i>	7920244
Xenium IAF-Monocyte-Neutrophil	<i>S100A9</i>	7905571
	<i>FCGR3B</i>	7921873
	<i>CSF3R</i>	7914950
	<i>BASP1</i>	8104601
	<i>OSM</i>	8075316
	<i>VCAN</i>	8106743
	<i>LYZ</i>	7957023
	<i>FCN1</i>	8165011
	<i>CST3</i>	8065403
	<i>CD14</i>	8114612
	<i>HLA-DRA</i>	8118548
	<i>HLA-DRB1</i>	8125445
	<i>TREM1</i>	8126303

Supplementary Table 7. iSCST gene signatures used for Gene Set Enrichment Analysis (GSEA). Numeric ID, Affymetrix numeric probe identifier corresponding to each gene.